The Tally Ho Shear Zone: Implications for the Tectonic Evolution of the Western Margin of Stikinia, Southern Yukon Territory, Canada

by

Amy Margaret Tizzard
B.Sc., Acadia University, 2003

A thesis submitted in partial fulfillment of the
requirements for the degree of

MASTER OF SCIENCE

in the School of Earth and Ocean Sciences

University of Victoria

2009

The Tally Ho Shear Zone: Implications for the Tectonic Evolution of the Western Margin of Stikinia, Southern Yukon Territory, Canada

by

Amy Margaret Tizzard
B.Sc., Acadia University, 2003

Supervisory Committee

_____
Dr. S.T. Johnston, Supervisor (School of Earth and Ocean Sciences)

_____
Dr. D. Canil, Departmental Member (School of Earth and Ocean Sciences)

_____
Dr. Robert Thompson, Outside Member (Geological Survey of Canada)

Supervisory Committee

Dr. Stephen T. Johnston, Supervisor

Dr. Dante Canil, Departmental Member

Dr. Robert Thompson, Outside Member

ABSTRACT

The Tally Ho shear zone (THSZ) is a 40-kilometre long, northwest-striking assemblage of highly-deformed rocks outcropping along the western margin of Stikinia in southern Yukon. The location of the THSZ adjacent to the boundary between the oceanic Stikine Terrane and pericratonic Nisling Assemblage of the Yukon-Tanana Terrane provides an opportunity to examine the tectonic significance of a terrane-marginal high-strain structure. Detailed geological mapping along the THSZ and adjacent rocks indicates that the shear zone is a crustal-scale thrust fault that places deep-seated arc rocks of Stikinia up-section and to the east onto a package of upper crustal volcanic and volcaniclastic rocks of the Upper Triassic Lewes River Group. Timing of movement along the THSZ is constrained by U-Pb zircon age determinations of a deformed section of cumulate leucogabbro in the hangingwall of the shear zone (208 ± 4.3 Ma) and by a post-kinematic cross-cutting megacrystic granite intrusion (~173 Ma). Positive ε_{Nd} values of Stikine magmatic rocks (+4.5 to +6.7) indicate magmas forming the oceanic terrane were formed with little to no input of continental crust until around the time of intrusion of a megacrystic granite unit in the mid-Jurassic (ε_{Nd} -4.0). The THSZ is therefore interpreted to have formed in response to the thick-skinned collision and underpinning of the Nisling Assemblage beneath western Stikinia in the Early Jurassic resulting in the imbrication of the Stikine magmatic arc along the THSZ.

TABLE OF CONTENTS

LIST OF TABLES

LIST OF FIGURES

CHAPTER 1

CHAPTER 2

ACKNOWLEDGEMENTS

Huge thanks to all the geologists at the Yukon Geological Survey for all their mentorship and support for this project. Also, thanks to Stephen Johnston for all your guidance and patience along the way. I wish to acknowledge the formal assistance of Derek Turner in the field, and the informal assistance of countless others. Finally, thanks to my family and friends for being supportive every step of the way.

CHAPTER 1

INTRODUCTION

INTRODUCTION

The Canadian Cordillera of western North America consists of a collage of accreted oceanic and pericratonic terranes that accreted to the continent in the Mesozoic. The timing of terrane accretion, the processes involved, the geometry of terranes, and their overall contribution to the growth of the continent are, however, topics of ongoing debate (e.g. Albarede 1998; Ben-Avraham *et al.* 1981; Erdmer *et al*. 2002; Johnston 2001; Johnston & Canil, 2007; McClelland *et al*. 2000; Patchett & Chase 2002; Sengor & Natalin 1996). Flake tectonic models of the Cordillera, for example, imply limited westward growth of the continent; terranes are portrayed as thin-flakes sitting atop a westward tapering basement wedge (Cook *et al.* 2004; Snyder *et al*. 2002). However, exhumation of rocks from depths of >100 kilometres during terrane accretion (MacKenzie *et al*. 2005) imply that at least locally, accretion was lithospheric in scale. Accordingly, if accreted oceanic terranes can be shown to occupy the entire lithosphere, their addition to the continent would be volumetrically significant. Insight into the geometry of accreted terranes, and therefore into the nature of accretion, can be found through detailed mapping along terrane margins, however these boundaries are commonly complicated by post-tectonic magmatism and overprinting structures. Nonetheless, unravelling and understanding the nature of tectonism along accretionary margins should aid in the overall understanding of the internal architecture of the orogen and place additional constraints on the tectonic history of the Canadian Cordillera.

The geometry and nature of the western contact between Stikinia, the largest of the accreted oceanic terranes, and the pericratonic Nisling Assemblage of the Yukon-Tanana Terrane (YTT) is, for example, uncertain. Geochemical and isotopic data for Stikinia indicates that the terrane developed in primitive oceanic setting

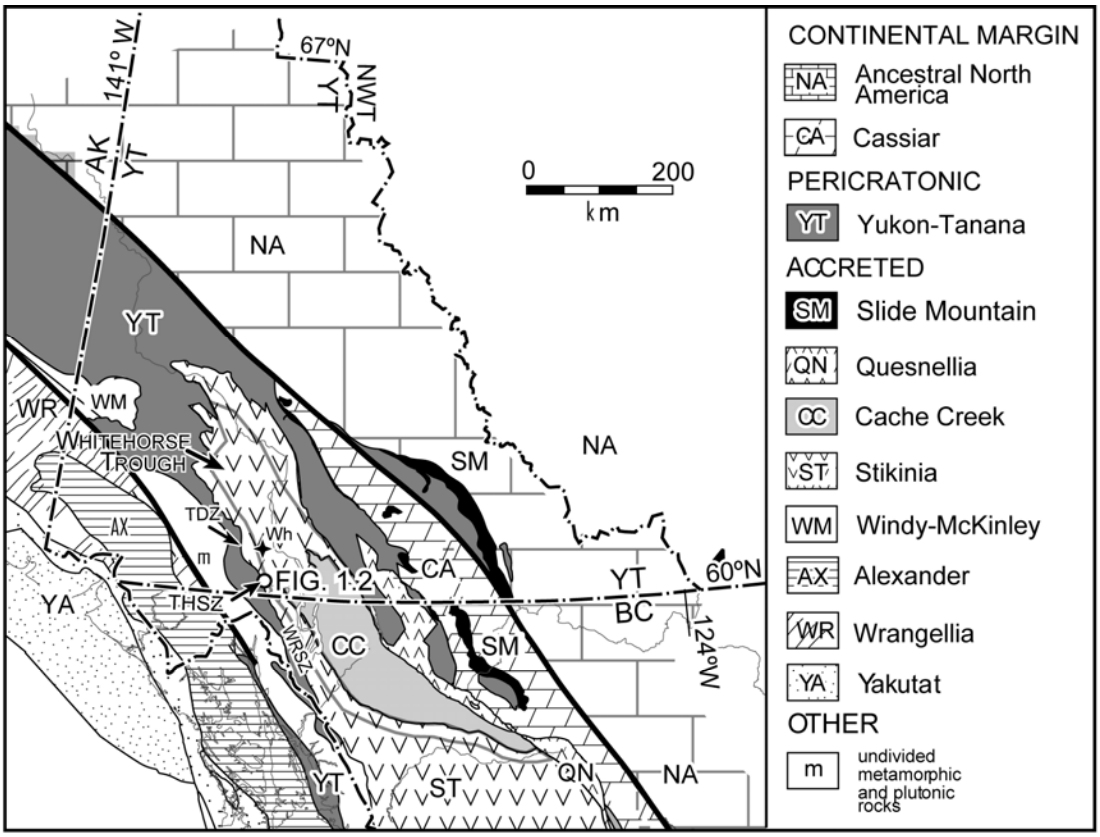

Figure 1.1. Simplified terrane map of the northern Canadian Cordillera (modified after Colpron *et al*. 2006). THSZ, Tally Ho shear zone; TDZ, Takhini deformation zone; WRSZ, Wann River shear zone; Wh, Whitehorse.

(Dostal *et al.* 1999; Monger *et al.* 1991; Samson *et al.* 1989). In contrast, immediately west of Stikinia, the Nisling Assemblage is characterised by a passive margin continental assemblage with an evolved isotopic signature (Mezger *et al*. 2001; Jackson *et al.* 1991). Despite the contrasting isotopic signatures, the contact between Stikinia and the Nisling Assemblage has been interpreted as both a stratigraphic boundary (Jackson *et al.* 1991) and as a tectonic contact (Currie & Parrish 1993)(Fig. 1.1). A stratigraphic terrane linkage implies Stikinia formed *in situ* on top of the Nisling Assemblage, and is not an exotic oceanic terrane. As such, its overall contribution to the growth of the continent would be minor. If, however, the contact is tectonic, then the origin and geometry of Stikinia must be determined in order to constrain its contribution to the westward growth of the continent. Resolving the nature of the Stikine-Nisling Assemblage contact is, therefore, an essential step in developing an accretionary history for part of the northern Canadian Cordillera.

This thesis examines the Tally Ho Shear Zone (THSZ), a 40-kilometre long, northwest-trending package of mylonite and schist along the western margin of Stikinia in southern Yukon (Fig. 1.2). The THSZ is adjacent to the Stikinia-Nisling Assemblage terrane boundary and thus provides an opportunity to investigate the tectonic significance of a terrane-marginal high-strain shear zone. The primary objectives of this thesis are:

- to characterize the structural style of the THSZ and develop a tectonic model for its formation using U-Pb isotopic ages;
- determine the tectonic affinity and environment in which magmatic rocks of Stikinia were emplaced;
- resolve the nature of the western Stikinia-Nisling Assemblage contact;

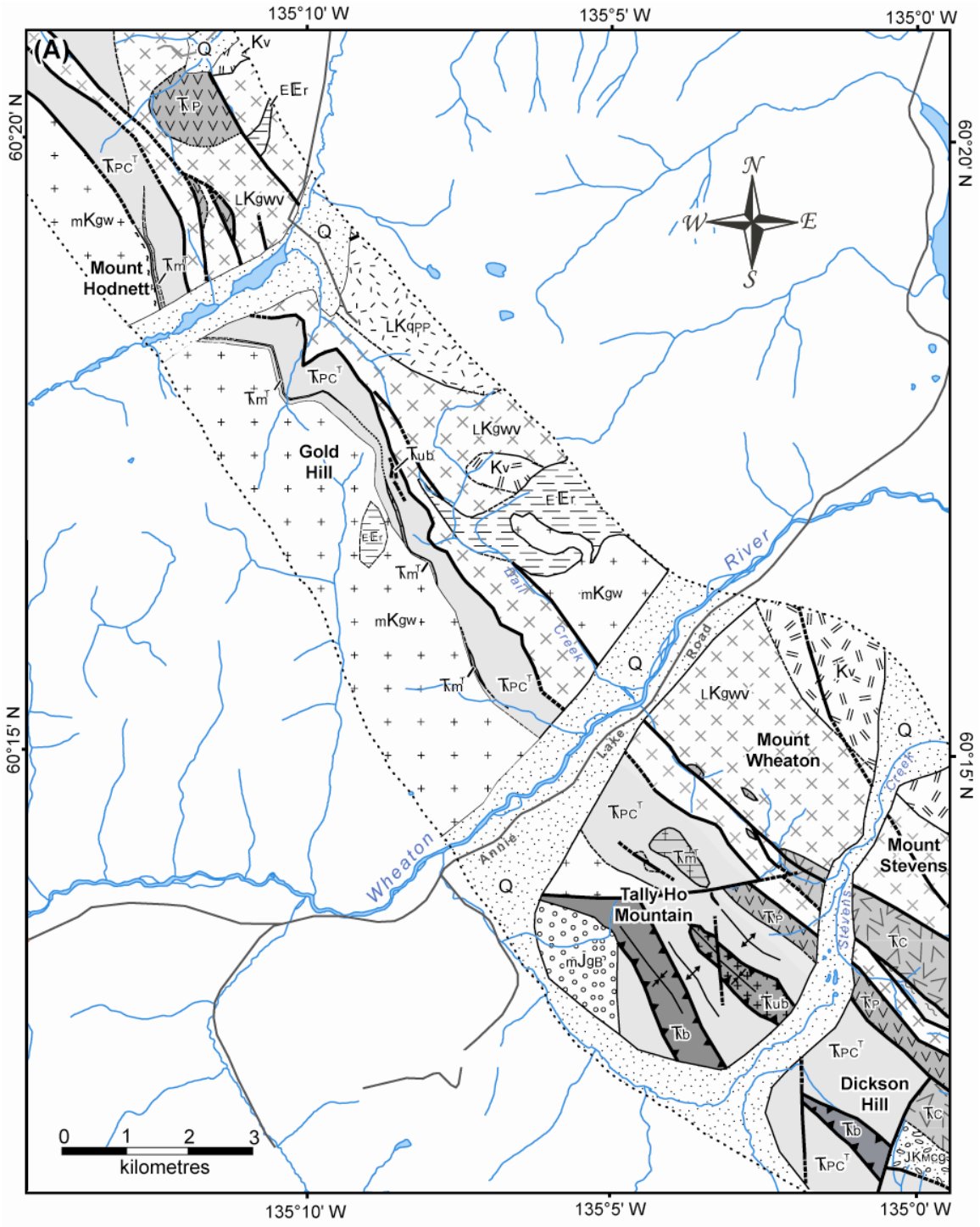

Figure 1.2. (A) Simplified geological map of the Tally Ho shear zone, southern Yukon Territory. (B) Legend for Figure 1.2. Names in parenthesis refer to unit names of Hart & Radloff (1990).

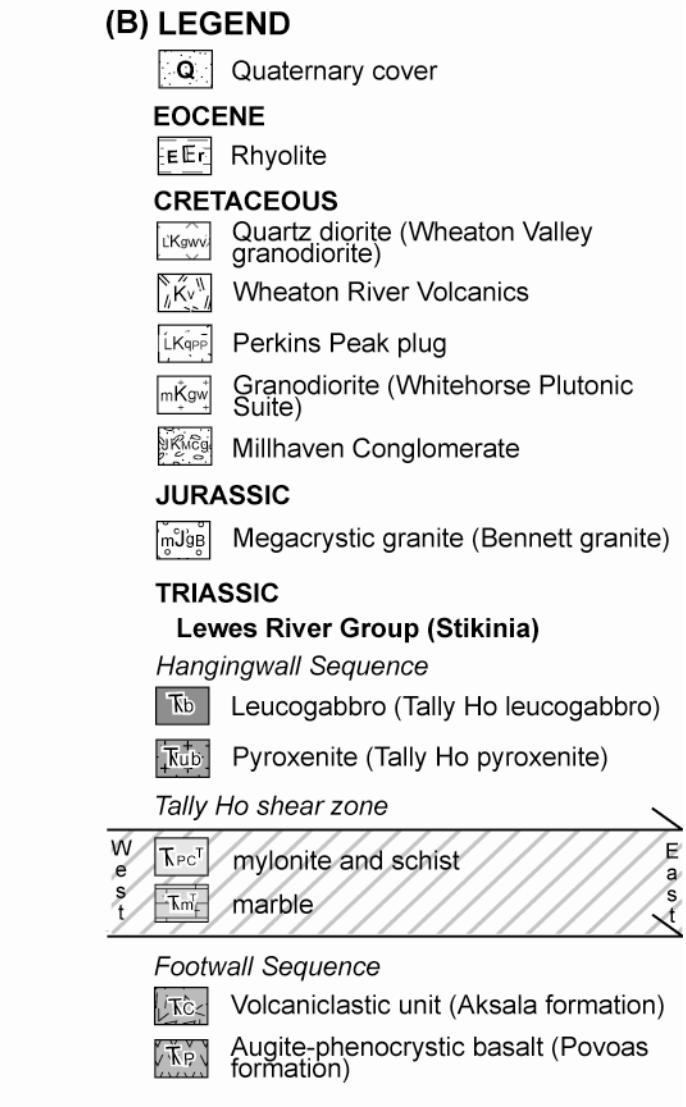
(B) LEGEND
Q
Quaternary cover
EOCENE
Er
Rhyolite
CRETACEOUS
Kgwv
Quartz diorite (Wheaton Valley granodiorite)
Kv
Wheaton River Volcanics
Kqpp
Perkins Peak plug
mKgw
Granodiorite (Whitehorse Plutonic Suite)
Kmcg
Millhaven Conglomerate
JURASSIC
mJgB
Megacrystic granite (Bennett granite)
TRIASSIC
Lewes River Group (Stikinia)
Hangingwall Sequence
Tkb
Leucogabbro (Tally Ho leucogabbro)
Tkub
Pyroxenite (Tally Ho pyroxenite)
Tally Ho shear zone
West
East
TkPC
mylonite and schist
Tkm
marble
Footwall Sequence
Tkc
Volcaniclastic unit (Aksala formation)
TkP
Augite-phenocrystic basalt (Povoas formation)

- examine the significance of the THSZ in a regional plate-tectonic framework; and,
- provide constraints on the amount of continental growth accomplished by oceanic terranes during Cordilleran orogenesis.

The thesis is presented in two papers with an accompanying 1:30,000 geological map (Appendix I). The first paper, Chapter 2, entitled "Arc imbrication during thick-skinned collision within the northern Cordilleran accretionary orogen, Yukon, Canada" was co-authored with Dr. Stephen Johnston (University of Victoria) and geochronologist Dr. Larry Heaman (University of Alberta). Chapter 2 focuses on the mapping and structural geology of the THSZ and places tight geochronological constraints on the timing of deformation along the shear zone. A model for the formation of the THSZ is presented.

Chapter 3, entitled "Geochemical and isotopic constraints on magmatic rocks along the western margin of Stikinia: implications for Mesozoic crustal growth in the Canadian Cordillera", was co-authored with Dr. Stephen Johnston and benefitted from the Sm-Nd isotopic analyses by Robert Creaser (University of Alberta). Chapter 3 focuses on the geochemical character and tectonic affinity of magmatic rocks in Stikinia using whole rock and trace element geochemistry and Sm-Nd isotopic ratios. The model put forth in Chapter 2 is re-examined using these geochemical constraints and the implications for crustal growth in the Canadian Cordillera are discussed.

Methodologies

The THSZ is located within NTS map sheets 105 D/2, 105 D/3 and 105 D/6 in southern Yukon with access granted via helicopter or 4WD vehicle from the Annie Lake Road. Field work along the THSZ was undertaken in June, July and August of 2004 with the aid of Dr. Stephen Johnston and the assistance of Derek Turner. Further guidance throughout the field season was provided by geologists at the Yukon Geological Survey. Mapping was performed at 1:30,000 scale from several different base camps with careful attention to shear zone kinematic indicators and contact relationships. A number of orientated samples were taken for micro-structural analysis. Previous 1:50,000 scale mapping by Hart & Radloff (1990) was utilized in the final compilation of the geological map (Appendix I).

Bulk samples of several intrusive units were taken for U-Pb isotopic analysis. Of those, only two were analysed. I undertook the geochronological analyses at the University of Alberta Radiogenic Isotope Facility under the guidance of Dr. Larry Heaman. Procedures for sample preparation follow that of Heaman & Parrish (1991). Additional samples were selected for whole rock and trace element geochemistry with a sub-set also analysed for Sm-Nd isotopic systematic at the Radiogenic Isotope Facility. A number of geochemical samples used in this study were analysed and described by Turner (2005), a project which was undertaken in tandem with this study.

REFERENCES CITED

Albarede, F. 1998. The growth of continental crust. *Tectonophysics*, **296**, 1-14.

Ben-Avraham, Z., Nur, A., Jones, D., & Cox, A. 1981. Continental accretion: from oceanic plateaus to allochthonous terranes. *Science*, **213**, 47-54.

Colpron, M., Nelson, J.L., & Murphy, D.C. 2006. A tectonostratigraphic framework for the pericratonic terranes of the northern Cordillera. *In:* Colpron, M., & Nelson, J.L. (eds) Paleozoic Evolution and Metallogeny of Pericratonic Terranes at the Ancient Pacific Margin of North America, Canadian and Alaskan Cordillera, Special Paper **45**, Geological Association of Canada, 1-23.

Cook, F.A., Clowes, R.M., Snyder, D.B., van der Velden, A.J., Hall, K.W., Erdmer, P., & Evenchick, C.A. 2004. Precambrian crust beneath the Mesozoic northern Canadian Cordillera discovered by Lithoprobe seismic reflection profiling. *Tectonics*, **23**, TC2010.

Currie, L., & Parrish, R.R. 1993. Jurassic accretion of Nisling terrane along the western margin of Stikinia, Coast Mountains, northwestern British Columbia. *Geology*, **21**, 235-238.

Dostal, J., Gale, V. & Church, B. 1999. Upper Triassic Takla Group volcanic rocks, Stikine Terrane, north-central British Columbia: geochemistry, petrogenesis, and tectonic implications. *Canadian Journal of Earth Sciences*, **36**, 1483-1494.

Erdmer, P., Moore, J.M., Heaman, L., Thompson, R.I., Daughtry, K.L. & Creaser, R.A. 2002. Extending the ancient margin outboard in the Canadian Cordillera: a record of Proterozoic crust and Paleocene regional metamorphism in the Nicola horst, southern British Columbia. *Canadian Journal of Earth Sciences*, **39**, 1605-1623.

Hart, C.J.R., & Radloff, J.K. 1990. Geology of Whitehorse, Alligator Lake, Fenwick Creek, Carcross and part of Robinson map areas (105D/11, 6, 3, 2, & 7), Open File 1990-4. Indian and Northern Affairs Canada, Whitehorse, 113 p.

Heaman, L. & Parrish, R.R. 1991. U-Pb geochronology of accessory minerals. *In*: Heaman, L. & Ludden, J.N. (eds) Applications of radiogenic isotope systems to problems in geology; short course handbook. Mineralogical Association of Canada, 59-102.

Jackson, J.L., Gehrels, G.E., Patchett, J.P., & Mihalynuk, M.G. 1991. Stratigraphic and isotopic link between the northern Stikine terrane and an ancient continental margin assemblage, Canadian Cordillera. *Geology*, **19**, 1177-1180.

Johnston, S.T. 2001. The Great Alaskan Terrane Wreck: Reconciliation of paleomagnetic and geological data in the northern Cordillera. *Earth and Planetary Science Letters*, **193**, 259-272.

Johnston, S.T., & Canil, D. 2007. Crustal structure of southwest Yukon, northern Cordillera: Implications for crustal growth in a convergent margin orogen. *Tectonics*, **26**, TC1006.

McClelland, W.C., Tikoff, B., & Manduca, C.A. 2000. Two-phase evolution of accretionary margins: examples from the North American Cordillera. *Tectonophysics*, **326**, 37-55.

Monger, J. W. H., Wheeler, J.O., Tipper, H.W., Gabrielse, H., Harms, T., Struik, L.C., Campbell, R.B., Dodds, C.J., Gehrels, G.E., & O'Brien, J. 1991. Upper Devonian to Middle Jurassic assemblages – Part B. Cordilleran terranes. *In*: Gabrielse, H., and Yorath, C.J. (eds) Geology of the Cordilleran Orogen in Canada: The Geology of North America: Denver, Colorado, Geological Society of America, p. 281-327.

Patchett, P.J., & Chase, C.G. 2002. Role of transform continent margins in major crustal growth episodes. *Geology*, **30**, 39-42.

Samson, S., McClelland, W.C., Patchett, P.J., Gehrels, G.E. & Anderson, R.G. 1989. Evidence from neodymium isotopes for mantle contributions to Phanerozoic crustal genesis in the Canadian Cordillera. *Nature,* **337**, 705-709.

Sengor, A.M.C., & Natalin, B.A. 1996. Turkic-type orogeny and its role in the making of the continental crust. *Annual Review of Earth and Planetary Sciences*, **24**, 263-337.

Snyder, D.B., Clowes, R.M., Cook, F.A., Erdmer, P., Evenchick, C.A., van der Velden, A.J., & Hall, K.W. 2002. Proterozoic prism arrests suspect terranes: Insights into the ancient Cordilleran margin from seismic reflection data. *GSA Today*, **12**, 4-10.

Turner, D. 2005. Geochemical and Petrological Analysis of the Tally Ho Shear Zone and Takhini Deformation Zone, South Central Yukon. Unpublished B.Sc. thesis, University of Victoria, 67p.

CHAPTER 2

Arc imbrication during thick-skinned collision within the northern Cordilleran accretionary orogen, Yukon, Canada

A.M. Tizzard & S. T. Johnston, School of Earth and Ocean Sciences, University of Victoria, PO Box 3055 STN CSC, Victoria, British Columbia, Canada V8W 3P6 stj@uvic.ca

L.M. Heaman, Department of Earth and Atmospheric Sciences, University of Alberta, Edmonton, Alberta, Canada T6G 2E3

Abstract

We present the results of geological mapping and geochronological studies of the Tally Ho shear zone (THSZ) and adjacent rocks. The shear zone crops out near the west margin of Stikinia, an oceanic arc and the largest of the accreted terranes within the Cordilleran orogen of western North America. The hangingwall of the largely flat-lying shear zone consists of coarsely crystalline leucogabbro and cumulate pyroxenite interpreted as the lower crustal and possibly lithospheric mantle roots of a magmatic arc. Rocks in the footwall consist of volcanic and volcaniclastic sequences of the Lewes River Arc, a Late Triassic magmatic arc characteristic of Stikinia. Because the shear zone places lower crustal plutonic rocks over a supracrustal sequence, we interpret it as a crustal scale thrust fault. Kinematic indicators imply top-to-the-east displacement across the shear zone. The geometry of folds of the shear zone is consistent with deformation in response to displacement over ramps in deeper seated thrust faults kinematically linked to the THSZ. Crystallization of the hangingwall leucogabbro at 208 ± 4.3 Ma provides a maximum age constraint for deformation, while a post-kinematic granitoid pluton that plugs the shear zone, and which crystallized at about 173 Ma provides a lower age limit. The THSZ is, therefore, coeval with (1) a series of latest Triassic – Early Jurassic shear and fault zones that characterize the length of the west margin of Stikinia; (2) the termination of isotopically juvenile arc magmatism of the Lewes River Arc; (3) crustal loading of Stikinia giving rise to a foreland basin that rapidly filled with westerly-derived orogenic molasse that includes clasts of ultra-high pressure metamorphic rocks; and (4) juxtaposition of Stikinia against continental crust of the Nisling Assemblage of the Yukon-Tanana Terrane to the west. These constraints are consistent with a model of

deformation in response to the entry of the continental Nisling Assemblage into the trench of the west facing Lewes River Arc, terminating subduction and imbricating the arc along a series of east-verging thrust faults, including the THSZ.

INTRODUCTION

The Canadian Cordillera Orogen, consisting of a mosaic of oceanic and pericratonic terranes, has developed in the absence of any terminal continental collision and is considered to be a classic accretionary orogen. As such, the Cordillera provides us with an opportunity to determine the processes involved in the development of accretionary orogens, and to better understand the role of crustal scale structures therein. Delineating and distinguishing between terrane bounding faults and structures internal to a terrane can, however, be complicated. It is rarely clear where one terrane ends and another begins, especially where similar oceanic or arc terranes have been juxtaposed. Post-accretionary dispersion of terranes by margin-parallel translations can "shuffle the deck", and syn- to post-accretionary magmatism commonly obscures both structure and stratigraphy. Nonetheless, understanding how strain is partitioned between and within accreting crustal blocks provides a first order constraint on the tectonic processes responsible for accretionary orogens.

In the northern Canadian Cordillera the Tally Ho shear zone (THSZ) crops out near the northwestern margin of Stikinia, a large accreted oceanic arc terrane (Fig. 2.1) (Hart & Radloff 1990; Tizzard & Johnston 2005). The THSZ is a 40-kilometre long, northwest-striking package of highly-strained rocks just north of the Yukon-British Columbia border. West of the THSZ is the pericratonic Nisling Assemblage of the Yukon-Tanana Terrane (Fig. 2.2) (Mortensen 1992). To the north the THSZ is covered by Neogene basalt flows, and to the south it is truncated by younger intrusive rocks. The tectonic location of the THSZ near the western margin of an accreted terrane (Stikinia) offers an example of a terrane-marginal structure and may therefore provide insight into

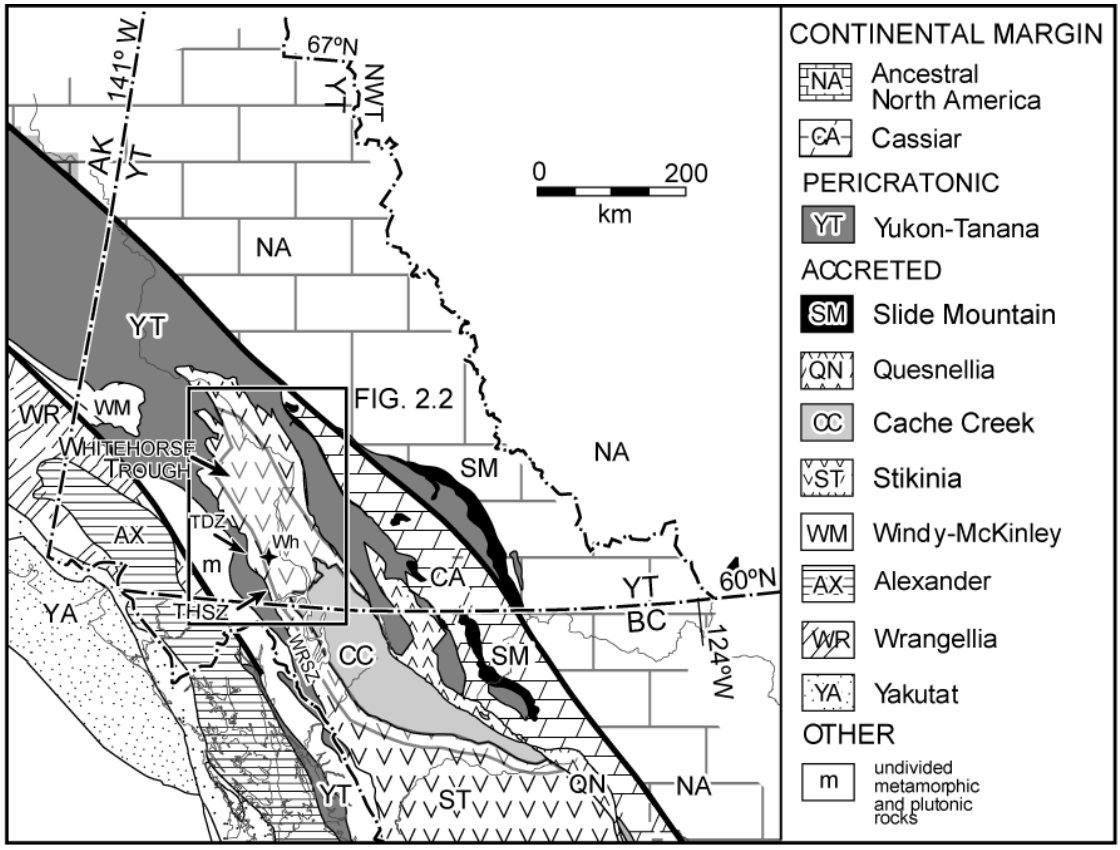

Figure 2.1. Simplified terrane map of the northern Canadian Cordillera (modified after Colpron *et al*. 2006). THSZ, Tally Ho shear zone; TDZ, Takhini deformation zone; WRSZ, Wann River shear zone; Wh, Whitehorse.

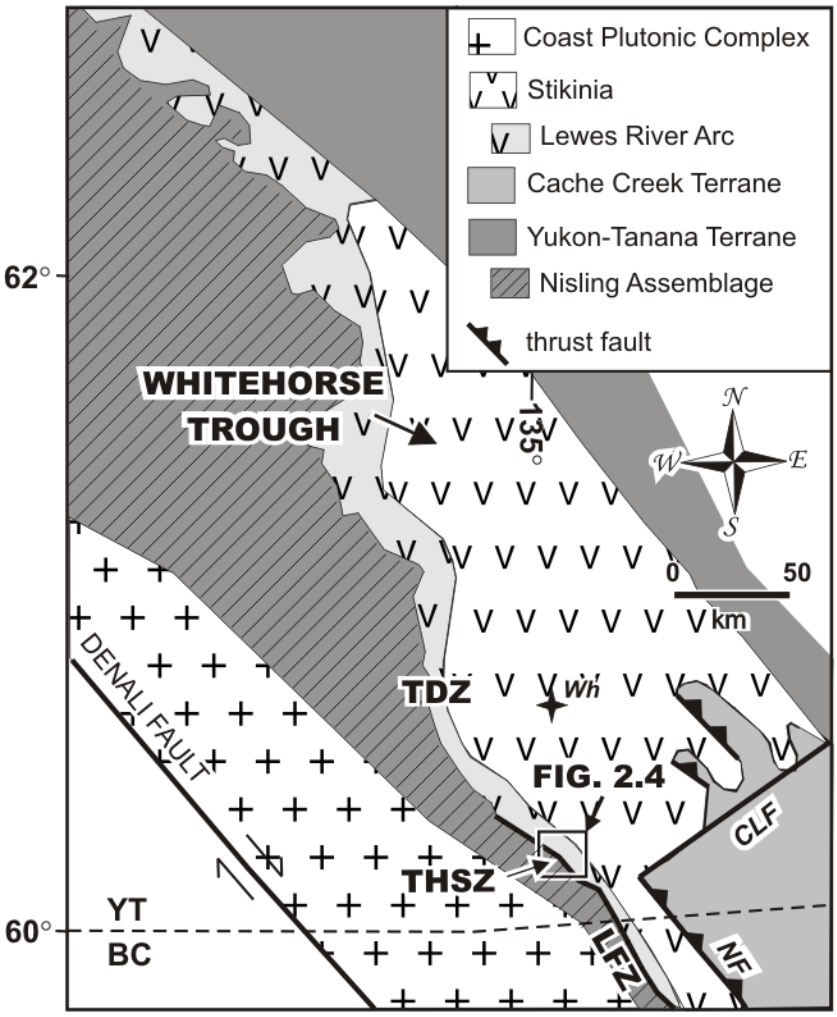

Figure 2.2. Simplified tectonic map of central southern Yukon showing location of mapping done in this study. THSZ, Tally Ho shear zone; TDZ, Takhini deformation zone; LFZ, Llewellyn fault zone; NF, Nahlin fault; CLF, Crag Lake fault; Wh, Whitehorse. Modified from Hart (1997).

the lithospheric-scale geometry of terranes and the nature of deformation along their bounding structures. Characterizing the structural style of the THSZ and applying geochronological constraints on the timing of deformation should aid in developing an accretionary history for part of the northern Canadian Cordillera. For example, is the THSZ the structure along which the oceanic Stikinia and continental Nisling Assemblage were juxtaposed? Alternatively, is the THSZ a secondary structure developed during collision, or is it a post-collisional or reactivated feature? Answering these questions may aid in improving our general understanding of terrane bounding structures.

This paper reports the results of detailed geologic mapping and U-Pb geochronology of the THSZ, and aims to: (1) establish the geometry and kinematics of the high-strain zone; (2) constrain the timing of deformation; (3) compare the THSZ to other structures along the northwestern margin of Stikinia; and (4) examine the significance of the THSZ in a regional context. We first describe Stikinia and the Nisling Assemblage and introduce the main structures along and adjacent to the boundary between these terranes. We then describe the lithologies and structures within and adjacent to the THSZ. Lastly we provide geochronological constraints on the deformation in the THSZ. A tectonic model for the evolution of the western margin of Stikinia is presented.

REGIONAL GEOLOGY

Stikinia

In Yukon, western Stikinia consists of the Upper Paleozoic Takhini Assemblage and the Upper Triassic to Lower Jurassic Lewes River and Laberge groups of the Whitehorse Trough (Fig. 2.3) (Hart 1997). The Takhini Assemblage consists of variably deformed and metamorphosed mafic volcanic rocks and minor felsic and sedimentary rocks. The Lewes River Group consists of a lower volcanic succession – the Povoas Formation, and an upper sedimentary succession – the Aksala Formation. In northern British Columbia the Stuhini Formation is correlative with the Povoas Formation and together they form the Lewes River Arc (Hart 1997). The Whitehorse Trough is an Upper Triassic to Middle Jurassic arc-marginal basin (Eisbacher 1981) in which volcanic and sedimentary rock of the Aksala Formation and Laberge Group accumulated. Based on detailed stratigraphy of the Laberge Group, Dickie & Hein (1995) interpreted the Whitehorse Trough as an east-facing (present day coordinates) fore-arc basin that developed above a west-dipping subduction zone. As we demonstrate below, the trough is a composite basin with a much more complicated history than previously envisaged.

The northwest margin of Stikinia is characterized by a series of high strain, shear and fault zones. These include, from north to south, the Takhini deformation zone, the THSZ (the subject of this paper), the Llewellyn fault zone, and the Wann River shear zone (Figs. 2.1, 2.2). The Takhini deformation zone lies 60 kilometres along strike to the northwest of the THSZ and consists of variably strained schist and phyllite with minor tuff, rhyolite, marble and greenstone of the Mississippian Takhini Assemblage. The deformation zone is intruded by unstrained granitic rocks of the Jurassic and Cretaceous

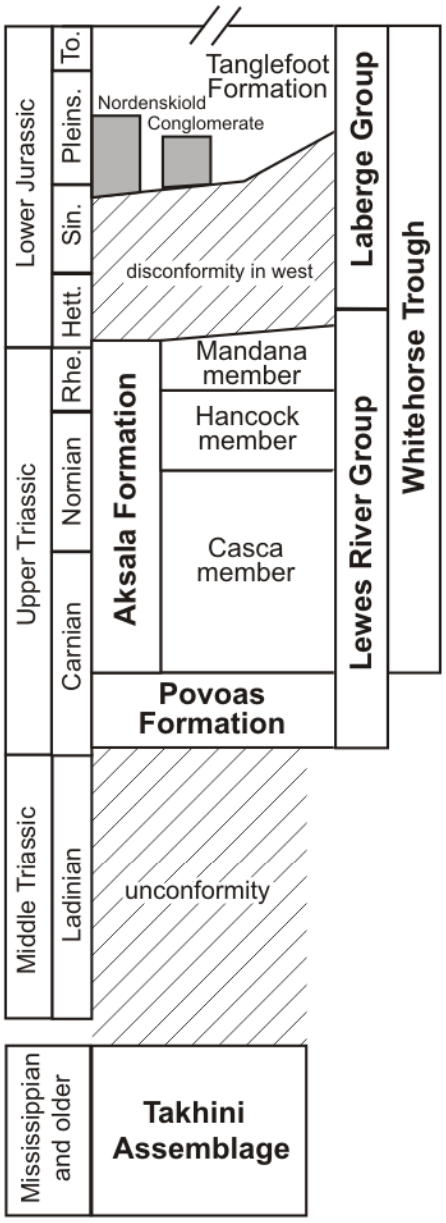

Figure 2.3. Stratigraphy of the western margin of Stikinia in southern Yukon. Names discussed in text are in bold. Modified from Hart (1997).

Little River (183 ± 2 Ma) and Annie Ned batholiths, respectively (Hart 1997). The Llewellyn fault zone is a northwest-striking brittle to brittle-ductile dextral strike-slip to dip-slip fault system that parallels the THSZ in southern Yukon and extends southeastwards into northern British Columbia (Hart & Radloff 1990) (Fig. 2.2). The Llewellyn fault zone in southern Yukon records dextral movement and is located along the eastern margin of the THSZ. The fault zone affects rocks as young as Eocene, although it may be in part a reactivation of an older fault zone (Mihalynuk & Rouse 1988). The Wann River shear zone is subvertical to subhorizontal, varies in strike from east-west to north-south, places Nisling Assemblage schist over Stikinia, and was active between 185 Ma (the crystallization age of a deformed pluton adjacent to the shear zone) and ~170 Ma U-Pb (cooling ages on titanite and rutile) (Currie & Parrish 1993).

Nisling Assemblage

Rocks of the Nisling Assemblage occur as pendants and blocks within the Coast Plutonic Complex, west of the THSZ and Takhini assemblage (Fig. 2.2) (Hart & Radloff 1990; Hart 1997). The Nisling Assemblage consists of regionally deformed and metamorphosed Paleozoic mica-quartz-feldspar schist, quartzite, marble and orthogneiss and is interpreted as part of the Yukon-Tanana Terrane, a pericratonic continental assemblage (Gehrels *et al*. 1990; Hart & Radloff 1990; Mortensen 1992). A U-Pb zircon age determination of meta-igneous rocks sampled along-strike 100 km to the north within the correlative Aishihik metamorphic suite provides a Mississippian age constraint for the Nisling Assemblage (Johnston *et al.* 1996).

LITHOLOGICAL UNITS

The map-area is divisible into three structural sequences; a high-strain central sequence (the THSZ) separates little strained rocks of an overlying hangingwall sheet from an underlying footwall sequence. A layered sequence of variably deformed gabbro and pyroxenite forms the hangingwall of the THSZ. The THSZ consists of mylonitic to schistose rocks, metabasalt, and minor marble. Rock units in the footwall are variably deformed and include augite-phenocrystic basalt, volcaniclastic, and sedimentary rocks. Megacrystic granite, granodiorite, quartz-diorite and numerous sub-volcanic rhyolite dykes are in intrusive- or fault-contact with the hangingwall, THSZ, and footwall rocks (Fig. 2.4).

Hangingwall Lithological Units

Leucogabbro

The leucogabbro unit consists of leucogabbro with rare lenses of pyroxenite (Fig. 2.5). The leucogabbro is medium- to coarse-grained and consists of plagioclase, amphibole, clinopyroxene and quartz with minor accessory magnetite. The occurrence of chlorite and amphibole replacing pyroxene suggests that the gabbro has been metamorphosed to at least greenschist facies. Chlorite and sericite alteration is common. The leucogabbro is weakly- to well-foliated and weakly- to non-lineated. The foliation planes are variably anastamosing and are defined by the preferential orientation of amphibole and pyroxene. Locally, elongate pyroxene-amphibole aggregates that lie in the foliation plane define a stretching lineation.

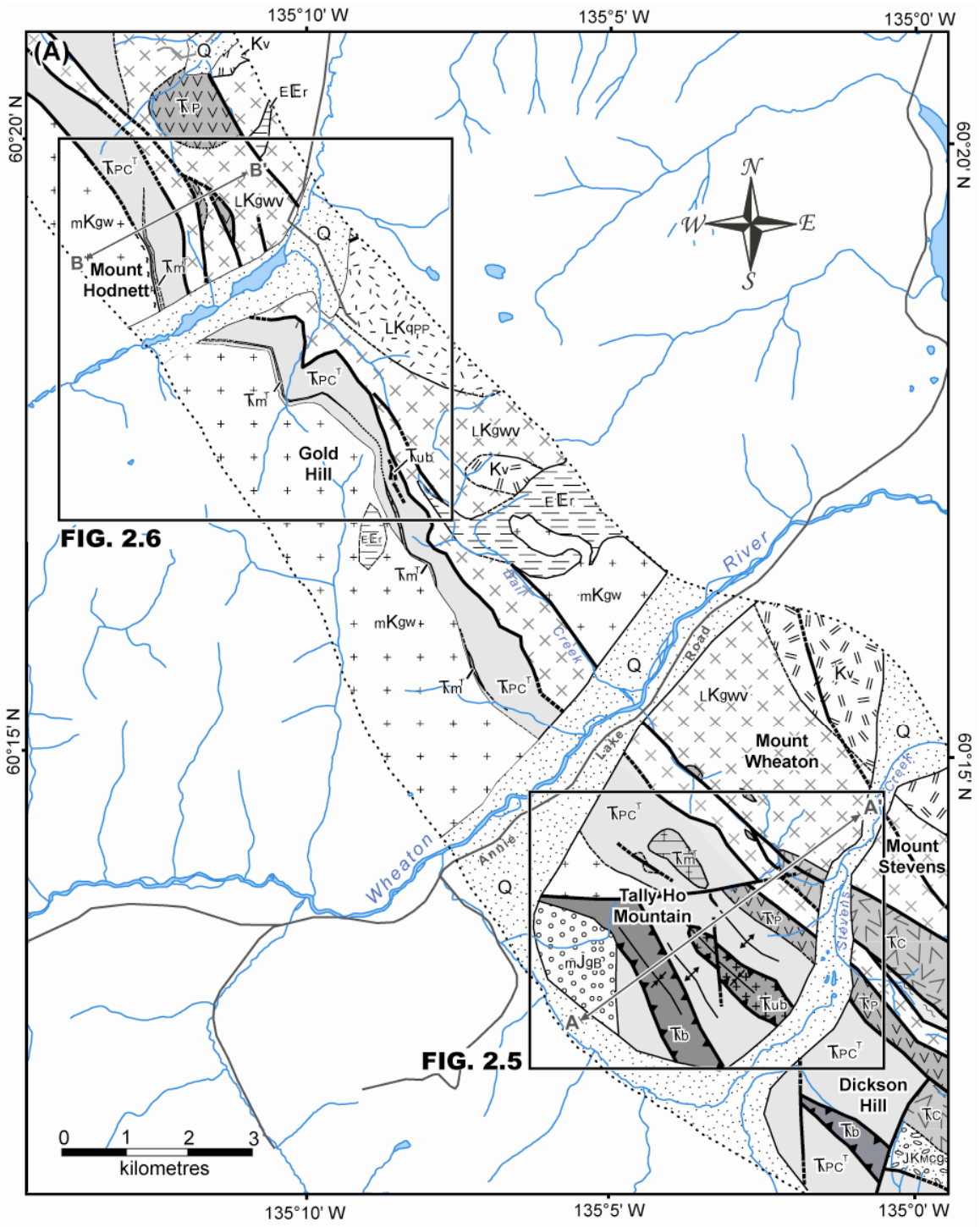

Figure 2.4. (A) Simplified geological map of the Tally Ho shear zone, southern Yukon Territory. (B) Legend for Figs. 2.4, 2.5 and 2.6. Names in parenthesis refer to unit names of Hart and Radloff (1990).

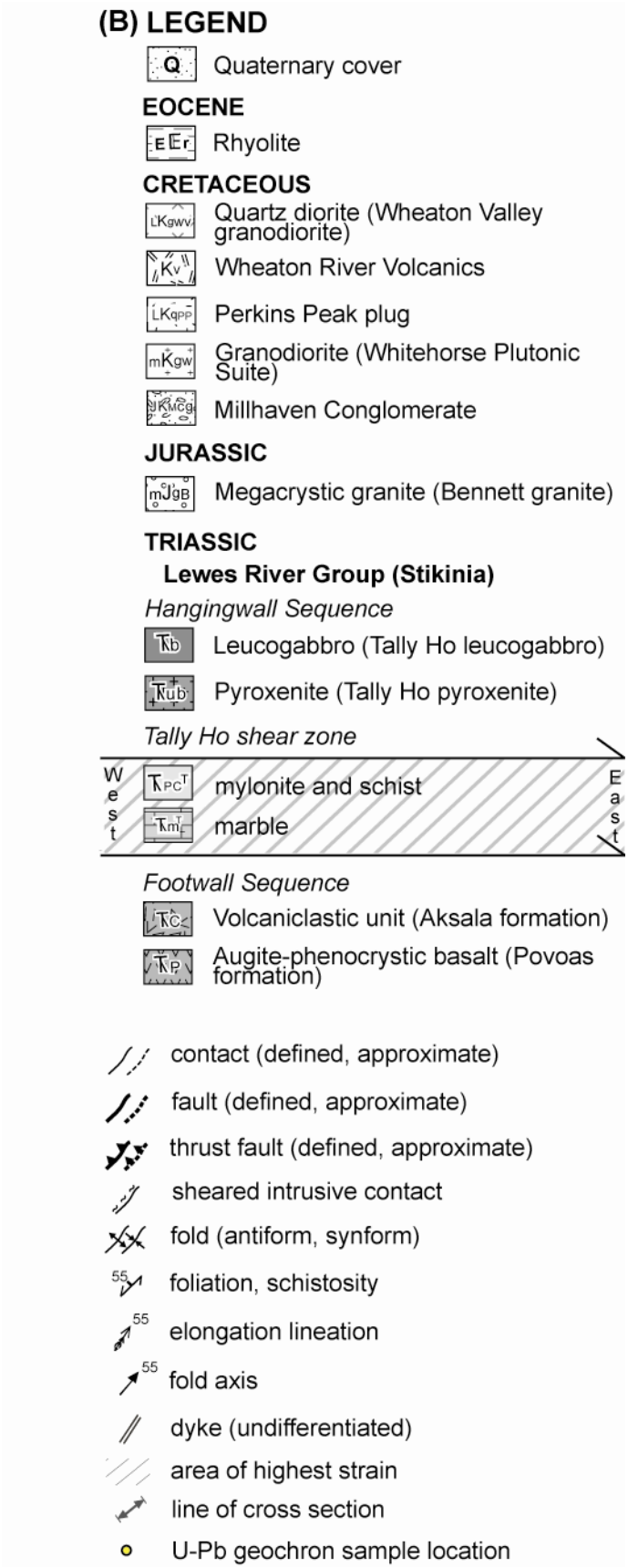
(B) LEGEND
Q
Quaternary cover
EOCENE
Er
Rhyolite
CRETACEOUS
Quartz diorite (Wheaton Valley granodiorite)
Kv
Wheaton River Volcanics
Perkins Peak plug
Granodiorite (Whitehorse Plutonic Suite)
Millhaven Conglomerate
JURASSIC
Megacrystic granite (Bennett granite)
TRIASSIC
Lewes River Group (Stikinia)
Hangingwall Sequence
Leucogabbro (Tally Ho leucogabbro)
Pyroxenite (Tally Ho pyroxenite)
Tally Ho shear zone
West
East
mylonite and schist
marble
Footwall Sequence
Volcaniclastic unit (Aksala formation)
Augite-phenocrystic basalt (Povoas formation)
contact (defined, approximate)
fault (defined, approximate)
thrust fault (defined, approximate)
sheared intrusive contact
fold (antiform, synform)
foliation, schistosity
elongation lineation
fold axis
dyke (undifferentiated)
area of highest strain
line of cross section
U-Pb geochron sample location

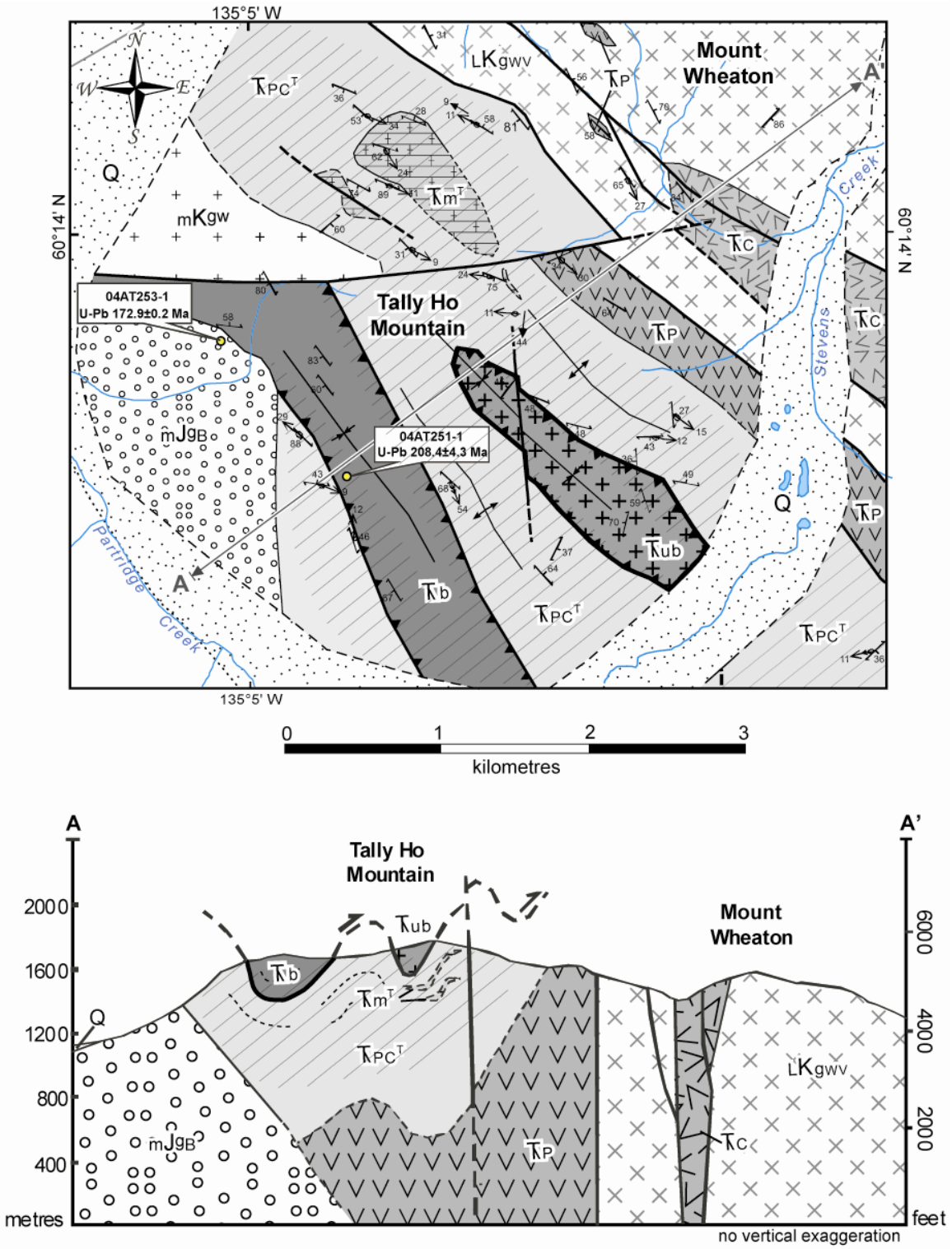

Figure 2.5. Geological map and cross-section of the Tally Ho shear zone showing locations of U-Pb zircon geochron samples in this study. Legend as in Figure 2.4(B).

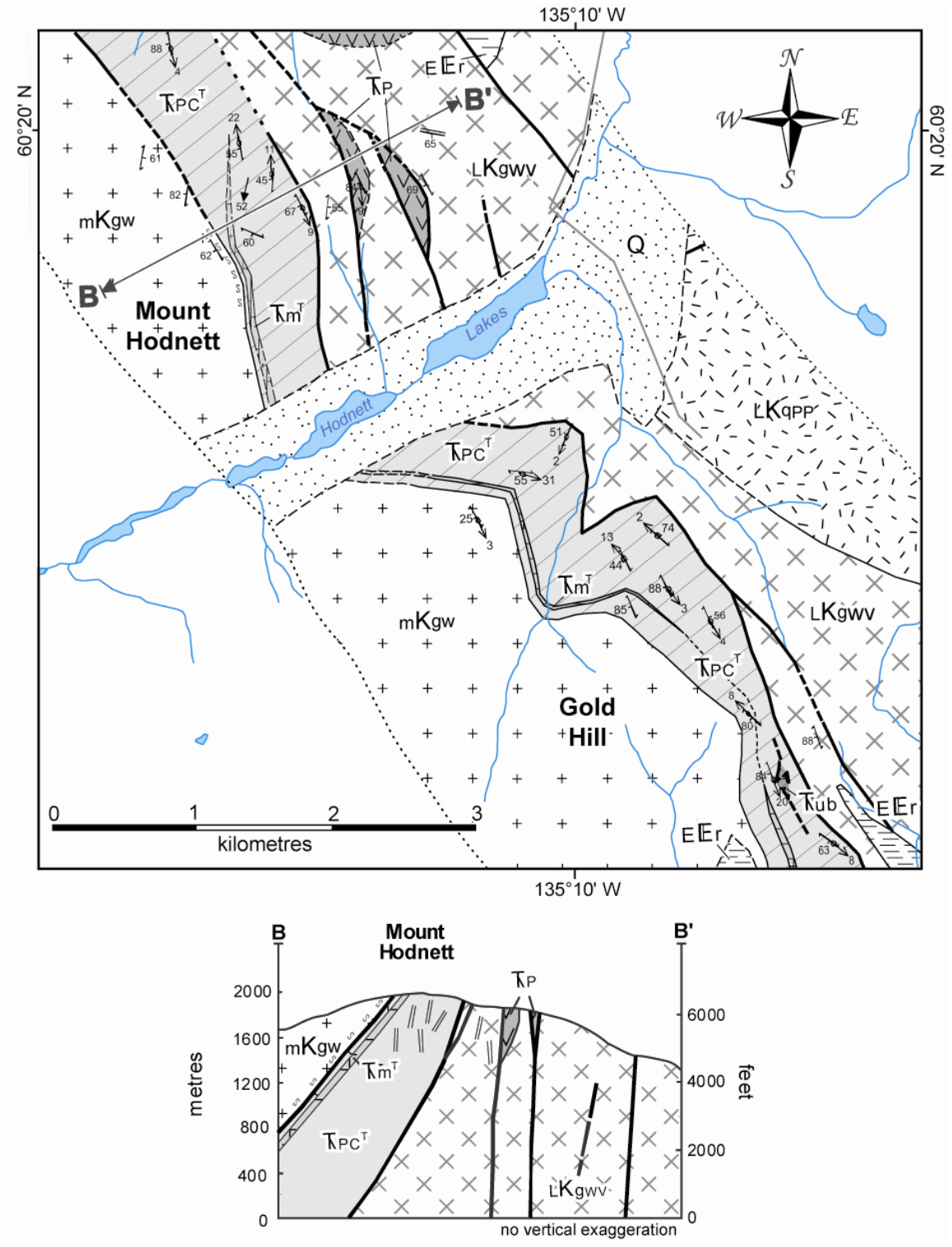

Figure 2.6. Geological map and cross-section of the Mount Hodnett and Gold Hill areas, Tally Ho shear zone. Legend as in Figure 4(B).

Lenses of pyroxenite up to one metre long have irregular and diffuse boundaries (Fig. 2.7a), are interpreted to be the result of magmatic processes, and therefore provide a temporal link between the leucogabbro and pyroxenite units (described below). A sharp contact exists between the leucogabbro and a megacrystic granite, with xenoliths of gabbro found in the megacrystic granite (Fig. 2.7b). The gabbro is, therefore, older than and has been intruded by the megacrystic granite. A contact with augite-porphyroclastic schist of the THSZ structural unit is covered. The contact is, however, interpreted as gradational; within 50 metres of the contact the leucogabbro is characterized by a weak foliation that increases in intensity toward the contact with the THSZ. The increasing strain toward the contact implies that the leucogabbro was caught up in the deformation that gave rise to the THSZ. The leucogabbro unit in the map area is lithologically similar to and continuous with the Tally Ho leucogabbro (Hart & Radloff 1990). A U-Pb zircon age date of 215 ± 1 Ma for the Tally Ho leucogabbro indicates crystallization in the Late Triassic (Hart *et al*. 1995).

Pyroxenite

The pyroxenite unit consists of black to dark green pyroxenite and outcrops along a blocky ridgeline on top of Tally Ho Mountain and near Gold Hill (Figs. 2.5, 2.6). The pyroxenite is medium to coarse-grained and dominantly consists of clinopyroxene with minor amounts of orthopyroxene, olivine and opaque minerals. Serpentine-rich layers 5-10 centimetres thick in the pyroxenite are interpreted as primary olivine-rich cumulate in which serpentine has subsequently replaced olivine. The presence of serpentine and chlorite indicate that the pyroxenite has been metamorphosed to at least greenschist facies.

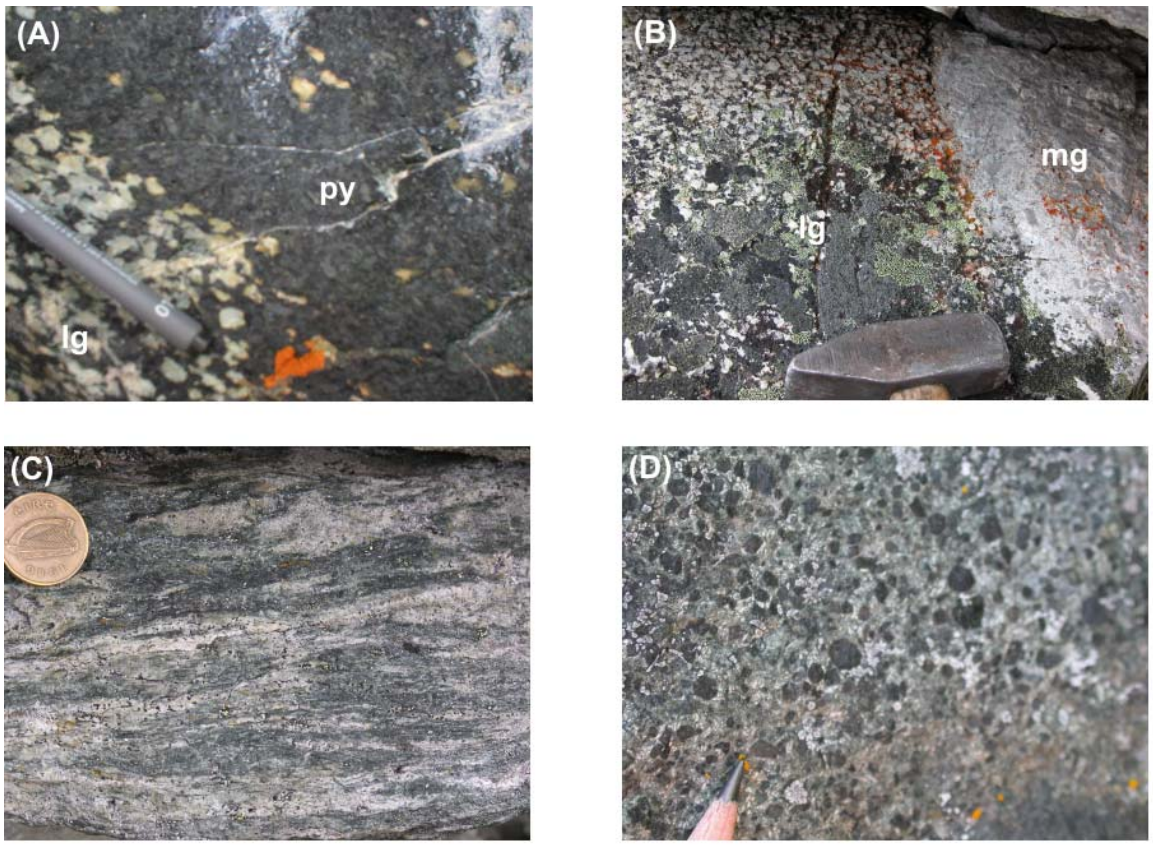

Figure 2.7. (A) pyroxenite lense (py) in leucogabbro (lg) on Dickson Hill; (B) intrusive contact between the leucogabbro (lg) and megacrystic granite (mg) on Tally Ho Mountain; (C) sheared pyroxenite near contact with THSZ on Tally Ho Mountain; (D) augite phenocrysts in undeformed augite-phenocrystic basalt adjacent to the Tally Ho shear zone on Dickson Hill.

The pyroxenite is massive to well-foliated with foliation planes defined by the preferential orientation of pyroxene and chlorite. Lineations are poorly developed. To the west, the contact of the pyroxenite with the leucogabbro is covered. Lenses of pyroxenite in the leucogabbro are inferred to indicate that the units are coeval. To the east the pyroxenite is increasingly strained and forms a gradational contact with mylonite of the THSZ structural unit (Fig. 2.7c). The transition zone from highly-strained pyroxenite to rocks of the THSZ varies in width from one to 50 centimetres.

The leucogabbro and pyroxenite are interpreted as being a coeval, cumulate-style magmatic body based on the presence of large pyroxenite lenses in the leucogabbro unit. Cumulate processes in the pyroxenite are also indicated by serpentinized cumulate olivine layers. The coarse crystallinity and petrology of the pyroxenite and leucogabbro units are consistant with their having originated within the deep crust and potentially lithospheric mantle part of an arc system (Hamilton 1988); hence the pyroxenite and leucogabbro units are interpreted as part of the roots of a volcanic arc, probably the Lewes River.

Footwall Lithological Units

Augite-phenocrystic basalt

East of the THSZ is a massive augite-phenocrystic to aphyric basalt unit (Fig. 2.4). The basalt consists of clinopyroxene, plagioclase and minor orthopyroxene and amphibole. Augite phenocrysts are up to 10 mm in diameter and the aphanitic matrix is variably epidotized, choloritized and sericitized (Fig. 2.7d). A granodiorite pluton

intrudes the basalt in the northern map area. Elsewhere, brittle faults form the contact between the basalt and granodiorite. To the west, the basalt becomes progressively strained over several hundred metres, forming a gradational contact with metabasaltic mylonite and schist of the THSZ. The augite-phenocrystic basalt unit is lithologically similar to and locally contiguous with basalt mapped as the Upper Triassic Povoas Formation (Hart & Radloff 1990).

Volcaniclastic unit

The volcaniclastic unit includes tuff, agglomerate, greywacke, pebble conglomerate and minor shale. The dominant lithology is fine- to coarse-grained tuff that contains both crystal and lithic fragments. Crystal fragments of plagioclase and pyroxene are common; lithic fragments are angular to sub-angular, up to cobble-size, and are dominantly fine-grained and mafic in composition. Epidote, chlorite and sericite are common alteration minerals, and characterize the volcaniclastic rocks adjacent to northwest-striking brittle faults. The volcaniclastic unit is well-bedded to moderately-well foliated with foliation planes defined by an anastomosing cleavage. On Mount Wheaton, xenoliths that are of a similar composition to the volcaniclastic unit are found in quartz diorite (Fig. 2.5). The volcaniclastic unit is therefore interpreted to be older than and has been intruded by quartz diorite. Elsewhere younger brittle faults juxtapose the volcaniclastic unit against quartz diorite and schist of the THSZ.

The volcaniclastic unit is lithologically similar to and locally continuous with the Upper Triassic Casca member of the Aksala formation (Hart & Radloff 1990) (Fig. 2.3).

The volcaniclastic and augite-porphyritic basalt units in the footwall of the THSZ are therefore interpreted as a part of the supracrustal sequence of Stikinia.

Tally Ho shear zone

The THSZ is a structural unit that separates the hangingwall Tally Ho pyroxenite and leucogabbro units from the footwall augite-porphyroclastic basalt and volcaniclastic units. The THSZ is composed of mylonite and augite-porphyroclastic schist with minor phyllite, foliated metabasalt and marble. The mylonite is laminated, very fine- to fine-grained and consists of quartz, amphibole, feldspar and minor clinopyroxene, biotite and opaque minerals. The augite-porphyroclastic schist is fine- to medium-grained and consists of clinopyroxene, plagioclase and minor amphibole and opaque minerals. Augite-porhyroclasts are up to 8 mm in diameter (Fig. 2.8a). The mylonite and the augite-porphyroclastic schist are moderately epidotized, sericitized and chloritized. The abundance of chlorite in the fine-grained matrix of the mylonite and schist is interpreted to indicate that the THSZ structural unit has been metamorphosed to at least greenschist facies. To the west, the THSZ structural unit grades up-section into strained and foliated pyroxenite and leucogabbro that in turn decrease in strain away from the mylonite and augite-porphyroclastic schist over a distance of 0.5 to 50 metres. The THSZ decreases in strain over 50 meters to the east where it grades into augite-phenocrystic basalt and volcaniclastic rocks down-section into the footwall units. Locally THSZ mylonite is faulted against granodiorite along younger steeply dipping brittle faults (Fig. 2.4).

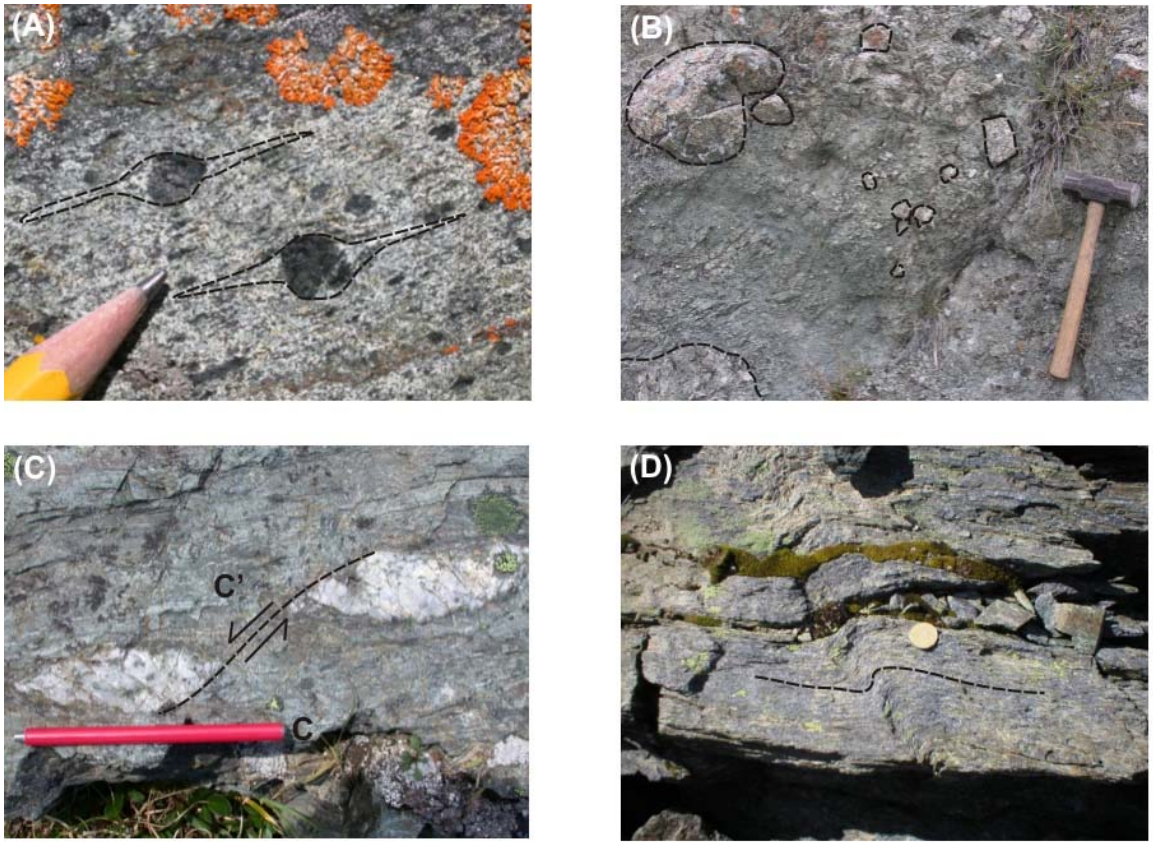

Figure 2.8. (A) rotated augite porphyroclasts in augite schist on Dickson Hill indicating a sinistral and top-to-the-east vorticity; (B) zone of fault gouge on the south face of Mount Hodnett containing clasts of the granodiorite unit. Larger clasts are outlined; (C) C' extensional shears in mylonite on Tally Ho Mountain indicating top-down and to-the-east movement; (D) east-vergent crenulations in mylonite on Gold Hill.

Younger Intrusions

Megacrystic granite unit

Four main intrusive units that cross-cut and therefore post-date the THSZ are recognized and include, from west to east (Fig. 2.4): a megacrystic granite, a granodiorite, a quartz-diorite, and a sub-volcanic rhyolite. The megacrystic granite is leucocratic, coarse-grained, and massive, and consists of quartz, plagioclase, orthoclase and minor biotite, hornblende and magnetite; alkali-feldspar megacrysts are up to two centimeters long. Sericite and chlorite alteration is locally evident, but not pervasive. Xenoliths in the megacrystic granite of a medium-grained gabbro and a sharp contact with the leucogabbro unit indicate that the megacrystic granite is younger than and intruded the leucogabbro (Fig. 2.7b). West of the map area the megacrystic granite intrudes rocks of the Nisling Assemblage of the Yukon-Tanana Terrane (Hart & Radloff 1990). The megacrystic granite unit is lithologically similar to and locally continuous with the Bennett granite (Hart & Pelletier 1989).

Granodiorite unit

Medium to coarse-grained leucocratic granodiorite consists of quartz, plagioclase and minor orthoclase and biotite ‘books’ up to 8 millimetres in diameter. Epidote, chlorite and sericite alteration is locally developed, although not pervasively. A foliation in the granodiorite, defined by an anastomosing cleavage, is present adjacent to and is associated with a fault that juxtaposes the granodiorite against the THSZ on Mount Hodnett (Figs. 2.5, 2.8b). Fine-grained and foliated xenoliths up to 50 centimeters in

width that are texturally similar to and interpreted as mylonitic rocks of the THSZ are found within the granodiorite in the Gold Hill area. The granodiorite unit is lithologically similar to and locally continuous with granodiorite of the Whitehorse plutonic suite (Hart & Radloff 1990). A U-Pb zircon age date of 119 Ma from Whitehorse plutonic suite granodiorite (Doherty & Hart 1988) is interpreted as the age of crystallization of the granodiorite unit.

Quartz diorite unit

The quartz diorite unit underlies much of the eastern portion of the map area (Fig. 2.4). Leucocratic quartz diorite is the most common lithology in this unit; granodiorite is a minor phase. The quartz diorite is coarse-grained and massive and consists of quartz, plagioclase, and minor orthoclase, hornblende and, less commonly, biotite. Chlorite and sericite alteration is common, and is pervasive adjacent to brittle faults. Locally, the quartz-diorite unit contains fine-grained, mafic xenoliths. A foliation defined by the weak alignment of hornblende and biotite is commonly developed adjacent to northwest-striking brittle faults. To the west, the quartz-diorite unit is in fault-contact with the THSZ and augite-phenocrystic basalt unit. The quartz diorite unit in the map area is lithologically similar to and locally continuous with the Wheaton Valley granodiorite (Hart & Radloff 1990). The quartz diorite unit is interpreted to be a Late Cretaceous intrusion based on a U-Pb zircon date of 77.1 ± 0.7 Ma (Hart 1995).

Rhyolite unit

Numerous rhyolite dykes and sills cross-cut all lithologies (Fig. 2.4). The dykes and sills, previously mapped by Hart & Radloff (1990), range in composition from feldspar-porphyritic rhyolite to aphanitic rhyolite and are 0.1 metres to several metres in width. In the Gold Hill area, feldspar-porphyritic rhyolite forms a map-scale sill that plugs a northwest-striking fault. In the Mount Hodnett area rhyolite dykes are cut by a northwest-trending fault. K-Ar age determinations have been interpreted as indicating a Paleocene to Early Eocene age for the dykes (Hart 1995; Breitsprecher & Mortensen 2004).

GEOCHRONOLOGY

One sample of each of the leucogabbro and megacrystic granite units was collected in the southwestern map area for U-Pb zircon geochronology to constrain the age of the THSZ (Fig. 2.5). The leucogabbro forms the hangingwall of, and passes into mylonites of the THSZ along a gradational contact. It is therefore inferred to have crystallized prior to the formation of the THSZ. The massive unstrained megacrystic granite intrudes the leucogabbro and mylonite of the THSZ and is inferred to post-date the deformation that gave rise to the THSZ. U-Pb geochronology can therefore provide us with the maximum age of formation of the THSZ (age of crystallization of the leucogabbro) and a minimum age (age of crystallization of the granite).

Methods

U-Pb geochron samples of the leucogabbro and megacrystic granite were processed at the Radiogenic Isotope Facility at the University of Alberta. The leucogabbro sample was very coarse-grained and weakly foliated. The megacrystic granite sample was massive, coarse-grained and alkali-feldspar megacrystic. Zircon was isolated from each 15 - 25 kilogram sample using conventional Wilfley table, heavy liquid and magnetic separation techniques (Heaman & Parrish 1991). Fractions for analysis were differentiated by grouping zircons with similar sizes, shapes, colour and clarity. Geochemical procedures followed that of Heaman *et al.* (2002). Concordia diagrams were generated using Isoplot 3.00 (Ludwig 1998) and all errors are given at the 2-σ level. The mean square of weighted derivatives (MSWD) for the discordia is provided as a measure of the quality of fit of the regression line between zircon fractions. Results for the leucogabbro and megacrystic granite analyses are presented in Table 2.1.

Leucogabbro

Three fractions of zircons were isolated from the leucogabbro. Each analysed fraction consisted of 3 to 17 tan-coloured zircon fragments that had no obvious zoning or inclusions. The data points lie below the concordia curve between 215 Ma and 221 Ma and form a linear array (Fig. 2.9a). A three-point regression line through the three fractions yielded an upper intercept age of 520 ± 140 Ma and a lower intercept age of 208.4 ± 4.3 Ma (MSWD = 0.034). The lower intercept of the discordia probably

Table 2.1. U-Pb zircon results for Yukon samples 04AT251-1 (leucogabbro) and 04AT253-1 (megacrystic granite). Th concentration calculated from amount of 208Pb and 207Pb/206Pb age with a slight correction for Pb-loss in some discordant fractions. All errors quoted in this table are reported at 1 sigma. Atomic ratios were corrected for fractionation and initial common Pb (Stacey & Kramers 1975). Number in parenthesis corresponds to the number of grains analysed. z, zircon; IF, initial Frantz; NM, non-magnetic (at indicated angle of tilt on Frantz Isodynamic Separator)

Description	Weight (mg)	U (ppm)	Th (ppm)	Pb (ppm)	Th/U	TCPb (pg)	$^{206}Pb/^{204}Pb$	$^{206}Pb/^{238}U$	$^{207}Pb/^{235}U$	$^{207}Pb/^{206}Pb$	Model Ages (Ma) $^{206}Pb/^{238}U$	Model Ages (Ma) $^{207}Pb/^{235}U$	Model Ages (Ma) $^{207}Pb/^{206}Pb$	% Disc
04AT251-1														
1z, tan fragments NM@1.2A (10)	24.6	2280.7	747.3	77.3	0.328	7	16640	0.03390±4	0.23683±30	0.05066±2	214.9±0.3	215.8±0.2	225.5±0.9	4.8
2z, tan fragments NM@1.2A (17)	34.8	901.1	353.1	31.7	0.392	9	7420	0.03443±4	0.24137±33	0.05085±3	218.2±0.3	219.6±0.3	233.8±1.5	6.8
3z, tan fragments NM@1.2A (3)	16.1	1299.3	357.9	44.3	0.275	3	15404	0.03460±5	0.24288±32	0.05092±3	219.2±0.3	220.8±0.3	237.1±1.3	7.7
04AT253-1														
1z, larger colourless 3:1 prisms NM@1.8A (19)	54.1	479.3	169.3	13.3	0.353	7	6643	0.02749±3	0.18833±24	0.04969±3	174.8±0.2	175.2±0.2	180.3±1.5	3.1
2z, smaller colourless 3:1 prisms NM@1.8A (50)	26.7	597.8	125.9	18.0	0.211	20	1418	0.02855±4	0.20765±43	0.05274±9	181.5±0.2	191.6±0.4	317.7±4.0	43.5
3z, large colourless prisms NM@1.8A (20)	44.0	489.4	176.3	13.4	0.360	4	8362	0.02718±3	0.18571±22	0.04956±3	172.9±0.2	173.0±0.2	174.3±1.3	0.8

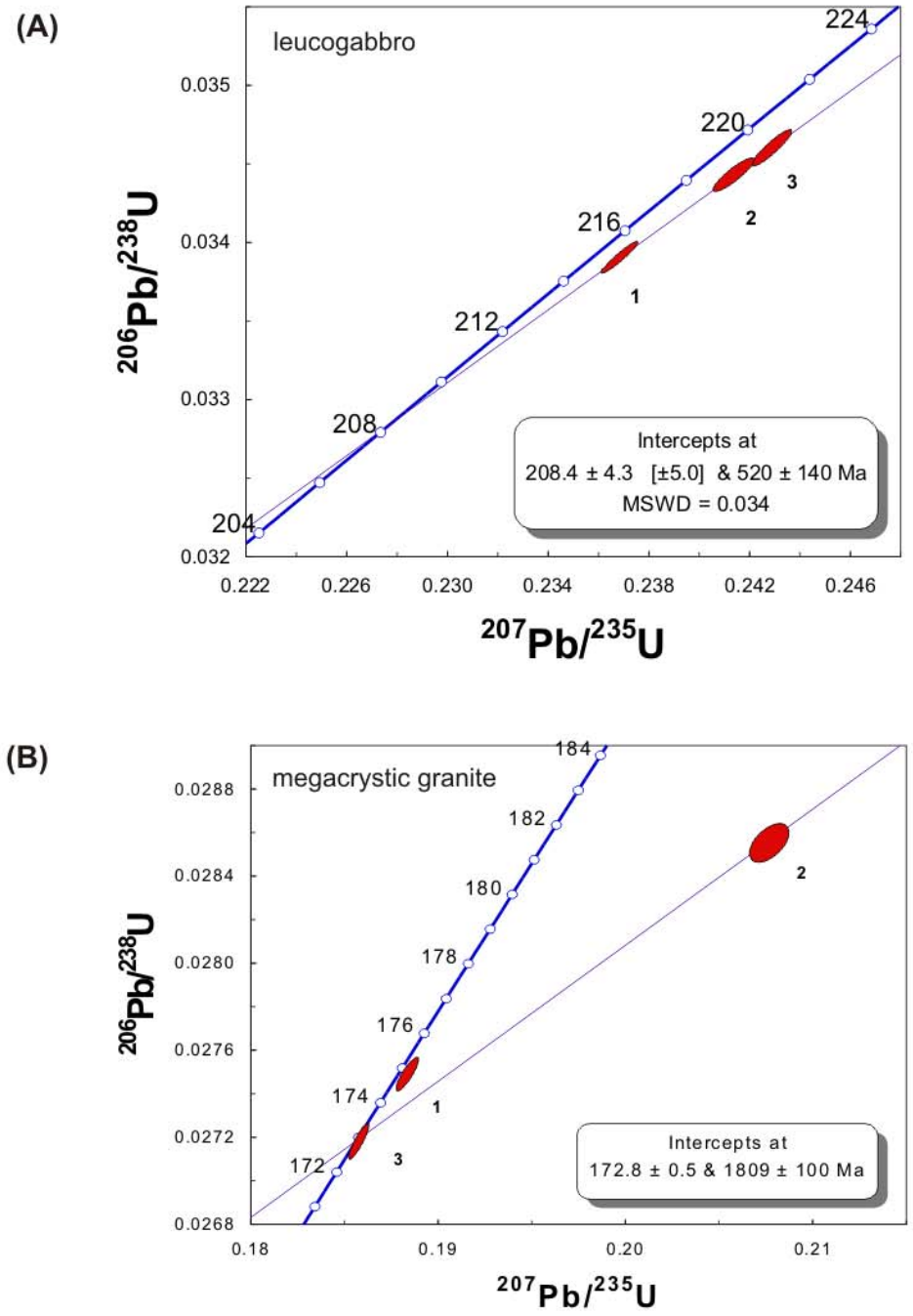

Figure 2.9. (A) U-Pb concordia diagram of 3 zircon fractions from leucogabbro (04AT251-1); (B) U-Pb concordia diagram of 3 zircon fractions from megacrystic granite (04AT253-1).

represents the age of crystallization of the leucogabbro. A Cambrian upper intercept of the discordia suggests some component of inherited zircon in the leucogabbro.

Megacrystic granite

Three fractions of zircon were isolated and analysed from the megacrystic granite. Each fraction consisted of 19 to 50 colourless prismatic zircons with crystal aspect ratios of 3 to 1. The zircons had no obvious zoning although colourless bubble-shaped inclusions were present in a small proportion of the grains. The data points lie below the concordia curve between 173 Ma and 183 Ma and do not form a linear array (Fig. 2.9b). The discordance in fraction 2 may be due in part to a component of inheritance in the granite; this fraction was characterized by an elevated level of total common lead (Table 2.1). The combination of only a few analysed fractions, potential inheritance, and an excess in total common lead in fraction 2 prevents precise determination of the age of crystallization of the megacrystic granite. Fraction 3 was concordant yielding a $^{206}Pb/^{238}U$ age of 172.9 ± 0.2 that is comparable to a 2-point regression through fractions 2 (least concordant) and 3 (most concordant) that yielded a lower intercept of 172.8 ± 0.5 Ma. The same regression yielded an upper intercept of 1809 ± Ma. The combination of the $^{206}Pb/^{238}U$ age of fraction 3 and the lower intercept of the fractions 3 and 2 discordia line probably provides the age range in which the granite crystallized (172.9 ± 0.2 to 172.8 ± 0.5 Ma).

STRUCTURE

THSZ

The THSZ consists of flaggy mylonite with a strong planar fabric, blastomylonite and schist. A well developed lineation is common. The mylonitic fabric is cut by brittle and brittle-ductile faults and shear zones. The strong flaggy foliation is referred to as S1 as it is the oldest observable planar fabric within the THSZ. S1 is defined by preferential alignment of minerals, including amphiboles, by a planar parting along which the rock readily breaks, by a finely developed lamination, and by compositional laminae, including quartz-feldspar layers. The S1 fabric parallels the margins of the THSZ, striking northwest-southeast (Fig. 2.10a). The well-developed lineation is defined by the alignment of elongate aggregates of amphibole and is interpreted as a stretching lineation (L1). L1 plunges shallowly to the northwest and southeast (Fig. 2.10b).

Kinematic indicators in the THSZ include rotated porphyroclasts, C-C' extensional shear bands and rare S-C fabric (Fig. 2.8). On Tally Ho Mountain and Dickson Hill the mylonites yield top to-the-southeast (n=6) and top to-the-east (n=7) kinematic indicators. A small number of kinematic indicators on Tally Ho Mountain and Dickson Hill (n=2), observed along steeply-dipping portions of the THSZ, yield sinistral indicators. Mount Hodnett is similarly dominated by top to-the-southeast kinematic indicators (n=5), however a small number of sinistral and dextral kinematic indicators were observed on steeply dipping portions of the THSZ (n=2 and n=1, respectively). C-C' extensional shear bands were the most commonly observed kinematic indicator in the THSZ (n=14) followed in frequency by rotated augite-porphyroclasts (n=10; Fig. 2.8c). The southeast trend of the L1 stretching lineation and the dominance of top-to-the-east

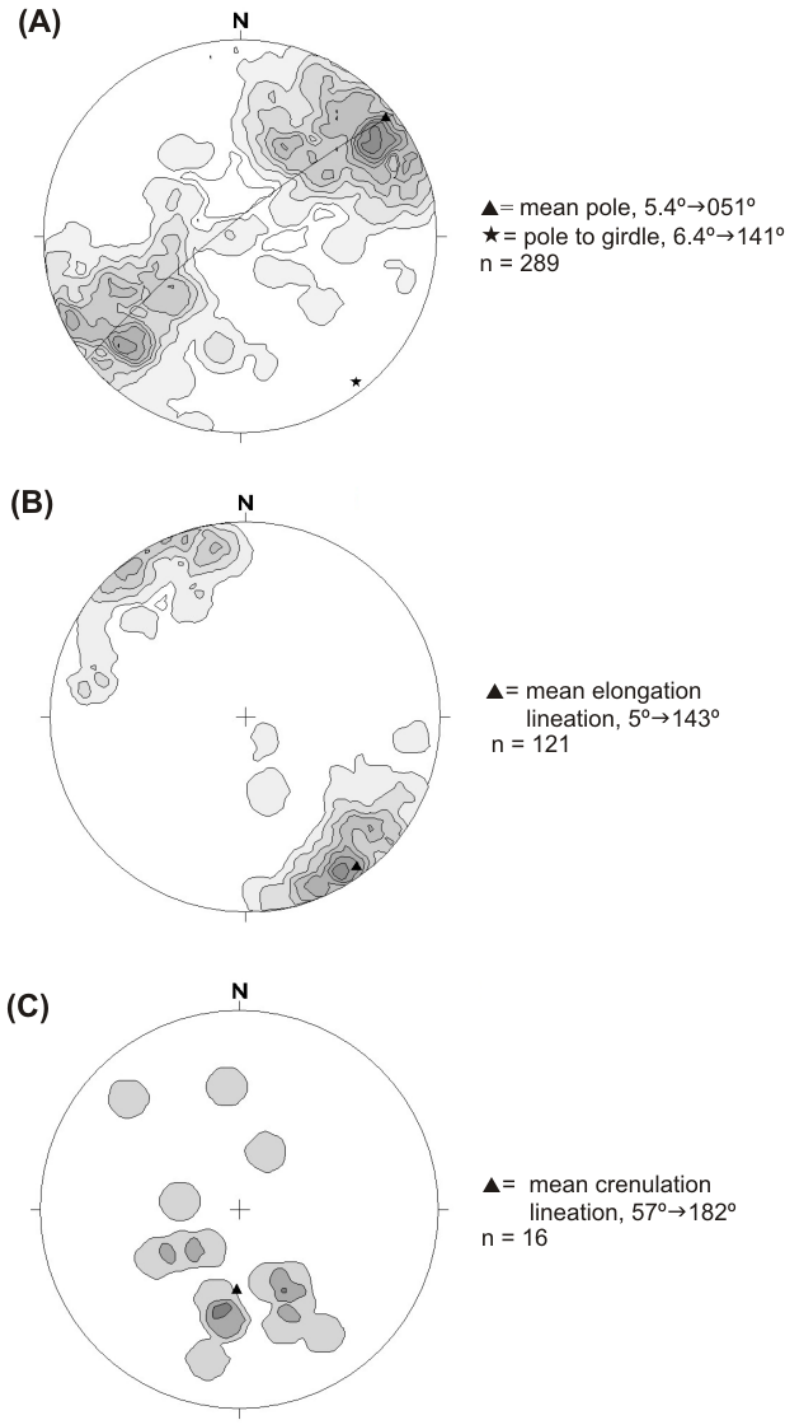

Figure 2.10. (A) stereographic plot of contoured poles to foliation plane in the THSZ; (B) stereographic contour plot of elongation lineations in the THSZ; (C) stereographic contour plot of crenulation lineations in the THSZ.

and top-to-the-southeast kinematic indicators suggest that the THSZ mylonites developed during and provide a record of top-to-the-east to southeast shear. Formation of the THSZ is limited to have occurred between about 208 Ma, the age of the hangingwall leucogabbro, and 173 Ma, the age of the cross-cutting, post-tectonic megacrystic granite.

The THSZ, including its contacts with the overlying hangingwall leucogabbro and pyroxenite and underlying footwall volcanic and volcaniclastic units, are folded. Folding is indicated by change in the orientation of the S1 mylonitic fabric, by meter to centimeter scale parasitic folds of S1, and by the presence of a crenulation lineation and cleavage. Folds of the S1 mylonitic fabric are referred to as F2. Crenulations of the S1 fabric are asymmetric with steeply west-dipping axial planes (S2), and short steep east-limbs, indicating eastward vergence (Fig. 2.8d). These parasitic folds are congruent to the interpreted shape of map-scale folds of the THSZ and its hanging- and footwall sequences (Fig. 2.5). The majority of crenulation lineations (L2) trend south, consistent with east-vergent kinematic indicators and the asymmetry of folds on Tally Ho Mountain and Dickson Hill (Fig. 2.10c). The eastward-vergence of the THSZ and of the F2 folds affecting the THSZ may indicate that the two phases of deformation are kinematically linked. F2 folding post-dates the formation of the S1 mylonitic fabric. The folds are, however, truncated by and older than the 173 Ma megacrystic granite (Fig. 2.5). Folding did not, therefore, significantly post-date formation of the THSZ, further strengthening the suggested kinematic link between mylonitization and subsequent folding.

Locally, on Tally Ho Mountain, where the THSZ is the best-exposed, two sets of lineations are identifiable: an east-west-trending elongation lineation and a south- to southeast-trending crenulation lineation. The lineation orientation most commonly

measured in the THSZ trends to the southeast (Fig. 2.10b), consistent with the orientation of the crenulation lineation measured on Tally Ho Mountain. The more poorly developed lineations observed throughout the rest of the THSZ may therefore be crenulation lineations and not elongation lineations as interpreted here. Alternatively, the orientation of the elongation lineation at a high angle to the predicted transport direction along the THSZ may be due to transpression (Oldow *et al.* 1990; Tikoff & Greene 1997). A more detailed structural study of the shear zone should resolve the nature of the lineation.

The THSZ separates structurally overlying coarse-grained ultramafic and mafic crystalline rocks from an underlying sequence of volcanic and volcaniclastic rocks. Strain decreases progressively structurally up- and down-section from mylonitic and schistose rocks into undeformed footwall and hangingwall lithological units, respectively. The mylonite is of similar composition to and is inferred to consist of highly strained rocks of the footwall volcaniclastic unit and locally of the hangingwall pyroxenite and leucogabbro units. Because the THSZ has an overall flat, sheet-like geometry (albeit subsequently folded), and places a lower crustal intrusive sequence inferred to be part of an arc root over top of a supracrustal arc sequence of volcanic and volcaniclastic rocks, we interpret the shear zone as a crustal scale, intra-arc thrust fault. The presence of coarsely-crystalline mafic and ultramafic rocks carried in the THSZ hangingwall indicates that the thrust fault rooted into the lower crust and potentially the lithospheric mantle of the arc. The distribution of hangingwall units west of the footwall units, the eastward extension of the footwall units into the more easterly Whitehorse Trough, and the overall eastward-vergence of the THSZ, all imply that the THSZ rooted to the west, and climbed up-section to the east. The east-vergence of F2 folds, and the close temporal

relationship between THSZ mylonites and the subsequent F2 folds, implies a genetic relationship. We interpret the map-scale F2 folds as fault-bend folds that developed during movement of the THSZ over ramps in structurally deeper-seated, kinematically-linked thrust faults, a commonly-observed relationship in fold and thrust belts.

Brittle deformation

Steeply-dipping, brittle to brittle-ductile fault zones strike parallel to and cross-cut the mylonitic THSZ, and are characterized by fault gouge, tension gashes, Riedel shears, slickenlines and rare S-C fabric. Tension gashes and Riedel shears on Mount Wheaton indicate sinistral (n=2) and dextral (n=2) slip. Brittle faults commonly contain gouge, strike northwest and dip subvertically (Fig. 2.8b). Although slickenline orientations along the fault zones are variable, strike-slip to oblique strike-slip displacements are most common. Dextral kinematic indicators were the most common sense of motion observed (n=33; sinistral n=2). Direct measurement of the amount of displacement along the brittle faults is difficult due to the lack of offset markers.

The brittle faults strike and dip similar to and are locally continuous with faults mapped as part of the Llewellyn fault zone (Hart & Radloff 1990). The steeply-dipping brittle to brittle-ductile faults that overprint and parallel the THSZ are therefore interpreted as part of the Llewellyn fault zone. Rocks as young as early Eocene are affected by the brittle deformation. However, near Gold Hill, an undeformed Eocene rhyolite intrusion truncates and therefore post-dates movement along the Llewellyn fault zone (Fig. 2.4) (Hart & Radloff 1990).

DISCUSSION

The THSZ places lower crust and potentially mantle of a Late Triassic arc onto the supracrustal volcanic and volcaniclastic rocks of the Late Triassic Lewes River Arc of Stikinia. The THSZ is, therefore, an intra-arc fault developed within and responsible for imbrication of Stikinia; it is not a terrane-bounding structure marking the primary contact between Stikinia and the more westerly Nisling Assemblage. Kinematic indicators, including S – C fabric, C' extensional shears, rotated porphyroclasts, and asymmetric parasitic folds and crenulations indicate that the subhorizontal shear zone was characterized by top-to-the-east shear. The geometry of folds of the THSZ are consistent with interpretation as fault-bend folds developed above ramps in deeper-seated shear zones kinematically linked to the THSZ. Hence the THSZ appears to be one of a series of faults forming an east-verging thrust belt.

The well-developed foliation in the leucogabbro and, to a lesser extent, the pyroxenite is typically defined by the parallel alignment of coarsely crystalline, unstrained elongate amphibole and pyroxene grains. The lack of internal strain of individual grains indicates that the foliation formed in response to flow within a deep crustal (high P, high T) setting. Exhumation of these rocks to shallow crustal levels resulted in retrogressive greenschist metamorphism and overprinted the high T ductile foliation with brittle-ductile shear zones and brittle fractures.

The age of the THSZ is tightly constrained. Leucogabbro carried in the hangingwall of the THSZ crystallized at 208.4 ± 4.3 Ma, providing a maximum age constraint on shear zone development. A minimum age constraint is provided by the megacrystic granite that intrudes into and plugs the THSZ and which crystallized at 173

Ma. Formation of the THSZ is, therefore, constrained to the latest Late Triassic to Early Jurassic.

The age, geometry and intra-Stikinian nature of the THSZ indicate that it is one of a series of Early Jurassic shear zones that characterize the Early Jurassic west margin of Stikinia. Timing constraints for the more northerly Takhini deformation zone, while few, are permissive of an Early Jurassic age. North and west of the Takhini deformation zone, in the Aishihik Lake region, little metamorphosed basalts of the Upper Triassic Lewes River Group are in fault contact with upper amphibolite facies schist and quartzite of the Aishihik metamorphic suite, which is here referred to as the Nisling Assemblage. The fault is plugged by and older than the 186 Ma Aishihik batholith and 185 Ma granitic intrusions of the Long lake plutonic suite. The Early Jurassic Wann River shear zone to the south is, of the documented Stikinian shear zones, perhaps the most similar to the THSZ, given its top-to-the-east sense of shear. Together, these coeval fault and shear zones, accommodated both intra-Stikinia strain as well as juxtaposition of isotopically juvenile arc crust of Stikinia against the continental Nisling Assemblage. Younger brittle-ductile shear zones, like the Llewellyn, are likely the product of reactivation of this network of crustal scale Early Jurassic faults that extend along and characterize the west margin of Stikinia.

Formation of the THSZ was coincident with the latest Triassic cessation of the isotopically juvenile Lewes River Arc magmatism and the formation of a major unconformity within the Whitehorse Trough, and immediately predated deposition of coarse clastics of the Lower Jurassic Laberge Group (Johannson 1994; Hart 1997) (Fig. 2.3). It is, therefore, likely that deformation coincided with and was related to the

termination of subduction beneath the Lewes River Arc. The termination of magmatism in arcs is commonly linked to collision with buoyant, unsubductable lithosphere along an arcs bounding trench. The development of coeval shear zones along the length of the western margin of Stikinia is consistent with a model of collision of Stikinia with continental crust to the west.

The deposition of orogenic clastic sediments across Stikinia in the Lower Jurassic, including boulder conglomerates of the Laberge Group, provide further support for involvement of Stikinia in a major Early Jurassic orogenic event. In northwestern British Columbia, Pleinsbachian greywacke of the Laberge Group is locally characterized by clasts of ultra-high pressure metamorphic rocks (MacKenzie *et al.* 2005). These sedimentary rocks provide a record of uplift and exhumation of crustal rocks that had been buried to depths of ~100 kilometers and constitute the only known vestiges of ultra-high pressure rocks in the entire Cordilleran orogen of western North America (MacKenzie *et al*. 2005; Canil *et al*. 2006). The rapid exhumation, erosion and subsequent deposition of ultra-high pressure minerals immediately post-dates the large-scale change in sedimentation in the Whitehorse Trough, consistent with the cessation of the Lewes River Arc being related to a latest Triassic – Lower Jurassic thick-skinned collisional event.

Juxtaposition of isotopically juvenile Triassic arc rocks of Stikinia against the isotopically evolved continental Nisling Assemblage of the Yukon-Tanana Terrane occurred in the Early Jurassic (Johnston *et al.* 1996). Hence it seems likely that it was the entry of the buoyant and unsubductable continental crust of the Nisling Assemblage into a subduction zone that dipped east beneath the west margin of Stikinia that resulted in

deformation and the cessation of arc magmatism. Evidence for deep tectonic burial of the Nisling Assemblage, consistent with its entry into a subduction zone in the Upper Triassic – Lower Jurassic, includes syn-kinematic, high pressure (pressures of 8 to 12 kbars) – high temperature regional metamorphism in the Lower Jurassic (Johnston & Erdmer 1995a), and the coeval development of an east-dipping axial planar foliation (Johnston & Erdmer 1995b). The Aiskihik batholith, which intrudes the Nisling Assemblage, crystallized at a depth of ~30 kilometres at 186.0 ± 2.8 Ma (Johnston *et al*. 1996). The high-level (intruded at depths of <6 kilometres) Long Lake plutonic suite intruded the Aishihik batholith and Nisling Assemblage at $185.6 \pm^{2.0}_{2.4}$ Ma, indicating rapid exhumation of the Aishihik batholith and previously deeply buried Nisling Assemblage (Johnston *et al*. 1996).

Collision of Nisling with Stikinia implies east-dipping subduction beneath the west margin of Stikinia (present day coordinates). In this model, the Upper Triassic Lewes River Arc, including the cumulate leucogabbro – pyroxenite that forms the hangingwall of the THSZ, faced west and developed in response to the consumption of oceanic lithosphere that was continuous with continental crust represented by the Nisling Assemblage (Fig. 2.11). Contrary to previous interpretations of the Whitehorse Trough as a forearc basin (Dickie & Hein 1995), in our model the trough forms the back arc located east of the west-facing Lewes River Arc in the Upper Triassic. Stratigraphic similarities between Stikinia and the Nisling Assemblage (Jackson *et al*. 1991; McClelland *et al*. 1992) may indicate that Stikinia and Nisling originated as part of one terrane that subsequently rifted apart.

Entry of the buoyant continental Nisling Assemblage into the trench bounding Stikinia to the west terminated subduction (Fig. 2.11). The collision drove structurally deep-seated portions of the Stikinia arc crust up-section to the east, giving rise to an east-verging intra-arc fold and thrust belt that included the THSZ. Thickening of the arc-crust loaded the upper plate lithosphere giving rise to a foreland basin east of the arc, within which the Laberge Group orogenic clastic sediments were deposited. The Lower Jurassic Whitehorse Trough was, therefore, neither a fore- or back-arc; it was a foreland basin. Confusion of the nature of the Whitehorse Trough in part results from the mis-interpretation of the foreland basin Laberge Group strata as the result of normal arc-marginal basin sedimentation. The presence of clasts of ultra-high pressure metamorphic rocks within the foreland basin indicate that collision resulted in the exhumation of rocks from depths of >100 km, probably along faults related to and kinematically linked to the THSZ. The post-collisional resumption of arc-magmatism, including the 185 Ma Long Lake plutonic suite to the north, and the 173 Ma megacrystic granite in the study area, implies that collision wasn't terminal and may indicate that the Nisling Assemblage was a narrow ribbon continent. The alkalic nature of some of the post-tectonic magmatism may, however, be better explained as a result of break off of the slab attached to the Nisling Assemblage.

Our model of the tectonic setting that gave rise to the THSZ rests in part on our interpretation of the pyroxenite and leucogabbro that forms the hangingwall to the shear zone as an arc root, rather than an ophiolite (slice of oceanic lithosphere) or upper crustal sill. Future geochemical and isotopic studies of the magmatic hangingwall sequence will, therefore, constitute a major test of our model. Furthermore, the complicated

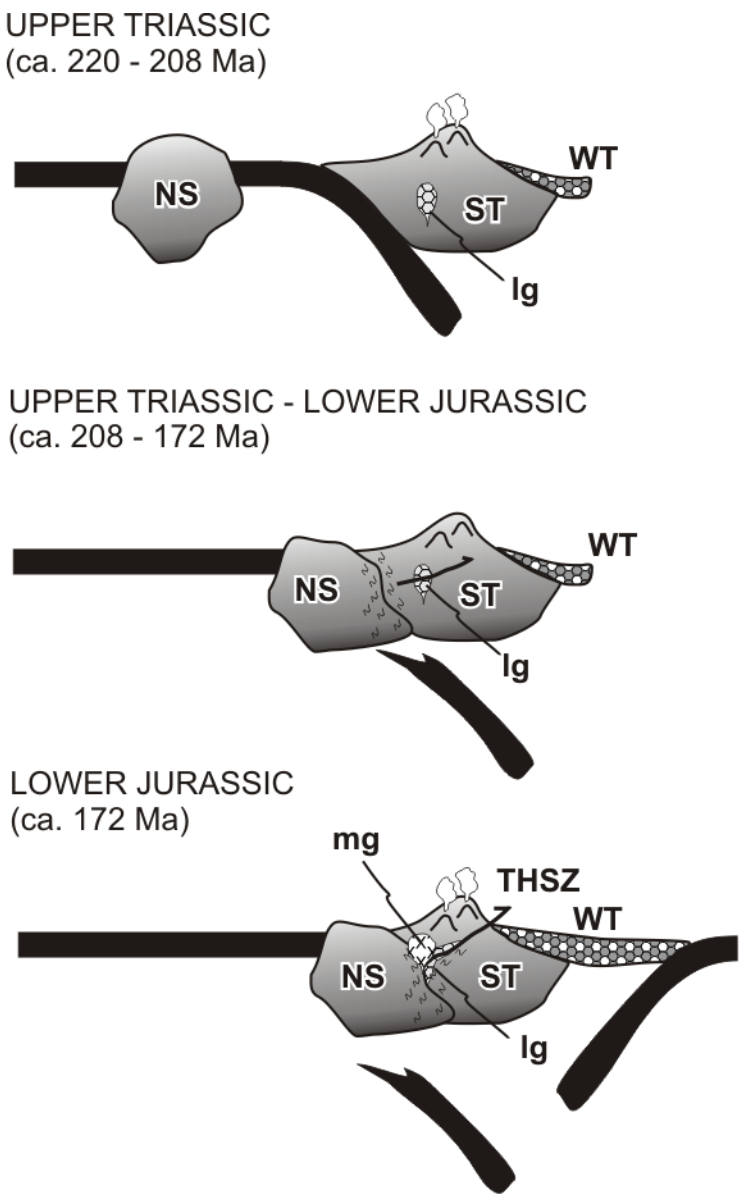

Figure 2.**11.** Schematic tectonic model for the development of the Tally Ho shear zone along the western margin of Stikinia (see text for explanation). NS, Nisling Assemblage; ST, Stikinia; WT, Whitehorse Trough; THSZ, Tally Ho shear zone; lg, leucogabbro and pyroxenite units; mg, megacrystic granite unit.

composite evolution of the Whitehorse Trough predicted by our model is testable by constraining subsidence rates through time by performing a back-stripping analysis of the strata that make up the Laberge and Lewes River groups.

CONCLUSIONS

The northern Canadian Cordillera is at least in part the product of thick-skinned collisions between a juvenile oceanic arc, Stikinia and a pericratonic terrane, the Nisling Assemblage. Entry of the buoyant Nisling Assemblage into the Stikine subduction zone resulted in the cessation of magmatism in the Lewes River Arc and the imbrication of the arc along crustal-scale east-vergent thrust faults like THSZ. The collision also resulted in the rapid exhumation of the Nisling Assemblage and Aishihik batholith to the west and deposition of ultra-high pressure rocks into the Whitehorse Trough to the east. Models of the Cordillera as an eastward amalgamation of thin-skinned crustal flakes that rode over North American continental basement (Snyder *et al*. 2002; Cook *et al*. 2004) are inconsistent with the tectonic model presented here. Collision of the Nisling Assemblage with Stikinia in the Early Jurassic demonstrates that thick-skinned accretion played a significant role in crustal growth along the ancient North American continental margin.

REFERENCES CITED

Breitsprecher, K. & Mortensen, J.K. 2004. YukonAge 2004: A database of isotopic age determinations for rock units from Yukon Territory, Canadian Geochronology Knowledgebase. Yukon Geological Survey, CD-ROM.

Canil, D., Mihalynuk, M. & Charnell, C. 2006. Sedimentary record for exhumation of ultrahigh pressure (UHP) rocks in the northern Cordillera, British Columbia. *Geological Society of America Bulletin*, **118,** 1171-1184.

Colpron, M., Nelson, J.L., and Murphy, D.C. 2006. A tectonostratigraphic framework for the pericratonic terranes of the northern Cordillera, in Colpron, M., and Nelson, J.L., eds., Paleozoic Evolution and Metallogeny of Pericratonic Terranes at the Ancient Pacific Margin of North America, Canadian and Alaskan Cordillera, Special Paper 45, Geological Association of Canada, p. 1-23.

Cook, F.A., Clowes, R.M., Snyder, D.B., van der Velden, A.J., Hall, K.W., Erdmer, P. & Evenchick, C.A. 2004. Precambrian crust beneath the Mesozoic northern Canadian Cordillera discovered by Lithoprobe seismic reflection profiling. *Tectonics*, **23,** TC2010.

Currie, L. & Parrish, R.R. 1993. Jurassic accretion of Nisling terrane along the western margin of Stikinia, Coast Mountains, northwestern British Columbia. *Geology*, **21,** 235-238.

Dickie, J.R. & Hein, F.J. 1995. Conglomeratic fan deltas and submarine fans of the Jurassic Laberge Group, Whitehorse Trough, Yukon Territory, Canada : fore-arc sedimentation and unroofing of a volcanic island arc complex. *Sedimentary Geology*, **98,** 263-292.

Doherty, R.A. & Hart, C.J.R. 1988. Preliminary Geology of Fenwick Creek (105D/3) and Alligator Lake (105D/6) map areas, Open File 1988-2. Exploration and Geological Services Division, Indian and Northern Affairs Canada, Yukon Region, **84**.

Eisbacher, G.H. 1981. Late Mesozoic - Paleogene Bowser Basin molasse and Cordilleran tectonics, western Canada. *In*: Miall, A.D. (ed) *Sedimentation and Tectonics in Alluvial Basins.* Geological Association of Canada, 125-151.

Gehrels, G.E., McClelland, W.C., Samson, S.D., Patchett, P.J. & Jackson, J.L. 1990. Ancient continental margin assemblage in the northern coast Mountains, southeast Alaska and northwest Canada. *Geology*, **18,** 208-211.

Hamilton, W.B. 1988. Plate tectonics and island arcs. *Geological Society of America Bulletin*, **100,** 1503-1527.

Hart, C.J.R. 1995. Magmatic and Tectonic Evolution of the Intermontane Superterrane and Coast Plutonic Complex in Southern Yukon Territory. M.Sc. thesis, University of British Columbia, 198 pp.

— 1997. A Transect Across Northern Stikinia: Geology of the Northern Whitehorse Map Area, Southern Yukon Territory (105D/13-16). *In*: Abbott, G. (ed) Exploration and Geological Services Division, Yukon Region, Indian and Northern Affairs Canada, Bulletin **112**.

Hart, C.J.R., Dickie, J.R., Ghosh, D.K. & Armstrong, R.L. 1995. Provenance constraints for Whitehorse Trough conglomerate: U-Pb zircon dates and initial Sr ratios of granitic clasts in Jurassic Laberge Group, Yukon Territory. *In*: Miller, D.M. & Busby, C. (eds) *Jurassic Magmatism and Tectonics of the North American Cordillera*. The Geological Society of America, 47-63.

Hart, C.J.R. & Pelletier, K.S. 1989. Geology of Carcross (105D/2) and part of Robinson (105D/7) map areas, Open File 1989-1. Exploration and Geological Services Division, Indian and Northern Affairs Canada, Yukon Region, **92**.

Hart, C.J.R. & Radloff, J.K. 1990. Geology of Whitehorse, Alligator Lake, Fenwick Creek, Carcross and part of Robinson map areas (105D/11, 6, 3, 2, & 7), Open File 1990-4. Indian and Northern Affairs Canada, Indian and Northern Affairs Canada, **113**.

Heaman, L. & Parrish, R.R. 1991. U-Pb geochronology of accessory minerals In: Heaman, L. & Ludden, J.N. (eds) Applications of radiogenic isotope systems to problems in geology; short course handbook. Mineralogical Association of Canada, 59-102.

Heaman, L.M., Erdmer, P. & Owen, J.V. 2002. U-Pb geochronologic constraints on the crustal evolution of the Long Range Inlier, Newfoundland. *Canadian Journal of Earth Sciences*, **39,** 845-865.

Jackson, J.L., Gehrels, G.E., Patchett, J.P. & Mihalynuk, M.G. 1991. Stratigraphic and isotopic link between the northern Stikine Terrane and an ancient continental margin assemblage, Canadian Cordillera. *Geology*, **19,** 1177-1180.

Johannson, G.G. 1994. Provenance constraints on Early Jurassic evolution of the northern Stikinian arc: Laberge Group, Whitehorse Trough, northwestern British Columbia. Unpublished M.Sc. thesis, University of British Columbia, 297 pp.

Johnston, S.T. & Erdmer, P. 1995a. Hot-side-up aurole in southwest Yukon and limits on terrane assembly of the northern Canadian Cordillera. *Geology*, **23,** 419-422.

—, 1995b. Magmatic flow and emplacement foliations in the Early Jurassic Aishihik Batholith, southwest Yukon: Implications for northern Stikinia. *In*: Miller, D.M. & Busby, C. (eds) *Jurassic magmatism and tectonics of the North American Cordillera*. Geological Society of America, 65-82.

Johnston, S.T., Mortensen, J.K. & Erdmer, P. 1996. Igneous and metaigneous age constraints for the Aishihik metamorphic suite, southwest Yukon. *Canadian Journal of Earth Sciences*, **33,** 1543-1555.

Ludwig, K.R. 1998. Isoplot/Ex (version 3.00): A geochronological toolkit for Microsoft Excel. Berkeley Geochronological Centre, Berkeley Geochronological Centre, 1-43.

MacKenzie, J.M., Canil, D., Johnston, S.T., English, J., Mihalynuk, M.G. & Grant, B. 2005. First evidence for ultrahigh-pressure garnet peridotite in the North American Cordillera. *Geology*, **33,** 105–108.

McClelland, W.C., Gehrels, G.E., Samson, S.D. & Patchett, P.J. 1992. Structural and geochronologic relations along the western flank of the Coast Mountains batholith: Stikine River to Cape Fanshaw, central southeastern Alaska. *Journal of Structural Geology*, **14,** 475-489.

Mihalynuk, M.G. & Rouse, J.N. 1988. Preliminary Geology of the Tutshi Lake Area, Northwestern British Columbia (104M/15), Geological Fieldwork 1987: A summary of Field Activities and Current Research, Paper 1988. Province of British Columbia, Ministry of Energy, Mines and Petroleum Resources, Mineral Resources Division, Geological Survey Branch, 217-232.

Mortensen, J.K. 1992. Pre-mid-Mesozoic tectonic evolution of the Yukon-Tanana Terrane, Yukon & Alaska. *Tectonics*, **11,** 836-853.

Oldow, J.S., Bally, A.W. & Lallemont, G.A. 1990. Transpression, orogenic float, and lithospheric balance. *Geology*, **18**, 991-994.

Snyder, D.B., Clowes, R.M., Cook, F.A., Erdmer, P., Evenchick, C.A., van der Velden, A.J. & Hall, K.W. 2002. Proterozoic prism arrests suspect terranes: Insights into the ancient Cordilleran margin from seismic reflection data. *GSA Today*, **12,** 4-10.

Stacey, J.S. & Kramers, J.D . 1975. Approximation of terrestrial lead isotope evolution by a two-stage model. *Earth and Planetary Science Letters*, **26**, 207-221.

Tikoff, B. & Greene, D. 1997. Stretching lineations in transpressional shear zones: and example from the Sierra Batholith, California. *Journal of Structural Geology*, **19**, 29-39.

CHAPTER 3

Geochemical and isotopic constraints on magmatic rocks along the western margin of Stikinia: Implications for Mesozoic crustal growth in the Canadian Cordillera

INTRODUCTION

In the Canadian Cordillera, much of the debate over the extent to which this accretionary orogen has been responsible for growth of the continent has centered on the origin of the major magmatic arc terranes, Stikinia and Quesnellia. These paleo-magmatic arcs are adjacent to pericratonic assemblages that include thick siliciclastic continental margin sequences. Did the volcanic arcs develop on these relic continental margins? If so, their contribution to the growth of the continent is limited (Erdmer *et al.* 2002; Erdmer *et al*. 2005; McClelland *et al*. 1992). The accretion of crust and lithosphere of truly exotic oceanic magmatic arcs would, however, contribute to significant continental growth (Johnston & Canil 2007).

Constraints on the petrogenesis of magmatic rocks, and the nature of the plumbing system that facilitated their intrusion or eruption, are provided by the geochemical and isotopic character of plutons and volcanic rocks. This information can, therefore, be exploited to constrain the timing and nature of terrane linkages. For instance, igneous rocks from oceanic terranes are characterized by juvenile isotopic signatures which distinguish them from the evolved, radiogenic character of magmas that have originated in or passed through continental lithosphere. A test, therefore, for determining the extent to which paleo-magmatic arcs, like Stikinia, contributed to the overall growth of the continent lies in the geochemical character of its rocks.

We sampled pristine and deformed pre-, syn- and post-tectonic magmatic and metamorphosed magmatic rocks within Stikinia near its western margin in southern Yukon (Fig. 3.1). Included in our sampling are mylonite of the Tally Ho shear zone

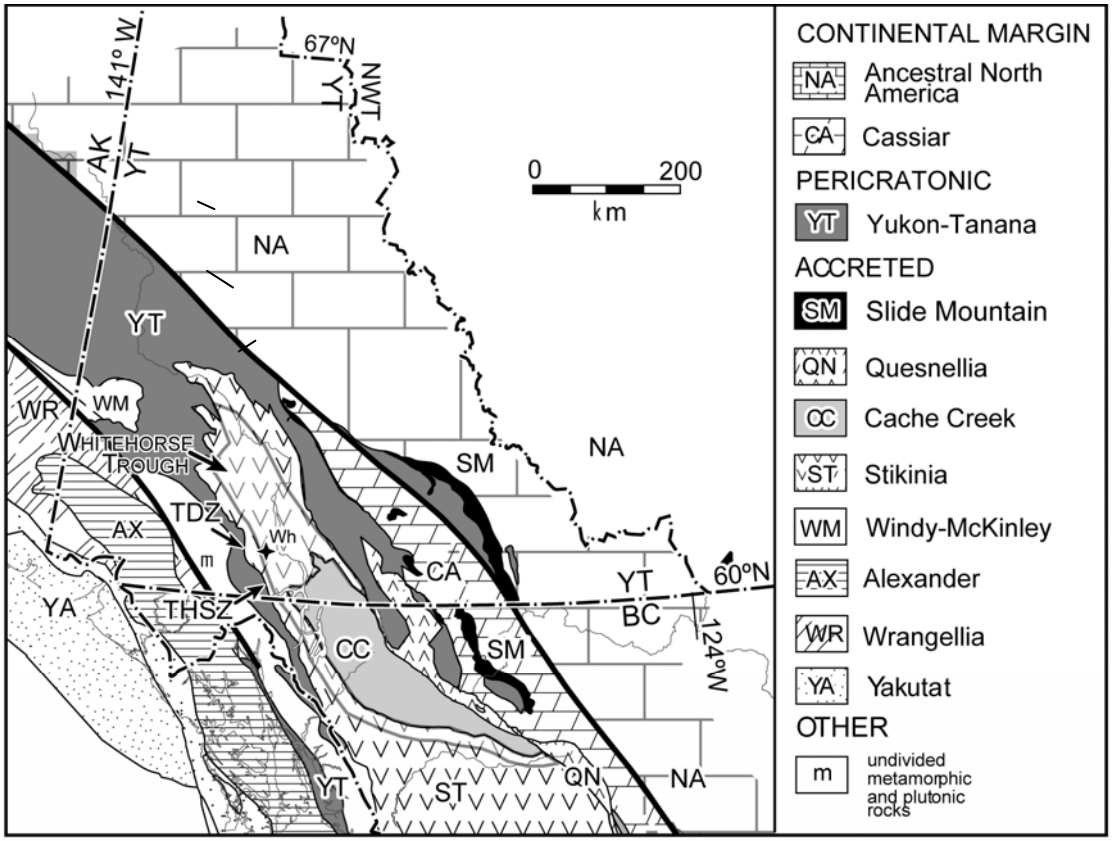

Figure 3.1. Simplified terrane map of the northern Canadian Cordillera (modified after Colpron *et al*. 2006). THSZ, Tally Ho shear zone; TDZ, Takhini deformation zone; Wh, Whitehorse.

(THSZ), an east-verging intra-arc thrust fault responsible for the imbrication of the Late Triassic Lewes River Arc that characterizes northern Stikinia (Tizzard *et al*. *in press*; Chapter 2). Immediately west of Stikinia, are schist and gneiss of the pericratonic Yukon-Tanana Terrane (YTT). The nature of the Stikinia-YTT contact remains a matter of conjecture. For example, some authors argue for a stratigraphic link between the terranes, implying Stikinia was built on the YTT (Jackson *et al*. 1993). Alternatively, the Stikinia - YTT boundary is interpreted as a result of tectonism due to terrane imbrication (Tizzard *et al. in press*; Currie & Parrish 1993; Johnston & Canil 2007).

Here we use our geochemical and isotopic data to determine the tectonic environment in which magmatic rocks of Stikinia were emplaced and if Stikinia developed on continental (YTT) or oceanic lithosphere. In doing so, we constrain the nature of the Stikinia-YTT contact, and limit the amount of continental growth accomplished during Cordilleran orogenesis. This paper reports the results of Sm-Nd isotopic systematics and major and trace element geochemistry of pre-tectonic magmatic rocks of Stikinia, syn-tectonic mylonite of the THSZ, a cross-cutting pluton that intrudes both Stikinia and the YTT, and an along strike high-strain zone consisting of the oldest known rocks of Stikinia in Yukon.

REGIONAL GEOLOGICAL SETTING

In southern Yukon, western Stikinia consists of the late Paleozoic Takhini Assemblage and the Upper Triassic to Lower Jurassic Lewes River and Laberge groups of the Whitehorse Trough (Fig. 3.2) (Hart, 1997). The Takhini Assemblage consists of

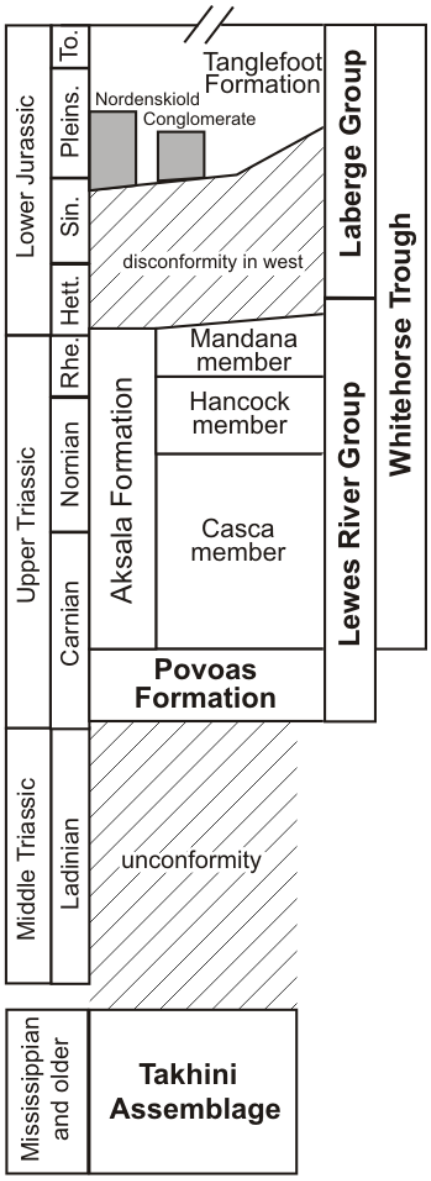

Figure 3.2. Stratigraphy of the western margin of Stikinia in southern Yukon. Names discussed in text are in bold. Modified from Hart (1997).

variably deformed volcanic and sedimentary rocks and comprises the oldest known Stikine stratigraphy in Yukon. The Upper Triassic volcanic and volcaniclastic Povoas Formation forms the base of the Lewes River Group and is correlative with the Stuhini Formation of northern British Columbia, together forming the Lewes River Arc (Hart 1997). Geochemical and isotopic data for Stikinia indicates that the terrane formed in an arc-setting (e.g. Monger *et al.* 1991 and references therein). Elevated ε_{Nd} isotopic values for plutonic, volcanic and sedimentary rocks of Stikinia imply that the terrane is primitive, having little or no involvement with evolved, continental source rocks (Dostal *et al*. 1999; Samson *et al*. 1989).

To the west of Stikinia, the pericrationic Nisling Assemblage of the YTT consists of early Paleozoic mica-schist, quartzite, marble and orthogneiss (Mortensen 1992; Hart & Radloff 1990). In contrast to Stikinia, negative ε_{Nd} isotopic values for the Nisling Assemblage imply an evolved continental source (Mezger *et al*. 2001; Jackson *et al*. 1991).

The contact between Stikinia and the YTT is commonly obscured by younger intrusions of the Coast Plutonic Complex and overprinted by Cretaceous and Tertiary steeply dipping strike-slip faults. Where observed, the western Stikinia-YTT contact is commonly tectonic (Tizzard *et al. in press*; Currie & Parrish 1993), although some authors argue a stratigraphic link between the terranes in the Upper Triassic (Jackson *et al.* 1991). In any case, cross-cutting plutons of the Long Lake Plutonic Suite that intrude and stitch together Stikinia and the YTT indicate that juxtaposition of the terranes took place by at least 185 Ma (Johnston *et al.* 1996; Hart 1997).

Sm-Nd ISOTOPIC ANALYSIS

A total of eight samples were selected for Sm-Nd isotopic analysis to test the tectonic affinity of magmas (evolved versus primitive) throughout the evolution of Stikinia. The Paleozoic Takhini Assemblage (n=2) represents the earliest known arc activity in northern Stikinia. Samples of leucogabbro (n=2), pyroxenite (n=1), and augite-phenocrystic basalt (n=1) from the Povoas Formation represent the pre-tectonic Upper Triassic Lewes River Arc. Mylonite from the THSZ (n=1) was sampled to assess the nature of syn-tectonic Stikinia in the Lower Jurassic. Lastly, a post-tectonic megacrystic granite (n=1) which intrudes both Stikinia and the YTT in the Lower Jurassic was also analysed for Sm-Nd isotopic systematics.

Leucogabbro samples are medium- to very coarse-grained and weakly- to moderately-foliated. The leucogabbro consists of plagioclase, amphibole, clinopyroxene, quartz and minor magnetite. A U-Pb zircon age of 208.4 ± 4.3 Ma was obtained by Tizzard *et al.* (*in press*; Chapter 2) for the leucogabbro. The pyroxenite is medium- to coarse-grained, massive to weakly-foliated and consists of clinopyroxene and minor orthopyroxene, olivine and opaque minerals. Both the pyroxenite and leucogabbro have been metamorphosed to at least greenschist facies. The pyroxenite and leucogabbro comprise part of a cumulate pluton that formed in the lower crust of the Lewes River Arc which was subsequently transposed up-section and to the east in the hangingwall of the THSZ (Tizzard *et al*. *in press*; Chapter 2). Augite-phenocrystic basalt of the Povoas Formation forms the footwall of and was caught up in the deformation that gave rise to the THSZ. The basalt is massive to weakly-foliated with augite phenocrysts up to 2 millimetres in diameter in a variably choloritized and sericitized aphanitic matrix.

Mylonite from the THSZ is very fine-grained and laminated and consists of clinopyroxene, plagioclase and minor amphibole and opaque minerals, and has been metamorphosed to at least greenschist facies. Deformation in the THSZ is constrained by the crystallization age of the leucogabbro in the hangingwall of the structure (208 Ma) and by the age of a cross-cutting pluton (172 Ma).

The Takhini deformation zone (TDZ) is a structural unit within the Paleozoic Takhini Assemblage (Fig. 3.1). The timing of deformation in the TDZ is poorly constrained to having occurred between the mid-Mississippian to Lower Jurassic (Hart 1997; Tizzard *et al*. *in press*; Chapter 2). The protolith of schist from the TDZ is assumed to have been a product of early arc activity in Stikinia (Hart 1997). Schist in the TDZ is moderately- to well-foliated and amphibole porphyroblastic. The fine-grained matrix consists of amphibole, plagioclase and quartz with minor calcite, epidote and opaque minerals.

Post-tectonic, massive, megacrystic granite intruded both Stikinia and the YTT in the Lower Jurassic. The granite is coarse-grained with alkali-feldspar megacrysts up to 2 centimeters in length. The granite consists of quartz, plagioclase, orthoclase and minor biotite, hornblende and magnetite. U-Pb zircon age determinations constrain the age of crystallization to between 179.9 ± 0.2 to 172 ± 0.5 Ma (Tizzard *et al. in press*; Chapter 2).

Samples were analysed at the Radiogenic Isotopic Facility at the University of Alberta and followed the techniques outlined by Untershutz *et al.* (2002) and references therein. The isotopic composition of Nd was determined in static mode by Multi-Collector ICP-Mass Spectrometry. All isotope ratios were normalized for variable mass

bias to a value of $^{146}Nd/^{144}Nd = 0.7219$ using the exponential fractionation law. The $^{143}Nd/^{144}Nd$ ratio of samples is presented relative to a value of 0.511850 for the La Jolla Nd isotopic standard, monitored by use of an Alfa Nd isotopic standard for each analytical session. Sm isotopic abundances were also measured in static mode by Multi-Collector ICP-Mass Spectrometry, normalized for variable mass bias to a value of 1.17537 for $^{152}Sm/^{154}Sm$ also using the exponential law. ε_{Nd} values for each sample were calculated using estimated ages of the Lewes River Arc and megacrystic granite from Tizzard *et al.* (*in press*; Chapter 2) and the Takhini Assemblage from Hart (1997). Sample locations are in Table 3.1.

Results

ε_{Nd} values range from a minimum of -4.0 for the megacrystic granite to a maximum of +6.9 for the Takhini Assemblage (Table 3.2). The Lewes River Arc samples of leucogabbro, pyroxenite, and augite-phenocrystic basalt have ε_{Nd} values of +4.5, +6.0, and +6.7 respectively. Mylonite from the THSZ has an ε_{Nd} value of +5.4. Model ages of the leucogabbro and pyroxenite range from 650 - 740 Ma whereas the megacrystic granite has a model age of 1190 Ma.

The negative ε_{Nd} signature of the megacrystic granite indicates an evolved crustal source or contamination from an evolved crustal source. In contrast, the positive ε_{Nd} signatures of samples from the Lewes River Arc and Takhini Assemblage indicate derivation from a more primitive mantle source with little or no involvement with evolved crustal material. From the Sm-Nd isotopic data it is clear that the megacrystic

Table 3.1. Sample locations.

Sample Number	UTM NAD83	Lat/Long
04AT207-1	496964mE 6676957mN	60º13’45.7” 135º3’17”
04AT219-1	497510mE 6677142mN	60º13’ 51.7” 135º 2’41.84”
04AT229-2	497236mE 6675449mN	60º13’45.7” 135º3’17.3”
04AT231-4	496938mE 6676443mN	60º13’29.2” 135º3’19.0”
04AT251-1	495901mE 6675861mN	60º13’10.3” 135º4’26.3”
04AT253-1	495159mE 6676819mN	60º13’41.2” 135º4”26.4”
04DT006-1	497983mE 6676264mN	60º13”23.4” 13ºd2”11.0’
04DT14-1	496153mE 6675179mN	60º12’48.2” 135º4’9.9”
04DT22-1	452894mE 6745054mN	60º13’45.7” 135º3’17.3”
04DT23-1	452786mE 6743031mN	60º49’11.7” 135º52’5.0”
04DT24-1	460397mE 6742637mN	60º48’55.0” 135º43’40.8”
04DT25-1	461178mE 6744066mN	60º49’48.0” 135º42”50.4”
04DT28-1	463339mE 6745079mN	60º49’15.4” 135º40’26.6”

Table 3.2. Sm and Nd analyses for Stikinia.

Sample No.	Rock Type	Sm (ppm)	Nd (ppm)	$\frac{^{147}Sm}{^{144}Nd}$	$\frac{^{143}Nd}{^{144}Nd_0}$	εNd_0	T_{DM} (Ga)	$\frac{^{143}Nd}{^{144}Nd_T}$	T (Ma)	εNd_T
04AT219-1	Augite-phenocrystc basalt	2.09	6.99	0.1807	0.512959	6.3	N/A	0.512699	208	6.7
04AT231-4	Pyroxenite	0.42	1.06	0.2393	0.513002	7.1	N/A	0.512676	208	6.0
04AT251-1	Leucogabbro	4.73	21.04	0.1360	0.512788	2.9	0.74	0.512603	208	4.5
04AT253-1	Megacrystic granite	1.74	9.78	0.1078	0.512334	-5.9	1.19	0.512212	172	-4.0
04DT006-1	Mylonite	4.95	21.97	0.1361	0.512830	3.7	0.65	0.512634	208	5.4
04DT14-1	Leucogabbro	2.64	12.45	0.1283	0.512778	2.7	0.69	0.512603	208	4.5
04DT24-1	Schist	1.95	6.55	0.1800	0.512951	6.1	N/A	0.512570	323	6.8
04DT25-1	Schist	2.66	9.79	0.1640	0.512922	5.5	N/A	0.512575	323	6.9
04AT219-1R*		2.09	6.99	0.1807	0.512952	6.1	N/A	0.512692	208	6.6

*R denotes repeated Nd analysis only, it is not a true replicate.

granite has been derived from or traveled through different source rocks than those comprising Stikinia. In addition, the significant difference between model ages of the megacrystic granite and Lewes River Arc also suggests different crustal sources.

MAJOR AND TRACE ELEMENT GEOCHEMISTRY

A first-order geochemical classification of magmatic rocks from Stikinia can be made using major element oxide ratios. Since many of the major elements are considered mobile during alteration and metamorphism, it is useful to compare the major element compositional classification with trace element classification schemes as a test of the mobility in the geochemical system. The minor and trace elements Ti, Zr, Hf, Nb, Ta, Y, Th, Ce, and most rare-earth elements (REE) are considered, among others, to be immobile during alteration and metamorphism up to green-schist facies (Pearce 1996; Winchester & Floyd 1977). The immobility of these elements can therefore be exploited to determine the tectonic environment in which the magmas were emplaced. In particular, Th is an effective discriminator of volcanic-arc basalts because it becomes selectively enriched during magmatism and is relatively unaffected by alteration and low-grade metamorphism (Pearce 1996; Wood *et al.* 1979).

A total of nine samples from Stikinia were analysed for major and trace element geochemistry. Samples were chosen to assess early (Takhini Assemblage), late (Lewes River Arc), syn-tectonic (THSZ), and post-tectonic (cross-cutting pluton) rocks of Stikinia. Like the suite of samples for Sm-Nd analysis, the Lewes River Arc is represented by samples of pyroxenite (n=3), leucogabbro (n=1) and augite-phenocrystic

basalt (n=1). Likewise, mylonite from the THSZ was also sampled (n=3). Samples from the Takhini Assemblage and megacrystic granite (n=1) are also identical to the ones previously described. Samples were analysed by X-Ray Flourescence for major and trace elements at XRAL Laboratories (A Division of SGS Canada Inc.) in North York, Ontario. A further nine samples, including leucogabbro, pyroxenite and a suite of samples from the Takhini Assemblage, were analysed in conjunction with this study and described by Turner (2005). Analytical techniques are discussed in Turner (2005). The combined major and trace element data is presented in Tables 3.3 and 3.4. Full geochemical analyses are presented in Appendix II.

Discrimination diagrams

The Total Alkalis versus Silica (TAS) discrimination diagram of Le Bas *et al*. (1986) uses the oxides ratio $Na_20 + K_2O$ versus SiO_2 to classify igneous rocks. A TAS plot of the Lewes River Arc, THSZ, and Takhini Assemblage shows a range of basaltic compositions (Fig. 3.3a). The classification of Winchester & Floyd (1977) which uses the trace element ratios Zr/TiO_2 versus Nb/Y to classify chemical compositions is consistent with the results shown on the TAS diagram (Fig. 3.3b).

The Th-Hf-Nb diagram of Wood *et al.* (1979) distinguishes between different mid-ocean ridge basalts (MORB), destructive plate-margin basalts (volcanic-arc), and within-plate (oceanic-island) basalts. A Th-Hf-Nb plot of volcanic rocks of the Lewes River Arc, THSZ, and Takhini Assemblage samples shows the majority of samples plotting in the volcanic-arc field, however, one sample of the Takhini Assemblage plots

Table 3.3. Selected major and trace element geochemistry results for volcanic and metamorphosed rocks of the Lewes River Arc, THSZ and Takhini Assemblage.

Sample:	**04AT 219-1**	**04AT 207-1**	**04DT 6-1**	**04AT 229-2**	**04DT 22-1***	**04DT 23-1***	**04DT 24-1***	**04DT 25-1***	**04DT 28-1***
Unit:	P	THSZ	THSZ	THSZ	TA	TA	TA	TA	TA
Rock type:	Augite basalt	Mylonite	Mylonite	Mylonite	Mylonite	Mylonite	Schist	Schist	Meta-basalt
Major elements (wt. %)									
Na_2O	1.89	3.2	1.99	3.21	4.3	3.69	2.41	2.04	3.19
MgO	9.2	4.76	5.07	5.5	5.46	5.51	12.11	10.22	8.57
Al_2O_3	11.65	15.41	19.92	17.08	16.09	22.06	11.63	11.44	15.89
SiO_2	47.53	54.69	46.46	47.7	48.9	44.58	48.43	47.59	47.65
K_2O	2.05	1.66	2.15	0.84	0.55	1.05	0.49	0.82	0.44
CaO	11.45	6.36	5.72	11.23	9.82	9.84	11.97	11.69	9.65
TiO_2	0.67	1.28	1.16	0.94	1.75	1.04	0.55	0.62	0.89
Cr_2O_3	0.06	0.01	0.01	0.01	n/d	n/d	n/d	n/d	n/d
MnO	0.182	0.147	0.171	0.187	0.18	0.15	0.18	0.18	0.23
FeO	n/d	n/d	n/d	n/d	11.78	9.93	9.81	11.52	10.89
P_2O_5	0.28	0.31	0.35	0.25	0.18	0.2	0.17	0.25	0.25
LOI	1.711	1.592	5.022	2.141	0.67	1.6	1.72	3.24	1.92
Total	98.44	99.73	98.75	99.74	99.7	99.68	99.48	99.63	99.59
Trace elements (ppm)									
Ba	510	274	974	310	285.33	117.71	107.27	217.42	73.95
V	268	260	231	344	269.68	225.98	237.19	228.60	239.86
Rb	39	28	38	17	11.15	1.84	2.61	5.02	0.90
Sr	311	569	427	1020	632.65	202.25	529.55	394.74	277.53
Y	13.8	30.6	20.2	16.6	12.40	24.25	8.25	7.58	7.76
Zr	35	141	119	50	6.69	6.83	4.56	6.57	27.39
Nb	1.1	7.2	4.8	1.5	2.53	3.16	0.96	0.86	2.03
Cs	1.9	2.7	1.1	0.8	0.75	0.07	0.07	0.15	0.07
La	3.8	14.8	15.9	8.94	7.22	3.98	3.47	5.53	5.91
Ce	8.88	33.1	34.8	19	18.13	13.83	8.27	13.17	15.26
Pr	1.37	4.71	4.8	2.66	2.36	2.36	1.22	1.80	2.11
Nd	6.62	20.3	20.1	11.9	12.42	13.96	6.28	9.18	10.59
Sm	2.00	5.35	4.67	3.21	3.25	4.4	1.83	2.43	2.60
Eu	0.772	1.68	1.57	1.19	1.18	1.6	0.64	0.81	0.92
Gd	2.51	5.71	4.51	3.49	2.23	5.24	1.73	1.69	2.35
Tb	0.43	0.97	0.71	0.55	0.50	0.88	0.34	0.37	0.37
Dy	2.54	5.29	3.74	3.08	3.03	5.55	2.04	2.14	2.13
Ho	0.51	1.05	0.73	0.59	0.59	1.11	0.40	0.41	0.40
Er	1.41	3.07	1.99	1.65	1.75	3.29	1.14	1.14	1.16
Tm	0.203	0.453	0.293	0.237	0.24	0.45	0.15	0.16	0.15
Yb	1.29	2.88	1.84	1.55	1.53	2.74	0.98	0.96	0.96
Lu	0.197	0.429	0.265	0.234	0.23	0.42	0.14	0.14	0.14
Hf	1	3.4	2.9	1.4	0.38	0.52	0.34	0.42	1.11
Ta	0.07	0.51	0.31	0.12	0.18	0.23	0.06	0.05	0.12
Pb	13	17	9	12	7.23	4.77	4.48	4.52	4.65
Th	0.53	1.63	1.95	1.26	0.91	0.1	0.36	0.58	0.62
U	0.39	0.83	1.23	0.75	1.12	0.09	0.39	0.42	0.46
Ti	n/d	n/d	n/d	n/d	4105.46	6954.6	2555.53	3165.27	3265.75
Cr	320	20	30	20	38.28	270.11	482.19	337.77	108.13
Co	42	23	29	31	32.32	43.99	49.87	48.16	28.31
Ni	70	20	20	20	28.51	100.53	158.15	90.54	38.21
Cu	110	90	100	90	106.44	31.12	134.60	124.38	112.42
Zn	90	120	130	70	81.51	113.06	72.81	91.88	68.74
Ga	13	19	23	19	50.17	31.05	23.02	34.31	28.62

Note: P, Povoas Formation; THSZ, Tally Ho shear zone; TA, Takhini Assemblage. Sample analyses denoted with * were taken from Turner (2005) and analyzed at Cominco Laboratories, Richmond, BC. All other samples were analysed by XRAL Laboratories - A Division Of SGS Canada Inc. Table is a compilation of selected trace elements; full analyses are presented in Appendix II.

Table 3.4. Selected major and trace element geochemistry results for the leucogabbro, pyroxenite and megacrystic granite samples.

Sample:	04AT 251-1	04DT 14-1*	04DT 14-2*	04AT 58-3*	04AT 231-3	04AT 231-4	04DT 004	04AT 339-2	04AT 253-1
Unit:	Leuco-gabbro	Leuco-gabbro	Leuco-gabbro	Leuco-gabbro	pyroxenite	pyroxenite	pyroxenite	pyroxenite	Megacrystic granite
Major elements (wt. %)									
Na_2O	3.08	3.15	0.89	4.42	0.08	0.14	0.31	0.71	8.88
MgO	4.3	6.73	10.47	2.51	19	19.36	16.36	16.61	0.79
Al_2O_3	16.18	13.4	6.69	20.39	1.68	1.76	2.2	9.53	18.51
SiO_2	50.84	47.72	43.47	52.95	51.42	50.14	44.75	47.49	62.14
K_2O	3.84	1.35	1.11	2.83	0.08	0.03	0.14	0.35	0.49
CaO	7.59	9.82	12.98	7.61	19.06	20.84	20.18	11.52	3.67
TiO_2	0.96	1.15	1.54	0.5	0.21	0.2	0.27	0.44	0.24
Cr_2O_3	<0.01	n/d	n/d	n/d	0.27	0.28	0.1	0.23	<0.01
MnO	0.21	0.23	0.4	0.11	0.12	0.122	0.114	0.19	0.07
FeO	10.32	14.25	20.39	6.25	5.8	n/d	n/d	n/d	2.91
P_2O_5	0.69	0.6	0.73	0.31	<0.01	0.01	0.01	0.05	0.08
LOI	1.45	1.37	0.81	1.64	1	1.175	8.369	2.746	1.6
Total	99.64	99.81	99.64	99.81	99.5	99.58	98.72	100	99.18
Trace elements (ppm)									
Sc	32.17	3.20	12.07	15.40	75.78	n/d	n/d	n/d	12.45
V	282.15	111.10	460.11	342.17	71.67	59	83	188	37.11
Rb	74.66	23.34	26.64	16.90	1.05	1	2	9	9.47
Sr	614.34	629.13	255.54	499.93	44.41	43	56	176	712.62
Y	21.14	2.79	31.11	16.98	2.50	2.5	3.3	9.7	9.61
Zr	55.01	6.47	25.84	11.26	1.86	6	4	23	98.64
Nb	3.12	1.70	3.50	2.03	0.12	0.7	0.3	1.2	9.33
Mo	0.93	1.04	2.15	0.95	n/d	2	2	2	0.25
Cs	0.61	0.64	2.02	1.20	0.31	0.4	0.1	0.3	0.27
Ba	980.76	539.93	212.06	342.81	3.37	8	46	208	66.93
La	17.01	4.63	19.60	13.84	0.28	0.42	0.25	3.12	16.39
Ce	38.38	11.20	50.72	34.12	0.91	1.18	0.9	6.58	28.38
Pr	4.99	1.31	7.21	4.69	0.18	0.22	0.21	0.95	2.91
Nd	20.82	6.18	32.82	21.85	1.09	1.35	1.51	4.55	9.27
Sm	4.91	1.30	7.94	5.12	0.36	0.47	0.58	1.3	1.59
Eu	1.49	0.66	1.38	1.29	0.13	0.169	0.21	0.506	0.52
Gd	4.98	1.24	7.67	3.79	0.53	0.58	0.73	1.56	1.53
Tb	0.69	0.17	1.25	0.74	0.09	0.1	0.13	0.27	0.22
Dy	4.19	1.00	7.32	4.28	0.49	0.55	0.71	1.67	1.45
Ho	0.83	0.19	1.40	0.80	0.11	0.1	0.13	0.34	0.30
Er	2.29	0.54	4.01	2.25	0.24	0.25	0.32	0.99	0.99
Tm	0.32	0.07	0.55	0.30	0.03	0.035	0.044	0.146	0.16
Yb	2.02	0.46	3.57	1.89	0.21	0.22	0.26	0.94	1.28
Lu	0.30	0.07	0.52	0.28	0.03	0.03	0.038	0.148	0.20
Hf	1.70	0.33	1.61	0.77	0.08	0.2	0.2	0.6	3.02
Ta	0.19	0.11	0.22	0.13	0.02	0.06	0.05	0.07	0.59
Pb	10.52	11.92	3.42	7.37	1.62	5	5	5	8.70
Th	2.62	0.91	3.04	1.73	0.18	0.05	0.05	0.4	5.71
U	1.32	1.14	1.81	1.10	0.07	0.06	0.04	0.23	2.89
Ti	5976.33	2016.33	6614.16	4517.78	1178.77	n/d	n/d	n/d	1309.32
Cr	58.48	13.91	69.21	31.83	2049.38	1520	530	1440	19.66
Co	28.40	12.98	57.96	36.63	44.48	38	35	49	4.45
Ni	16.06	10.60	45.51	27.05	128.35	120	110	210	3.01
Cu	100.49	62.51	218.64	150.09	2.25	10	10	30	4.06
Zn	96.84	56.44	198.28	121.73	34.97	30	30	70	30.64
Ga	1.37	2.95	9.32	6.54	2.11	2.7	2.9	1.7	1.69

Note: Sample analyses denoted with * were taken from Turner (2005) and analyzed at Cominco Laboratories, Richmond, BC. All other samples were analysed by XRAL Laboratories - A Division Of SGS Canada Inc. Table is a compilation of selected trace elements; full analyses are presented in Appendix II.

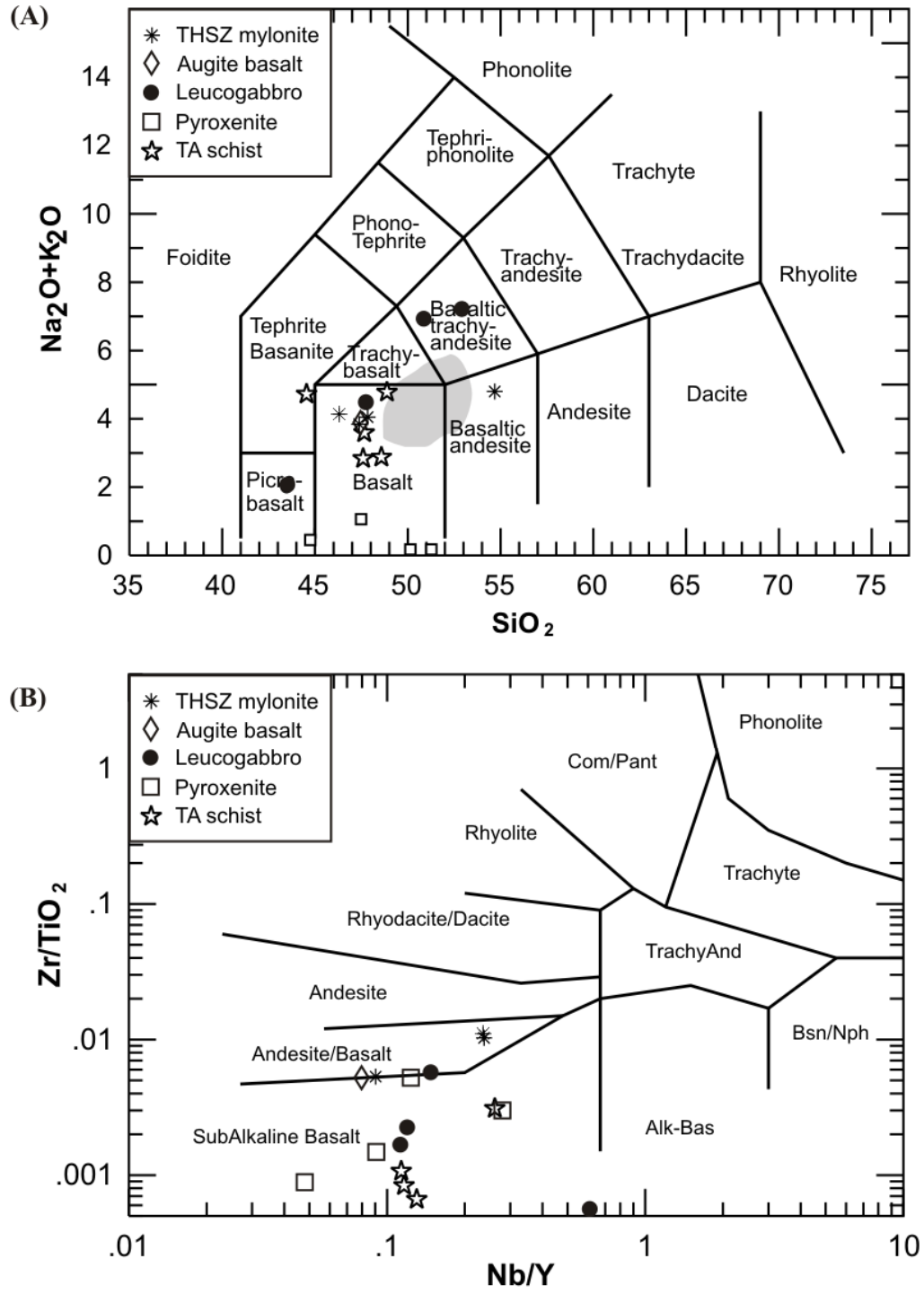

Figure 3.3. Geochemical discrimination diagrams of different parts of Stikinia. (A) TAS diagram of Le Bas *et al*. (1986). Shaded area represents range of compositions of the Povoas Formation from Hart & Pelletier (1988), Hart & Radloff (1990), and Hart (1997); (B) Zr/TiO2-Nb/Y diagram of Winchester & Floyd (1977).

in the E-MORB field (Fig. 3.4). The reason for this anomalous data is not yet known but may be due to alteration in the samples or inconsistencies between analytical techniques. Alternatively, fractionation processes or an abundance of Fe-Ti oxide minerals in the samples may have caused the data to plot erroneously (Rollinson 1993).

The Nb-Y discrimination diagram of Pearce *et al*. (1984) differentiates between volcanic-arc and syn-collisional granite, within-plate granite, and ocean-ridge granite. The megacrystic granite that intrudes both Stikinia and the YTT plots in the volcanic-arc/syn-collisional field (Fig. 3.5). The data point is consistent with geochemical data from the Little River Batholith, another Early Jurassic pluton that stitches together YTT and Stikinia (Hart 1997).

REE

The REE are generally immobile and resistant to alteration and low-grade metamorphism and are thus useful petrogenetic indicators (Rollinson 1993). A chondrite-normalized REE plot (Sun & McDonough 1989) of mylonitic and schistose rocks of the THSZ and Takhini Assemblage shows a low negative slope indicating enrichment in the light-REE and an enriched mantle source (Fig 3.6a). Samples from the Lewes River Arc show two differing patterns: a low negative slope of all the leucogabbro, augite-phenocrystic basalt and one pyroxenite sample, and an upward bowed pattern of remaining pyroxenite samples (Fig 3.6b). The low negative slope indicates a relative enrichment of the light-REE to the heavy-REE, reflecting an enriched mantle source. The

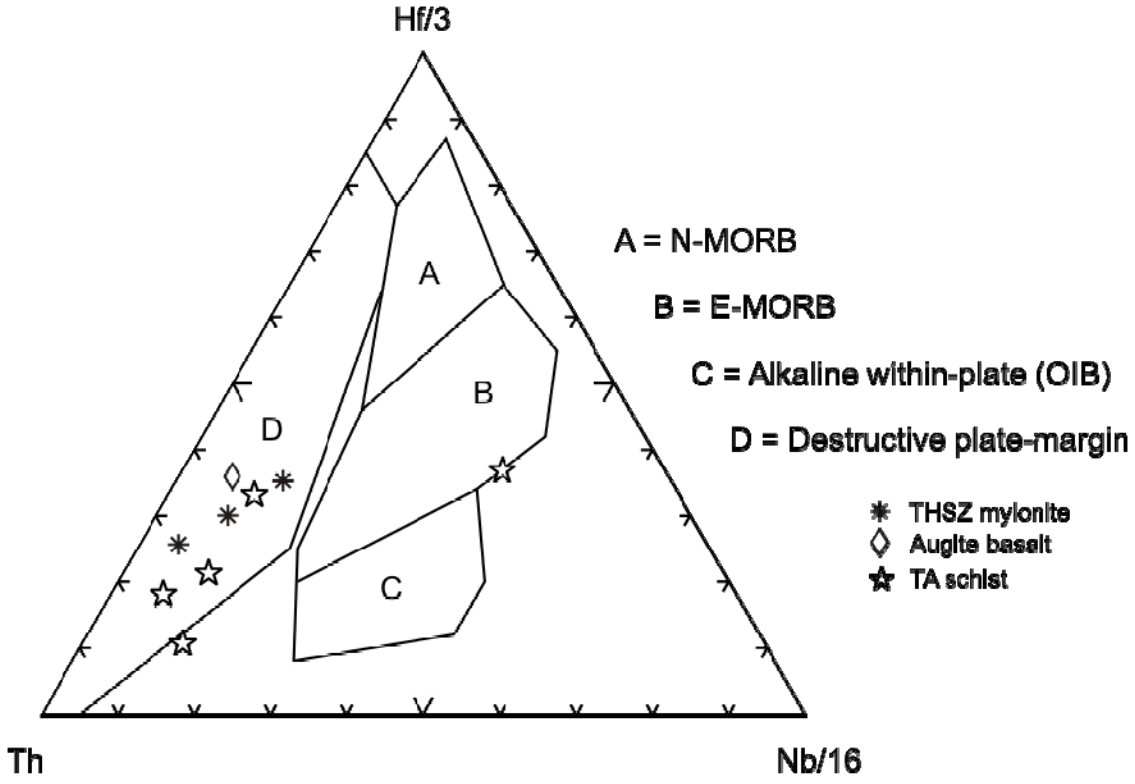

Figure 3.4. Th-Hf/3-Nb/16 discrimination diagram of Wood *et al.* (1979).

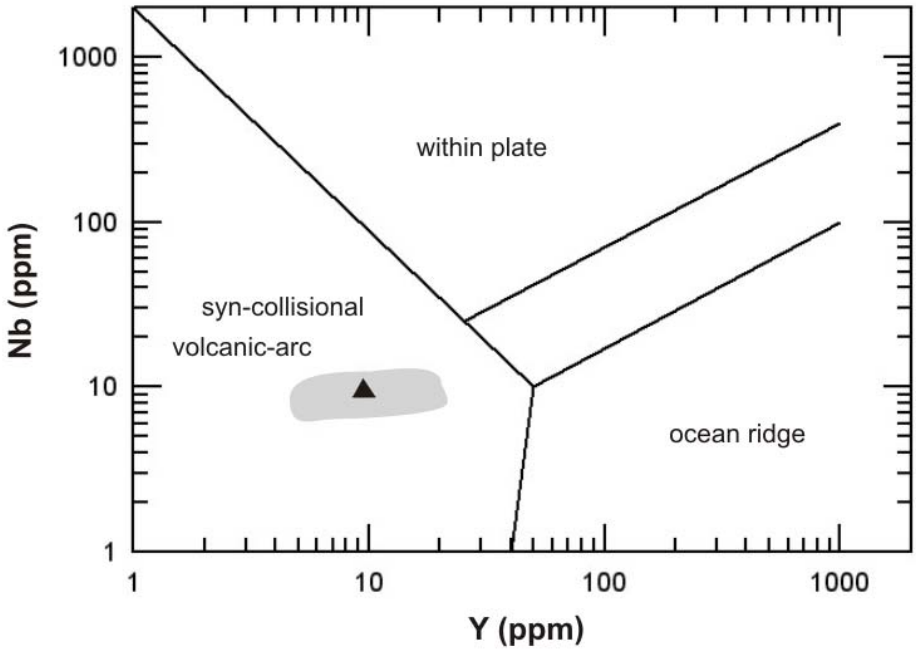

Figure 3.5. Nb-Y discrimination diagram for megacrystic granite (04AT253-1; from Pearce *et al*. 1984). Shaded area represents range of analyses from the Little River batholith (Hart 1997).

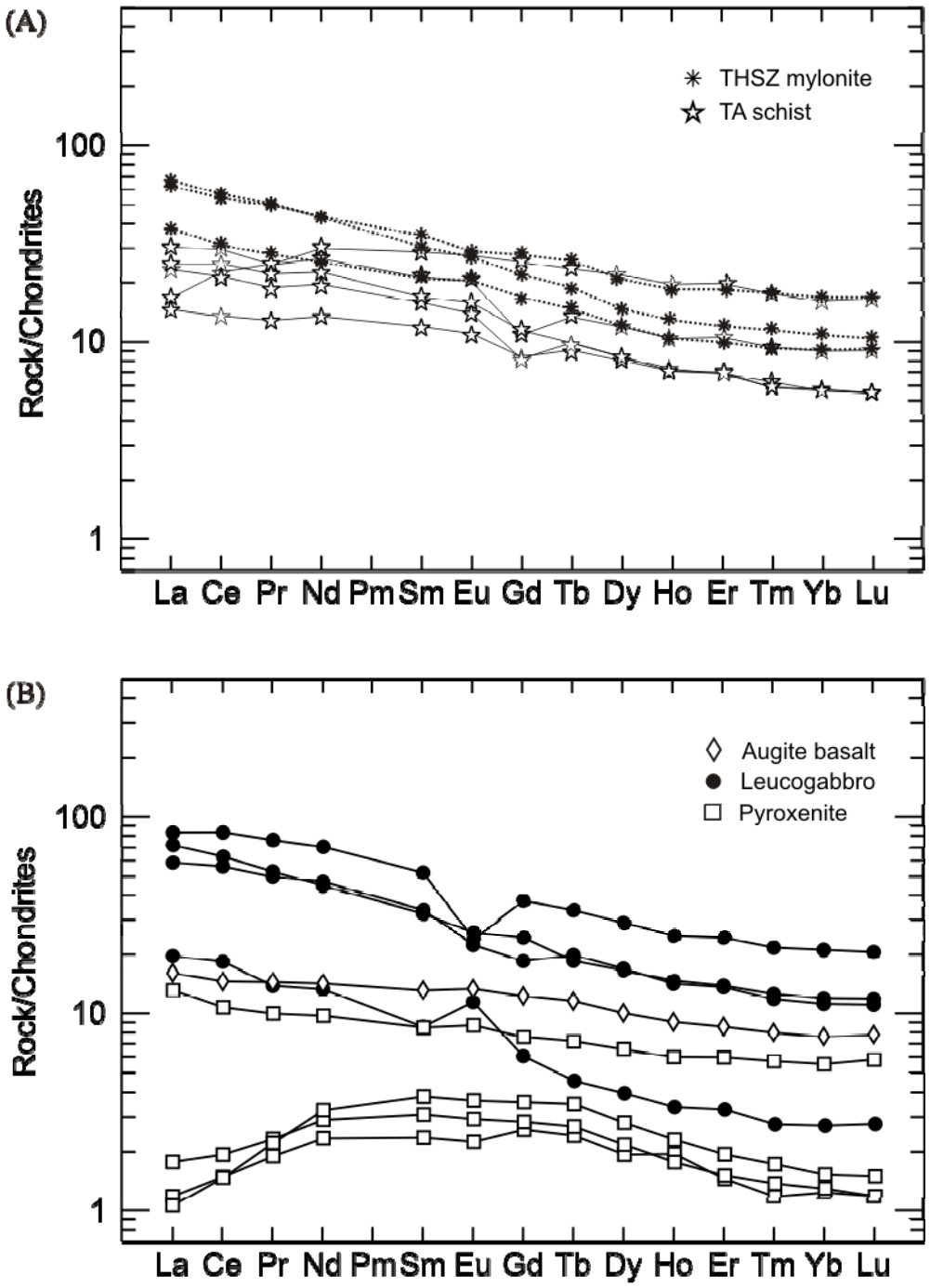

Figure 3.6. Chondrite-normalized REE patterns for (A) the THSZ and Takhini Assemblage (TA); and (B) Lewes River Arc. Normalizing values from s-Sun & McDonough (1989).

bowed pattern of pyroxenite samples indicates enrichment in the middle-REE relative to the light- and heavy-REE. The chief component of pyroxenite samples is clinopyroxene which preferentially incorporates the middle-REEs during crystallization, which may explain the bow-shaped pattern; hornblende also preferentially partitions into the middle-REEs and may also give rise to the bowed pattern of the REE plot (Rollison 1993).

The distribution of leucogabbro samples higher on the chondrite-normalized graph than the pyroxenite samples indicates a higher relative enrichment in light- and heavy-REE. If fractionation in the magma chamber occurred, the melt would have become enriched in the REE relative to the cumulus because the REE are moderately to highly incompatible (Rollinson 1993). The leucogabbro samples, therefore, appear to reflect a more evolved component of the original magma chamber.

Trace element spider diagrams

The geochemical signature of volcanic-arc rocks is characterized by a significant negative Nb anomaly relative to Th and Ce, a signature commonly explained as the result of wet melting above a subducting oceanic slab (Pearce 1996). Enrichment in Th and Ce indicates that dehydration and partial melting processes were involved in the generation of magma, while Nb was preferentially retained in the down-going slab (Pearce 1996). Primitive mantle normalized plots (Sun & McDonough 1989) of Lewes River Arc, THSZ, and Takhini Assemblage rocks display the characteristic oceanic-arc signature which is consistent with the arc affinity indicated by the REE and primitive isotopic signature (Fig. 3.7a). The data set has a very similar distribution pattern and overlaps moderately well

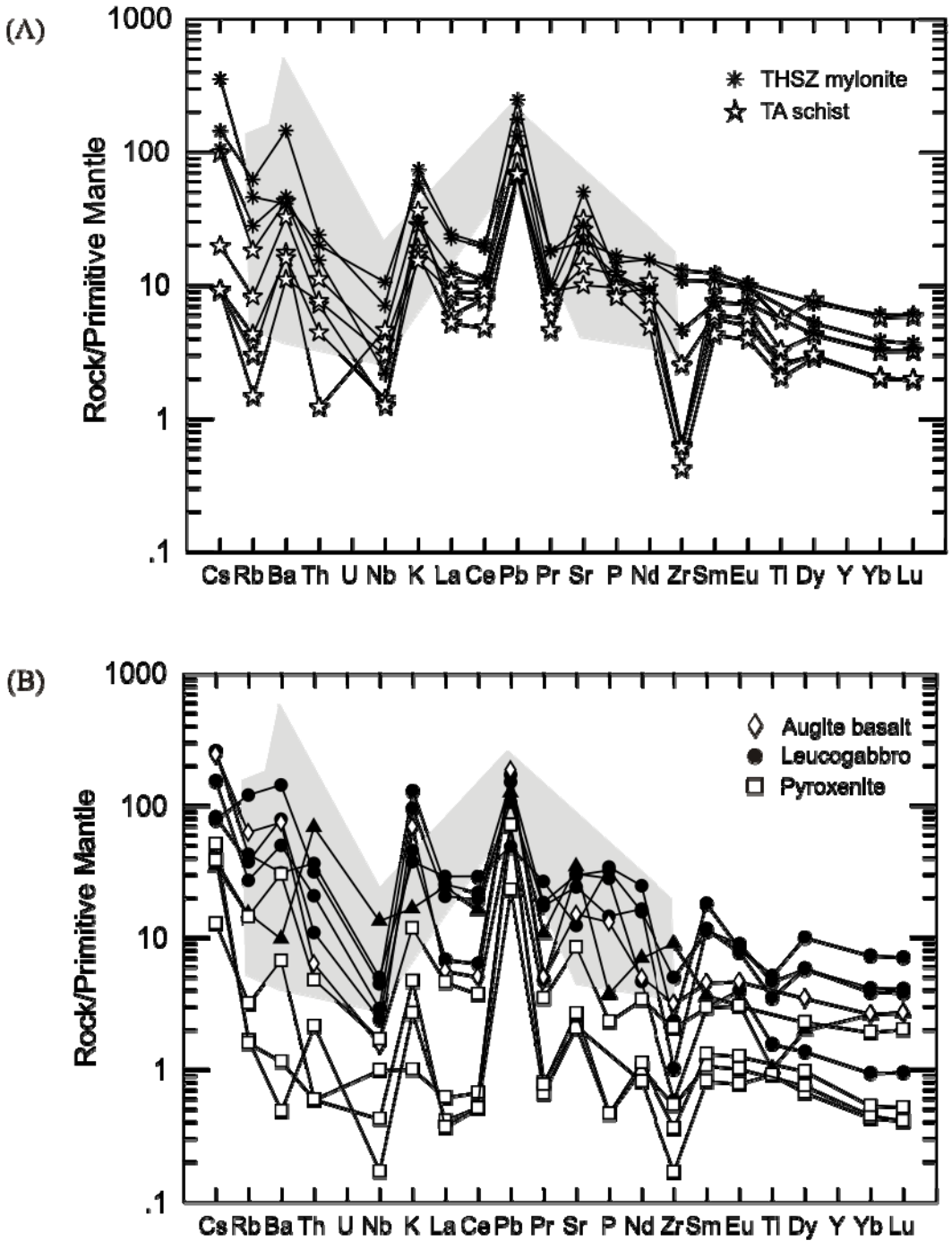

Figure 3.7. Primitive-mantle normalized trace element patterns of: (A) THSZ and Takhini Assemblage (TA); and (B) Lewes River Arc. Shaded area is bulk pattern from limited data set of the Povoas Formation extracted from Hart & Pelletier (1988), Hart & Radloff (1990), and Hart (1997). Normalizing values are from Sun & McDonough (1989).

with a limited data set from samples of the Povoas Formation (Hart 1997; Hart & Pelletier 1988; Hart & Radloff 1990).

Leucogabbro and pyroxenite samples have a similar distribution pattern on primitive mantle normalized diagram, however, the leucogabbro plots higher on the diagram than the pyroxenite (Fig. 3.7b). The pyroxenite samples lack a Ti anomaly, while the leucogabbro samples exhibit a negative Ti anomaly. These relationships are best explained as resulting from fractionational crystallization, with Ti being preferentially removed from the increasingly felsic, incompatible element-rich magma by the crystallization of a Ti-bearing mineral (probably magnetite).

DISCUSSION

Interpretation of major and trace element geochemistry of late Paleozoic to Upper Triassic magmatic rocks of northern Stikinia shows that the terrane was derived from an enriched mantle source and formed in an oceanic-arc setting. Analysis of Sm-Nd isotopic ratios indicate that Stikinia is a primitive terrane, neither composed of re-worked continental rocks nor of magmas that have passed through or interacted with evolved crust. Hence, geochemistry and isotopic ratios are consistent and confirm that Stikinia developed on oceanic crust, distal from any continental margin. Models of Stikinia forming on top of older sialic crust such as the YTT (Jackson *et al*. 1991) are therefore untenable.

To the west, the contact between Stikinia and the YTT is plugged by an early Middle Jurassic megacrystic granite pluton. Isotopic analysis of the granite shows that

magmatism occurred in the presence of or was derived from an evolved source, demonstrating that the isotopic character of the region changed from primitive to evolved sometime in the Lower Jurassic. This sudden shift in isotopic character is suggestive of a major tectonic event occurring in the Lower Jurassic in order to juxtapose primitive Stikinia against a more isotopically evolved source, presumably the YTT.

The THSZ, an east-verging intra-arc thrust fault within Stikinia, formed in response to the collision and records imbrication of the terrane during tectonic emplacement of YTT beneath Stikinia in the Upper Triassic to Lower Jurassic (Tizzard *et al. in press*; Chapter 2). Timing of tectonism is constrained by the age of a deformed cumulate pluton in the hanging wall of the shear zone (208 Ma) and by the age of the cross-cutting and undeformed megacrystic granite (172 Ma). Timing of terrane amalgamation, however, is further constrained by the intrusion of the Long Lake Plutonic Suite to the north of the THSZ that intrudes and stitches together Stikinia and the YTT in the Lower Jurassic (185 Ma) (Johnston *et al*. 1996; Hart 1997). The transition from primitive magmatic rocks in Stikinia to the evolved nature of the megacrystic granite is therefore consistent with the timing of formation of the THSZ and the tectonic emplacement of YTT beneath Stikinia; the presence of the YTT adjacent to and beneath Stikinia gave rise to the evolved isotopic character of the megacrystic granite (Fig. 3.8).

The movement of deep-seated arc rocks and potentially mantle peridotite along the THSZ to upper crustal levels and the exhumation and deposition of ultra-high pressure minerals from depths of ~100 kilometres in Laberge Group sedimentary rocks (Canil *et al.* 2006; MacKenzie *et al*. 2005) demonstrates that the collision of Stikinia and the YTT was thick-skinned (Tizzard *et al. in press*; Chapter 2). Flake-tectonic models of

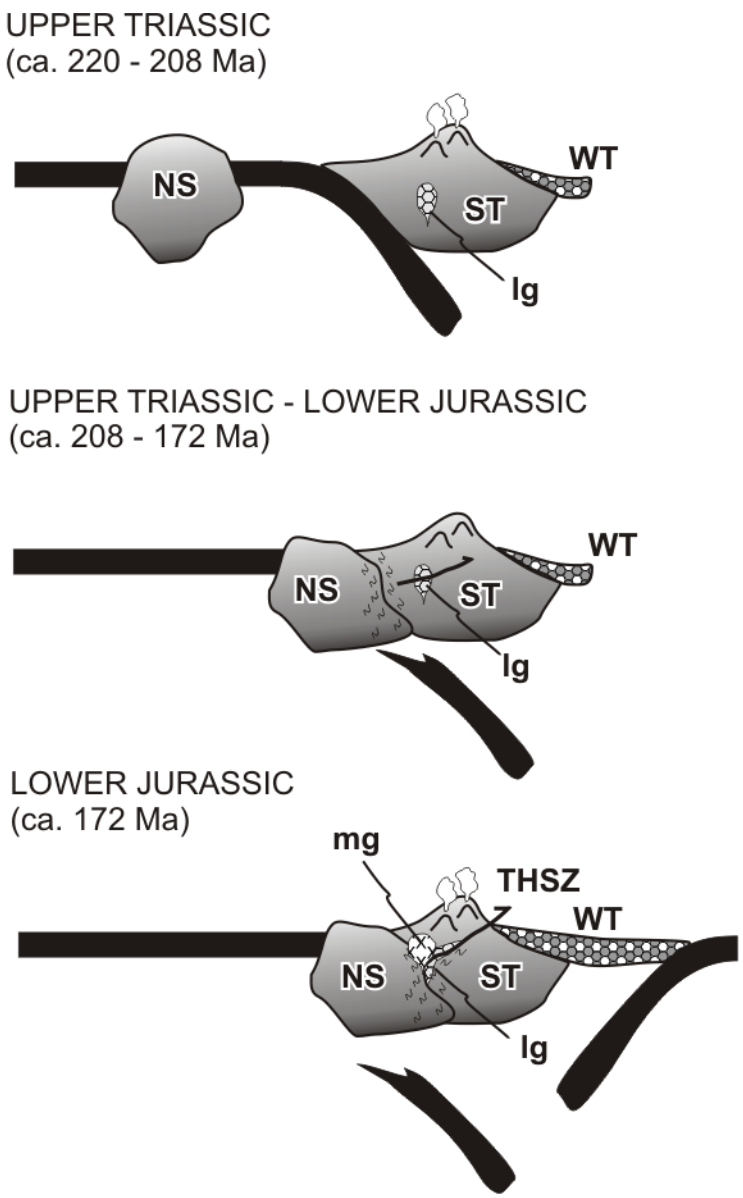

Figure 3.8. Schematic tectonic model showing the collision and underpinning of the Nisling Assemblage of the Yukon-Tanana Terrane beneath Stikinia in the Lower Jurassic (Tizzard *et al*. *in press*; Chapter 2). NS, Nisling Assemblage; ST, Stikinia; WT, Whitehorse Trough; THSZ, Tally Ho shear zone; lg, leucogabbro and pyroxenite units; mg, megacrystic granite unit.

the Canadian Cordillera predict a conveyor-like movement of allochthonous terranes carried in thin thrust sheets over a westward tapering basement wedge that extends nearly the width of the Cordillera (Cook *et al.* 2004; Snyder *et al*. 2002). These models de-emphasize the degree in which exotic oceanic-arc terranes like Stikinia have contributed to the overall growth of the continent; the allochthonous terranes are portrayed as thin flakes above the basement wedge and are volumetrically insignificant. Thick-skinned accretion of Stikinia, the largest of the allochthonous Cordilleran terranes, would however, constitute extensive continental growth accomplished by an exotic oceanic-arc.

CONCLUSIONS

Stikinia is a long-lived oceanic magmatic arc that formed outboard of the ancient continental margin throughout the Paleozoic and early Mesozoic. Geochemical and isotopic data confirm that no evolved crustal material was present during formation of the terrane until the collision and underpinning of the YTT beneath Stikinia in the Lower Jurassic. In contrast to the primitive nature of Stikine magmas, voluminous post-collision magmas intruding the boundary between Stikinia and the YTT are characterized by an evolved isotopic signature. This shift in isotopic character, owing to the tectonic emplacement of the YTT, confirms a tectonic link between the terranes in the Lower Jurassic.

Exhumation and deposition of ultra-high pressure minerals in the Whitehorse Trough and the movement of lower crust and potentially mantle rocks of Stikinia to upper crustal levels along the THSZ are evidence of thick-skinned collision between the YTT

and Stikinia. Hence, a thick section of juvenile Stikine crust, and not a thin sliver, was accreted to the YTT. Unlike predictions put forth by flake-tectonic models, thick-skinned collision and the underpinning of buoyant pericratonic terranes beneath primitive oceanic-arcs therefore contributed significantly to the westward growth of the continent in at least the Jurassic. Consequently, calculations of crustal growth made assuming that accretion was thin-skinned likely significantly underestimate growth attributable to the accretion of allochthonous terranes like Stikinia.

REFERENCES CITED

Canil, D., Mihalynuk, M., & Charnell, C. 2006. Sedimentary record for exhumation of ultrahigh pressure (UHP) rocks in the northern Cordillera, British Columbia. *Geological Society of America Bulletin*, **118**, 1171-1184.

Colpron, M., Nelson, J.L., & Murphy, D.C. 2006. A tectonostratigraphic framework for the pericratonic terranes of the northern Cordillera. *In*: Colpron, M., & Nelson, J.L. (eds) Paleozoic Evolution and Metallogeny of Pericratonic Terranes at the Ancient Pacific Margin of North America, Canadian and Alaskan Cordillera. Special Paper 45, Geological Association of Canada, p. 1-23.

Cook, F.A., Clowes, R.M., Snyder, D.B., van der Velden, A.J., Hall, K.W., Erdmer, P. & Evenchick, C.A. 2004. Precambrian crust beneath the Mesozoic northern Canadian Cordillera discovered by Lithoprobe seismic reflection profiling. *Tectonics*, **23,** TC2010.

Currie, L., & Parrish, R.R. 1993. Jurassic accretion of Nisling terrane along the western margin of Stikinia, Coast Mountains, northwestern British Columbia. *Geology*, **21**, 235-238.

Dostal, J., Gale, V., & Church, B. 1999. Upper Triassic Takla Group volcanic rocks, Stikine Terrane, north-central British Columbia: geochemistry, petrogenesis, and tectonic implications. *Canadian Journal of Earth Sciences,* **36,** 1483-1494.

Erdmer, P., Moore, J.M., Heaman, L., Thompson, R.I., Daughtry, K.L. & Creaser, R.A. 2002. Extending the ancient margin outboard in the Canadian Cordillera: record of Proterozoic crust and Paleocene regional metamorphism in the Nicola horst, southern British Columbia. *Canadian Journal of Earth Sciences*, **39**, 1605-1623.

Erdmer, P., Mihalynuk, M.G., Gabrielse, H., Heaman, L.M. & Creaser, R.A. 2005. Mississippian volcanic assemblage conformably overlying Cordilleran miogeoclinal strata, Turnagain River area, northern British Columbia, is not part of an accreted terrane. *Canadian Journal of Earth Science*, **42**, 1449-1465.

Hart, C.J.R. 1997. A Transect Across Northern Stikinia: Geology of the Northern Whitehorse Map Area, Southern Yukon Territory (105D/13-16): Whitehorse YT, Exploration and Geological Services Division, Yukon Region, Indian and Northern Affairs Canada, 112 p.

Hart, C.J.R. & Pelletier, K.S. 1989. Geology of Carcross (105D/2) and part of Robinson (105D/7) map areas, Open File 1989-1: Whitehorse YT, Exploration and Geological Services Division, Indian and Northern Affairs Canada, Yukon Region, p. 92.

Hart, C.J.R. & Radloff, J.K. 1990. Geology of Whitehorse, Alligator Lake, Fenwick Creek, Carcross and part of Robinson map areas (105D/11, 6, 3, 2, & 7), Open File 1990-4: Whitehorse, Indian and Northern Affairs Canada, p. 113.

Jackson, J.L., Gehrels, G.E., Patchett, J.P., & Mihalynuk, M.G. 1991. Stratigraphic and isotopic link between the northern Stikine terrane and an ancient continental margin assemblage, Canadian Cordillera. *Geology*, **19**, 1177-1180.

Johnston, S.T., & Canil, D. 2007. Crustal structure of southwest Yukon, northern Cordillera: Implications for crustal growth in a convergent margin orogen. *Tectonics*, **26**, TC1006.

Johnston, S.T., Mortensen, J.K., & Erdmer, P. 1996. Igneous and metaigneous age constraints for the Aishihik metamorphic suite, southwest Yukon. *Canadian Journal of Earth Sciences*, **33**, 1543-1555.

Le Bas, M.J., Le Maitre, R.W., Streckeisen, A., & Zanettin, B. 1986. A chemical classification of volcanic rocks based on the total alkali-silica diagram. *Journal of Petrology*, **30**, 1299-1312.

MacKenzie, J.M., Canil, D., Johnston, S.T., English, J., Mihalynuk, M.G., & Grant, B. 2005. First evidence for ultrahigh-pressure garnet peridotite in the North American Cordillera. *Geology*, **33**, 105-108.

McClelland, W.C., Gehrels, G.E., Samson, S.D., & Patchett, P.J. 1992. Structural and geochronologic relations along the western flank of the Coast Mountains batholith: Stikine River to Cape Fanshaw, central southeastern Alaska. *Journal of Structural Geology*, **14**, 475-489.

Mezger, J., Chacko, T. & Erdmer, P. 2001. Metamorphism at a late Mesozoic accretionary margin: a study from the Coast Belt of the North American Cordillera. *Journal of Metamorphic Geology*, **19**, 121-137.

Monger, J. W. H., Wheeler, J. O., Tipper, H. W., Gabrielse, H., Harms, T., Struik, L. C., Campbell, R. B., Dodds, C. J., Gehrels, G. E., & O'Brien, J. 1991. Upper Devonian to Middle Jurassic assemblages - Part B. Cordilleran terranes. *In:* Gabrielse, H., and Yorath, C. J. (eds) Geology of the Cordilleran Orogen in Canada: The Geology of North America: Denver, Colorado, Geological Society of America, p. 281-327.

Mortensen, J.K. 1992. Pre-mid-mesozic tectonic evolution of the Yukon-Tanana terrane, Yukon and Alaska. *Tectonics*, **11**, 836-853.

Pearce, J. A. 1996. A user's guide to basalt discrimination diagrams. *In:* Wyman, D. A., (ed.) Trace element geochemistry of volcanic rocks: Applications for massive sulphide exploration. Geological Association of Canada, Short Course Notes, p. 79-113.

Pearce, J.A., Harris, N.B.W., & Tindle, A.G. 1984. Trace element discrimination diagrams for the tectonic interpretation of granitic rocks. *Journal of Petrology*, **25**, 956-983.

Rollinson, H. 1993. Using Geochemical Data: Evaluation, Presentation, Interpretation, Prentice Hall, Toronto, 352 p.

Samson, S., McClelland, W.C., Patchett, P.J., Gehrels, G.E. & Anderson, R.G. 1989. Evidence from neodymium isotopes for mantle contributions to Phanerozoic crustal genesis in the Canadian Cordillera. *Nature*, **337**, 705-709.

Snyder, D.B., Clowes, R.M., Cook, F.A., Erdmer, P., Evenchick, C.A., van der Velden, A.J. & Hall, K.W. 2002. Proterozoic prism arrests suspect terranes: Insights into the ancient Cordilleran margin from seismic reflection data. *GSA Today*, **12,** 4-10.

Sun, S., & McDonough, W. F. 1989. Chemical and isotopic systematics of oceanic basalts: Implications for mantle composition and processes. *In:* Saunders, A. D., & Norry, N. J. (eds) Magmatism in the ocean basins, Geological Society of London, p. 313-345.

Tizzard, A.M., Johnston, S.T., & Heaman, L.M. *in press*. Arc imbrication during thick-skinned collision within the northern Cordilleran accretionary orogen, Yukon, Canada. *Geological Society of London.*

Turner, D. 2005. Geochemical and Petrological Analysis of the Tally Ho Shear Zone and Takhini Deformation Zone, South Central Yukon. Unpublished B.Sc. thesis, University of Victoria, 67p.

Unterschutz, J.L., Creaser, R.A., Erdmer, P., Thompson, R.I., & Daughtry, K.L. 2002. North American margin origin of Quesnel terrane strata in the southern Canadian Cordillera: Inferences from geochemical and Nd isotopic characteristics of Triassic metasedimentary rocks. *Geological Society of America Bulletin*, **114**, 462-475.

Winchester, J. A., & Floyd, P. A. 1977. Geochemical discrimination of different magma series and their differentiation products using immobile elements. *Chemical Geology*, **20**, 325-343.

Wood, D.A., Joron, J., & Treuil, M. 1979. A re-appraisal of the use of trace elements to classify and discriminate between magma series erupted in different tectonic settings. *Earth and Planetary Science Letters*, **45**, 326-336.

Wood, D. A. 1980. The application of a Th-Hf-Ta diagram to problems of tectonomagmatic classification and to establishing the nature of crustal contamination of basaltic lavas of the British Tertiary volcanic province. *Earth and Planetary Science Letters*, **50**, 11-30.

CHAPTER 4

CONCLUSIONS

CONCLUSIONS

Detailed mapping and geochronology of the western margin of Stikinia in southern Yukon have shown that the THSZ is an intra-arc shear zone within Stikinia that developed in response to the thick-skinned collision and underpinning of the Nisling Assemblage of the YTT beneath Stikinia in the Lower Jurassic. The THSZ is therefore not a primary terrane bounding structure. Uranium-Pb zircon dating of a deformed leucogabbro caught up in the deformation in the THSZ, and an undeformed cross-cutting pluton, provide constraints on the maximum (208 Ma) and minimum (173 Ma) timing of movement along the THSZ. Kinematic indicators indicate that the shear zone is an east-vergent thrust fault that juxtaposed a deep-seated pyroxenite-gabbro cumulate intrusion on top of a package of upper crustal volcanic and volcaniclastic rocks of the Lewes River Group. Entry of the buoyant pericratonic Nisling Assemblage into the Stikine subduction zone, in response to closure of oceanic lithosphere continuous with the Nisling Assemblage by subduction beneath Stikinia, resulted in the cessation of arc magmatism in the Lewes River Arc, and led to imbrication of Stikinia along the THSZ. Tectonic burial of the Nisling Assemblage beneath the thickened crust of Stikinia was followed by return of the buoyant continental lithosphere to the near surface, explaining the exhumation and deposition of ultra-high pressure minerals eastwards into the Whitehorse Trough. In the Lower Jurassic, the Whitehorse Trough also evolved from a back-arc basin into a foreland basin. The Takhini deformation zone to the north and the Wann River shear zone to the south of the THSZ are additional high-strain zones along the western margin of Stikinia that may be tectonically-linked to the THSZ. Post-tectonic brittle faulting and magmatism have obscured the primary contact between the Nisling

Assemblage and Stikinia in southern Yukon and make it difficult to determine if along-strike Takhini and Wann River shear zones are correlative structures that developed at the same time as the THSZ, or if they owe their origin to other processes that affected the west margin of Stikinia.

Whole rock and trace element geochemistry and a Sm-Nd isotopic analysis of pre-, syn- and post-tectonic magmatic rocks of Stikinia have shown that Stikinia was a primitive oceanic arc that developed in the absence of any significant amount of evolved continental crust. In contrast, a megacrystic granite unit intruding the Stikinia-Nisling Assemblage boundary around 173 Ma has an evolved isotopic signature, demonstrating a shift in isotopic character of magmatic rocks from primitive to evolved in the Lower Jurassic. As such, the contact between Stikinia and the pericratonic Nisling Assemblage is confirmed as tectonic, and not stratigraphic. The shift in isotopic character was due to the tectonic emplacement of the Nisling Assemblage beneath Stikinia in the Lower Jurassic.

The THSZ appears to have transected the entire crust of Stikinia, while Nisling Assemblage lithosphere was emplaced at depth beneath the arc, indicating a thick-skinned collision. None of the geological relationships documented in the course of this research are consistent with collision involving the emplacement of thin, upper crustal flakes as suggested by interpretations of deep seismic sections across the Cordillera.

SUGGESTIONS FOR FUTURE WORK

- The interpretation of the THSZ as a lithospheric-scale intra-arc shear zone rests, in part, on the assumption of the pyroxenite and leucogabbro in the hangingwall

of the shear zone as originating in the lower crust of the Stikine magmatic arc. A detailed petrographic and pressure-temperature study is required to confirm the interpretation presented here.

- Detailed mapping and geochronology to the north and south of the THSZ is necessary to provide further constraints on the nature of tectonism along the western margin of Stikinia. For example, constraints on the age of the Takhini assemblage and timing of deformation in the Takhini deformation zone are few. Further work is necessary to determine if the Takhini deformation zone developed concurrently with the THSZ or is part of an earlier deformation event.
- We predict a complex evolution of the Whitehorse Trough. Our interpretation of the Whitehorse Trough as evolving from an early back-arc basin in the Upper Triassic to a foreland basin in the Lower Jurassic is testable with detailed mapping, stratigraphy, geochemistry and isotopic studies. A provenance study, for example, should highlight the change in sedimentation from dominantly volcanic and volcaniclastic source rocks of the Lewes River Arc to a mixed protolith shedding from deep crustal and exhumed pericratonic rocks to the west. Accordingly, the bulk radiogenic character of the Whitehorse Trough is predicted to become more evolved through time.
- There is a need to reassess interpretations of deep seismic profiles across the northern Cordillera. Current interpretations (Cook *et al.* 2004; Snyder *et al*. 2002) imply a westward continuity of North American basement and lithospheric mantle beneath the accreted terranes for most of the orogen. The accreted terranes are depicted as thin upper crustal flakes emplaced onto a passive and

little deformed lower plate. On the contrary, our findings indicate thick-skinned collision and deeply-rooted imbrication of Stikinia took place in the Early Jurassic.

REFERENCES CITED

Cook, F.A., Clowes, R.M., Snyder, D.B., van der Velden, A.J., Hall, K.W., Erdmer, P. & Evenchick, C.A. 2004. Precambrian crust beneath the Mesozoic northern Canadian Cordillera discovered by Lithoprobe seismic reflection profiling. *Tectonics*, **23,** TC2010.

Snyder, D.B., Clowes, R.M., Cook, F.A., Erdmer, P., Evenchick, C.A., van der Velden, A.J. & Hall, K.W. 2002. Proterozoic prism arrests suspect terranes: Insights into the ancient Cordilleran margin from seismic reflection data. *GSA Today*, **12,** 4-10.

APPENDIX I (MAP POCKET)

Geological Map of the Tally Ho Shear Zone

APPENDIX II

Geochemistry Results

WHOLE ROCK MAJOR ELEMENT GEOCHEMISTRY RESULTS

Sample	Na2O	MgO	Al2O3	SiO2	K2O	CaO	TiO2	Cr2O3	MnO	FeO	P2O5	LOI	Total
04AT207-1[€]	3.2	4.76	15.41	54.69	1.66	6.36	1.28	0.01	0.147	-	0.31	1.592	99.73
04AT219-1[€]	1.89	9.2	11.65	47.53	2.05	11.45	0.67	0.06	0.182	-	0.28	1.711	98.44
04AT229-2[€]	3.21	5.5	17.08	47.7	0.84	11.23	0.94	0.01	0.187	-	0.25	2.141	99.74
04AT231-3[€]	0.08	19	1.68	51.42	0.08	19.06	0.21	0.27	0.12	5.8	<0.01	1	98.72
04AT231-4[€]	0.14	19.36	1.76	50.14	0.03	20.84	0.2	0.28	0.122	-	0.01	1.175	100
04AT251-1[€]	3.08	4.3	16.18	50.84	3.84	7.59	0.96	<0.01	0.21	10.32	0.69	1.45	99.64
04AT253-1[€]	8.88	0.79	18.51	62.14	0.49	3.67	0.24	<0.01	0.07	2.91	0.08	1.6	99.5
04AT339-2[€]	0.71	16.61	9.53	47.49	0.35	11.52	0.44	0.23	0.19	-	0.05	2.746	99.93
04DT004[€]	0.31	16.36	2.2	44.75	0.14	20.18	0.27	0.1	0.114	-	0.01	8.369	99.18
04DT6-1[€]	1.99	5.07	19.92	46.46	2.15	5.72	1.16	0.01	0.171	-	0.35	5.022	98.75
04DT14-1*[£]	3.15	6.73	13.4	47.72	1.35	9.82	1.15	-	0.23	14.25	0.6	1.37	99.81
04DT14-2*[£]	0.89	10.47	6.69	43.47	1.11	12.98	1.54	-	0.4	20.39	0.73	0.81	99.5
04DT22-1*[£]	4.3	5.46	16.09	48.9	0.55	9.82	1.75	-	0.18	11.78	0.18	0.67	99.7
04DT23-1*[£]	3.69	5.51	22.06	44.58	1.05	9.84	1.04	-	0.15	9.93	0.2	1.6	99.68
04DT24-1*[£]	2.41	12.11	11.63	48.43	0.49	11.97	0.55	-	0.18	9.81	0.17	1.72	99.48
04DT25-1*[£]	2.04	10.22	11.44	47.59	0.82	11.69	0.62	-	0.18	11.52	0.25	3.24	99.63
04DT28-1*[£]	3.19	8.57	15.89	47.65	0.44	9.65	0.89	-	0.23	10.89	0.25	1.92	99.59
04AT58-3*[£]	4.42	2.51	20.39	52.95	2.83	7.61	0.5	-	0.11	6.25	0.31	1.64	99.58

[€]Sample analyses courtesy of the Yukon Geological Survey. X-Ray Flourescence analyses were performed at XRAL Laboratories-A Division Of SGS Canada Inc., North York, Ontario.
*From: Turner, D. 2005. Geochemical and Petrological Analysis of the Tally Ho Shear Zone and Takhini Deformation Zone, South Central Yukon. Unpublished B.Sc. thesis, University of Victoria, 67p. (part of this study)
[£]Analysis at Cominco Laboratories, Richmond, BC

WHOLE ROCK TRACE ELEMENT GEOCHEMISTRY RESULTS

Sample	Li	Ba	Sc	V	Rb	Sr	Y	Zr	Nb	Mo	Cs	Ba	La	Ce	Pr
04AT 207-1[€]	-	274	-	260	28	569	30.6	141	7.2	2	2.7	274	14.8	33.1	4.71
04AT 219-1[€]	-	510	-	268	39	311	13.8	35	1.1	2	1.9	510	3.8	8.88	1.37
04AT 229-2[€]	-	310	-	344	17	1020	16.6	50	1.5	2	0.8	310	8.94	19	2.66
04AT231-3[€]	7.09	-	75.78	71.67	1.05	44.41	2.50	1.86	0.12	-	0.31	3.37	0.28	0.91	0.18
04AT 231-4[€]	-	8	-	59	1	43	2.5	6	0.7	2	0.4	8	0.42	1.18	0.22
04AT251-1[€]	5.42	-	32.17	282.15	74.66	614.34	21.14	55.01	3.12	0.93	0.61	980.76	17.01	38.38	4.99
04AT253-1[€]	3.96	-	12.45	37.11	9.47	712.62	9.61	98.64	9.33	0.25	0.27	66.93	16.39	28.38	2.91
04AT 339-2[€]	-	208	-	188	9	176	9.7	23	1.2	2	0.3	208	3.12	6.58	0.95
04DT 004[€]	-	46	-	83	2	56	3.3	4	0.3	2	0.1	46	0.25	0.9	0.21
04DT 6-1[€]	-	974	-	231	38	427	20.2	119	4.8	2	1.1	974	15.9	34.8	4.8
04DT14-1*[£]	-	0.04	3.20	111.10	23.34	629.13	2.79	6.47	1.70	1.04	0.64	539.93	4.63	11.20	1.31
04DT14-2*[£]	-	0.02	12.07	460.11	26.64	255.54	31.11	25.84	3.50	2.15	2.02	212.06	19.60	50.72	7.21
04DT22-1*[£]	-	0.02	16.91	269.68	11.15	632.65	12.40	6.69	2.53	2.83	0.75	285.33	7.22	18.13	2.36
04DT23-1*[£]	-	0.03	16.12	225.98	1.84	202.25	24.25	6.83	3.16	1.2	0.07	117.71	3.98	13.83	2.36
04DT24-1*[£]	-	0.01	7.22	237.19	2.61	529.55	8.25	4.56	0.96	0.45	0.07	107.27	3.47	8.27	1.22
04DT25-1*[£]	-	0.02	12.42	228.60	5.02	394.74	7.58	6.57	0.86	0.84	0.15	217.42	5.53	13.17	1.80
04DT28-1*[£]	-	0.02	9.55	239.86	0.90	277.53	7.76	27.39	2.03	0.84	0.07	73.95	5.91	15.26	2.11
04AT58-3*[£]	-	0.06	15.40	342.17	16.90	499.93	16.98	11.26	2.03	0.95	1.20	342.81	13.84	34.12	4.69

[€]Sample analyses courtesy of the Yukon Geological Survey. X-Ray Flourescence analyses were performed at XRAL Laboratories-A Division Of SGS Canada Inc., North York, Ontario.
*From: Turner, D. 2005. Geochemical and Petrological Analysis of the Tally Ho Shear Zone and Takhini Deformation Zone, South Central Yukon. Unpublished B.Sc. thesis, University of Victoria, 67p. (part of this study)
[£]Analysis at Cominco Laboratories, Richmond, BC

WHOLE ROCK TRACE ELEMENT GEOCHEMISTRY RESULTS

Sample	Nd	Sm	Eu	Gd	Tb	Dy	Ho	Er	Tm	Yb	Lu	Hf	Ta	Tl	Pb
04AT 207-1[€]	20.3	5.35	1.68	5.71	0.97	5.29	1.05	3.07	0.453	2.88	0.429	3.4	0.51	0.29	17
04AT 219-1[€]	6.62	2	0.772	2.51	0.43	2.54	0.51	1.41	0.203	1.29	0.197	1	0.07	0.52	13
04AT 229-2[€]	11.9	3.21	1.19	3.49	0.55	3.08	0.59	1.65	0.237	1.55	0.234	1.4	0.12	0.15	12
04AT231-3[€]	1.09	0.36	0.13	0.53	0.09	0.49	0.11	0.24	0.03	0.21	0.03	0.08	0.02	-	1.62
04AT 231-4[€]	1.35	0.47	0.169	0.58	0.1	0.55	0.1	0.25	0.035	0.22	0.03	0.2	0.06	0.05	5
04AT251-1[€]	20.82	4.91	1.49	4.98	0.69	4.19	0.83	2.29	0.32	2.02	0.30	1.70	0.19	0.08	10.52
04AT253-1[€]	9.27	1.59	0.52	1.53	0.22	1.45	0.30	0.99	0.16	1.28	0.20	3.02	0.59	-	8.70
04AT 339-2[€]	4.55	1.3	0.506	1.56	0.27	1.67	0.34	0.99	0.146	0.94	0.148	0.6	0.07	0.05	5
04DT 004[€]	1.51	0.58	0.21	0.73	0.13	0.71	0.13	0.32	0.044	0.26	0.038	0.2	0.05	0.05	5
04DT 6-1[€]	20.1	4.67	1.57	4.51	0.71	3.74	0.73	1.99	0.293	1.84	0.265	2.9	0.31	0.27	9
04DT14-1*[£]	6.18	1.30	0.66	1.24	0.17	1.00	0.19	0.54	0.07	0.46	0.07	0.33	0.11	-	11.92
04DT14-2*[£]	32.82	7.94	1.38	7.67	1.25	7.32	1.40	4.01	0.55	3.57	0.52	1.61	0.22	-	3.42
04DT22-1*[£]	12.42	3.25	1.18	2.23	0.50	3.03	0.59	1.75	0.24	1.53	0.23	0.38	0.18	-	7.23
04DT23-1*[£]	13.96	4.4	1.6	5.24	0.88	5.55	1.11	3.29	0.45	2.74	0.42	0.52	0.23	-	4.77
04DT24-1*[£]	6.28	1.83	0.64	1.73	0.34	2.04	0.40	1.14	0.15	0.98	0.14	0.34	0.06	-	4.48
04DT25-1*[£]	9.18	2.43	0.81	1.69	0.37	2.14	0.41	1.14	0.16	0.96	0.14	0.42	0.05	-	4.52
04DT28-1*[£]	10.59	2.60	0.92	2.35	0.37	2.13	0.40	1.16	0.15	0.96	0.14	1.11	0.12	-	4.65
04AT58-3*[£]	21.85	5.12	1.29	3.79	0.74	4.28	0.80	2.25	0.30	1.89	0.28	0.77	0.13	-	7.37

[€]Sample analyses courtesy of the Yukon Geological Survey. X-Ray Flourescence analyses were performed at XRAL Laboratories-A Division Of SGS Canada Inc., North York, Ontario.

*From: Turner, D. 2005. Geochemical and Petrological Analysis of the Tally Ho Shear Zone and Takhini Deformation Zone, South Central Yukon. Unpublished B.Sc. thesis, University of Victoria, 67p. (part of this study)

[£]Analysis at Cominco Laboratories, Richmond, BC

WHOLE ROCK TRACE ELEMENT GEOCHEMISTRY RESULTS

Sample	Bi	Th	U	P	Ti	Cr	Co	Ni	Cu	Zn	Ge	As	Ag
04AT 207-1[€]	0.3	1.63	0.83	-	-	20	23	20	90	120	3.2	5	-
04AT 219-1[€]	0.3	0.53	0.39	-	-	320	42	70	110	90	2.2	5	-
04AT 229-2[€]	0.2	1.26	0.75	-	-	20	31	20	90	70	2.3	5	-
04AT231-3[€]	0.04	0.18	0.07	30.98	1178.77	2049.38	44.48	128.35	2.25	34.97	2.11	3.00	0.05
04AT 231-4[€]	0.2	0.05	0.06	-	-	1520	38	120	10	30	2.7	5	-
04AT251-1[€]	0.02	2.62	1.32	3186.87	5976.33	58.48	28.40	16.06	100.49	96.84	1.37	5.59	0.13
04AT253-1[€]	0.06	5.71	2.89	403.06	1309.32	19.66	4.45	3.01	4.06	30.64	1.69	1.52	0.02
04AT 339-2[€]	0.5	0.4	0.23	-	-	1440	49	210	30	70	1.7	5	-
04DT 004[€]	0.1	0.05	0.04	-	-	530	35	110	10	30	2.9	5	-
04DT 6-1[€]	0.2	1.95	1.23	-	-	30	29	20	100	130	1.6	5	-
04DT14-1*[£]	-	0.91	1.14	-	2016.33	13.91	12.98	10.60	62.51	56.44	2.95	-	-
04DT14-2*[£]	-	3.04	1.81	-	6614.16	69.21	57.96	45.51	218.64	198.28	9.32	-	-
04DT22-1*[£]	-	0.91	1.12	-	4105.46	38.28	32.32	28.51	106.44	81.51	5.38	-	-
04DT23-1*[£]	-	0.1	0.09	-	6954.6	270.11	43.99	100.53	31.12	113.06	5.58	-	-
04DT24-1*[£]	-	0.36	0.39	-	2555.53	482.19	49.87	158.15	134.60	72.81	4.75	-	-
04DT25-1*[£]	-	0.58	0.42	-	3165.27	337.77	48.16	90.54	124.38	91.88	5.68	-	-
04DT28-1*[£]	-	0.62	0.46	-	3265.75	108.13	28.31	38.21	112.42	68.74	25.20	-	-
04AT58-3*[£]	-	1.73	1.10	-	4517.78	31.83	36.63	27.05	150.09	121.73	6.54	-	-

[€]Sample analyses courtesy of the Yukon Geological Survey. X-Ray Flourescence analyses were performed at XRAL Laboratories-A Division Of SGS Canada Inc., North York, Ontario.

*From: Turner, D. 2005. Geochemical and Petrological Analysis of the Tally Ho Shear Zone and Takhini Deformation Zone, South Central Yukon. Unpublished B.Sc. thesis, University of Victoria, 67p. (part of this study)

[£]Analysis at Cominco Laboratories, Richmond, BC

WHOLE ROCK TRACE ELEMENT GEOCHEMISTRY RESULTS

Sample	Sn	Sb	W	Hg	Mn	Ga
04AT 207-1[€]	1	2.8	0.5	-	-	19
04AT 219-1[€]	1	3	0.5	-	-	13
04AT 229-2[€]	1	2.6	0.6	-	-	19
04AT231-3[€]	1.07	0.47	0.35	-	972.13	2.61
04AT 231-4[€]	1	2	0.5	-	-	3
04AT251-1[€]	0.86	0.33	0.24	-	1731.56	18.06
04AT253-1[€]	0.90	0.65	ud	-	477.26	15.58
04AT 339-2[€]	1	2.4	0.5	-	-	9
04DT 004[€]	1	2.5	0.5	-	-	4
04DT 6-1[€]	1	3.2	0.5	-	-	23
04DT14-1*[£]	-	-	-	-	614.50	68.25
04DT14-2*[£]	-	-	-	-	3399.70	36.21
04DT22-1*[£]	-	-	-	-	1343.21	50.17
04DT23-1*[£]	-	-	-	-	1456.94	31.05
04DT24-1*[£]	-	-	-	-	1504.27	23.02
04DT25-1*[£]	-	-	-	-	1556.80	34.31
04DT28-1*[£]	-	-	-	-	1694.57	28.62
04AT58-3*[£]	-	-	-	-	1901.90	48.07

[€]Sample analyses courtesy of the Yukon Geological Survey. X-Ray Flourescence analyses were performed at XRAL Laboratories-A Division Of SGS Canada Inc., North York, Ontario.
*From: Turner, D. 2005. Geochemical and Petrological Analysis of the Tally Ho Shear Zone and Takhini Deformation Zone, South Central Yukon. Unpublished B.Sc. thesis, University of Victoria, 67p. (part of this study)
[£]Analysis at Cominco Laboratories, Richmond, BC

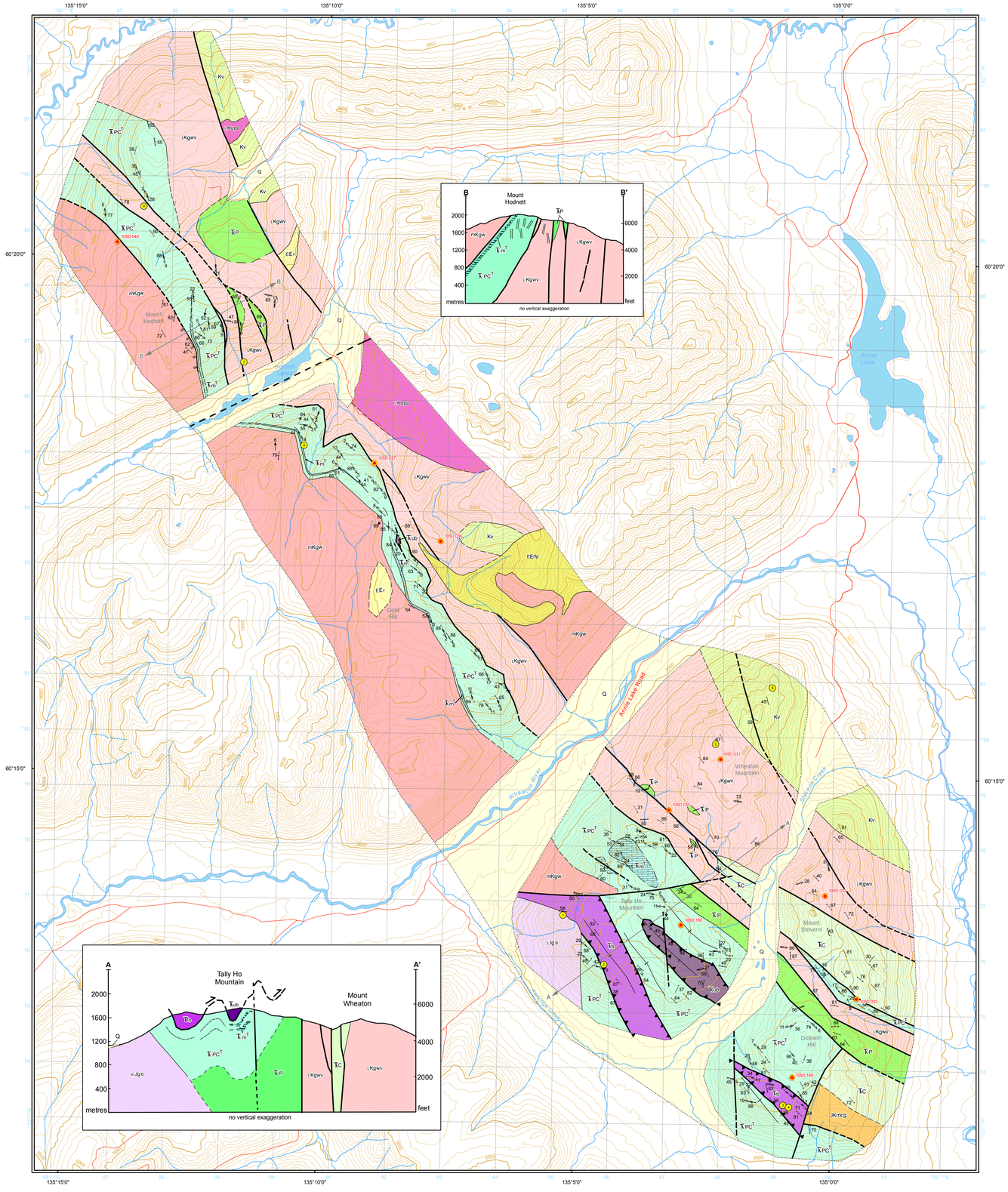

1:50 000-scale topographic base data produced by CENTRE FOR TOPOGRAPHIC INFORMATION, NATURAL RESOURCES CANADA

ONE THOUSAND METRE GRID
Universal Transverse Mercator Projection
North American Datum 1983
Zone 8

CONTOUR INTERVAL 100 FEET
Elevations in feet above Mean Sea Level

BEDROCK GEOLOGY

TALLY HO SHEAR ZONE

YUKON

SCALE 1:30 000

0 1 2 3 4
kilometres

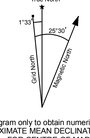

Use diagram only to obtain numerical values
APPROXIMATE MEAN DECLINATION 2005
FOR CENTRE OF MAP

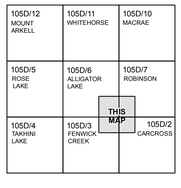

LEGEND

QUATERNARY

Q — unconsolidated gravel, sand, silt and clay of fluvial, glaciofluvial and/or glaciolutrice origin.

EOCENE

Mount Skukum Volcanic Complex

EErfp — buff weathering domes, plugs and locoliths of coarse-grained rhyolite feldspar porphyry (Hart et al., 1990).

EEr — flaggy, orange, rusty orange to white orange, mauve or tan, fine-grained rhyolite dykes, dyke swarms, and flow domes (Hart et al., 1990).

CRETACEOUS

LKgwv — QUARTZ DIORITE UNIT (Wheaton Valley granodiorite): light to dark grey weathering, medium- to coarse-grained quartz diorite and granodiorite; variably chloritized and locally foliated; xenolithic (U-Pb zircon 77.1 ± 0.7 Ma; Hart, 1995).

Kv — WHEATON RIVER VOLCANICS: pale green to grey weathering, aphanitic and porphyritic andesite to dacite flows, heterolithic breccia, agglomerate, tuff and associated epiclastic rocks (Hart et al., 1990).

LKgpp — PERKINS PEAK PLUG: pale pink weathering, white porphyricic alaskite and granite with plagioclase and quartz-eye phenocrysts in fine-grained mafic matrix; coarse-grained and mafic phases (Hart et al., 1990).

mKgw — GRANODIORITE UNIT (Whitehorse Plutonic Suite): buff to grey weathering, medium-grained granodiorite and diorite; locally weakly foliated and xenolithic (K/Ar 116 Ma; Hart, 1995).

JKcg — MILLHAVEN CONGLOMERATE: dark reddish brown-weathering polymictic orthoconglomerate; clasts include quartz, quartzite, schist, granite, chert and volcanic rock up to 6 cm in diameter that are subangular to subrounded (Hart et al., 1990).

JURASSIC

mJgs — MEGACRYSTIC GRANITE UNIT (Bennett granite): light grey weathering, coarse-grained, massive feldspar megacrystic granite (U-Pb 172.8 ± 0.5 Ma; this study).

UPPER TRIASSIC

LEWES RIVER GROUP

Aksala Formation

TrC — VOLCANICLASTIC UNIT (Casca Member; formally the Annie Member of Hart and Radloff, 1990): dark reddish to green-grey weathering, massive to well-bedded tuff, agglomerate, greywacke, pebble conglomerate, and laharric debris flows; variably chloritized and locally foliated (Tizzard and Johnston, 2005; Hart et al., 1990; Hart, 1997).

Povoas Formation

TrP — AUGITE-PHENOCRYSTIC BASALT UNIT: dark green to grey weathering, massive basalt to moderately-well foliated augite-phenocrystic basalt; variably chloritized and augite phenocrysts up to 1 cm in diameter.

TrPC^T — TALLY HO SHEAR ZONE: green to grey weathering, moderate- to well-foliated greenschist, augite-pophyroclastic schist and mylonite; variably chloritized and epidotized.

white to buff weathering marble and sandy marble; highly strained and recrystallized.

TrLb — LEUCOGABBRO UNIT (Tally Ho leucogabbro): mottled, dark green, black and white, medium- to very coarse-grained plagioclase-hornblende gabbro; weakly- to well-foliated (U-Pb 208.4 +/- 4.3 Ma; this study).

TrPo — PYROXENITE UNIT (Tally Ho pyroxenite); dark green to brown weathering, medium- to coarse-grained pyroxenite and peridotite; variably serpentinized and locally strongly foliated; chrysotile and magnetite veinlets; probably co-eval with leucogabbro unit.

SYMBOLS

geologic contacts (defined, approximate, inferred, covered)
fault; movement not known (defined, approximate, inferred, covered)
thrust fault (defined, approximate, inferred)
fold (synform, antiform)
sheared intrusive contact
limit of mapping/outcrop
foliation (dominant)
elongation or mineral lineation
crenulation lineation
fold axis (dominant phase)
dyke
mineral lineation (slickenline)
fault (orientation known)
line of cross-section
radiometric date (see table 1 for details)
MINFILE locality (see table 2 for details)
road/trail

NOTES

The geology of the Tally Ho shear zone and adjacent areas benefited from 1:50,000 scale mapping by Hart et al. (1990a) and Hart et al. (1990b). Names in parentheses in legend refer to unit names ascribed by Doherty and Hart (1988), Hart et al. (1990a) and Hart et al. (1990b) . Unit descriptions are taken from Hart et al. (1990a) and Hart et al. (1990b) except for Tally Ho shear zone and associated units discussed in Tizzard et al.(in press). See text for explanatory notes. This map is formatted in the style of the Yukon Geological Survey.

Table 1. Radiometric Ages

Symbol #	Dating Method	Mineral Dated*	Rock Type	Age (Ma)	Reference
1	K/Ar	w	quartz-feldspar porphyry dyke	54.7 ± 3.8	Breitsprecher & Mortensen (2004)
2	K/Ar	w	andesite porphyry dyke	65.3 ± 2.3	Hart (1995)
3	U-Pb	z	hornblende granodiorite	77.1 ± 0.7	Hart (1995)
4	K/Ar	h	pyroxene diorite	106 ± 4	Hart (1995)
5	K/Ar	h	hornblende gabbro	113 ± 3	Hart (1995)
6	U-Pb	z	megacrystic granite	172.8 ± 0.5	Tizzard et al. (in press)
7	U-Pb	z	hornblende gabbro	208.4 ± 4.3	Tizzard et al. (in press)
8	U-Pb	z	hornblende gabbro	215 ± 0.6	Hart (1995)

* z = zircon; h = hornblende; w = whole rock

Table 2. Mineral Occurrences
Yukon MINFILE (Deklerk, 2005)

Minfile #	Name	Deposit Type	Major Commodity	Minor Commodity
105D 030	Tally Ho	Epithermal Au-Ag-Cu: high sulphidation	Au, Ag	Pb, Cu
105D 031	Wheaton Mountain	Epithermal Au-Ag-Cu: high sulphidation	Au, Ag	Pb, Cu
105D 032	Buffalo Hump	Au-quartz veins	Au, Ag	Pb, Ag
105D 033	Mt. Stevens, Midnight, Hidden Ore, Hawk Eye	Au-quartz veins	Au, Ag	Cu, Pb, Zn
105D 036	Gold Hill, Dail	Au-quartz veins	Ag, Au	
105D 037	Gold Reef	Polymetallic veins	Ag, Au	Pb, Cu
105D 040	Legal Tender, Lucky Boy, Mineral Hill	Au-quartz veins	Au, Pb, Ag	Cu, Zn
105D 168	Dickson Hill	Epithermal Au-Ag-Cu: high sulphidation	Au	Ag
105D 180	Silver Queen	Porphyry Cu-Mo-Au	Ag	Cu, Au, Pb

REFERENCES

Deklerk, R., 2005. Yukon MINFILE 2005 - A database of mineral occurrences. Yukon Geological Survey.

Doherty, R.A., Hart, C.J.R. 1988. Preliminary Geology of Fenwick Creek (105 D/3) and Alligator Lake (105 D/6) Map Areas, Open File 1988-2. Indian and Northern Affairs Canada, Exploration and Geological Services Division, Yukon Region.

Breitspreher, K., Mortensen, J.K. 2004. YukonAge 2004: A database of isotopic age determinations for rock units from Yukon Territory, Canadian Geochronology Knowledgebase. Yukon Geological Survey, CD-ROM.

Hart, C.J.R. 1995. Magmatic and Tectonic Evolution of the Intermontane Superterrane and Coast Plutonic Complex in Southern Yukon Territory. M.Sc. thesis, University of British Columbia, 198 pp.

Hart, C.J.R. 1997. A Transect Across Northern Stikinia: Geology of the Northern Whitehorse Map Area, Southern Yukon Territory (105D/13-16). *In:* Abbott, G. (ed.) Exploration and Geological Services Divisions, Yukon Region, Indian and Northern Affairs Canada, Bulletin 112.

Hart, C.J.R., Doherty, R.A., Radloff, J.K., Hunt, J.A., Fingland, M.P., Wegenast, J. 1990a. Geological Map of Fenwick Creek (105 D/3) Map Area, Open File 1990-4. Indian and Northern Affairs Canada, Exploration and Geological Services Division, Yukon Region.

Hart, C.J.R., Doherty, R.A., Radloff, J.K., Hunt, J.A., Fingland, M.P., Wegenast, J. 1990b. Geological Map of Alligator Creek (105 D/6) Map Area, Open File 1990-4. Indian and Northern Affairs Canada, Exploration and Geological Services Division, Yukon Region.

Tizzard, A.M., Johnston, S.T., Hearman, L.M. *In press.* Arc imbrication during thick-skinned collision within the northern Cordilleran accretionary orogen, Yukon, Canada. Geological Society of London.

Geological map of the Tally Ho shear zone (parts of NTS 105D/2, 3, 6 & 7) (1:30,000 scale)

by

Amy Tizzard and Stephen Johnston
University of Victoria, Victoria, British Columbia

APPENDIX I

The Tally Ho Shear Zone: Implications for the Tectonic Evolution of the Western Margin of Stikinia, Southern Yukon Territory, Canada

University of Victoria